National Technical University of Athens
**School of Civil Engineering**
Institute of structural analysis and anti-seismic research
*Analysis and Design of Earthquake Resistant Structures* ***(ADERS)***

# POSTGRADUATE DISSERTATION

## *«Development of computer program for the second order inelastic analysis of frames»*

**IOANNIS A. KAPOGIANNIS**

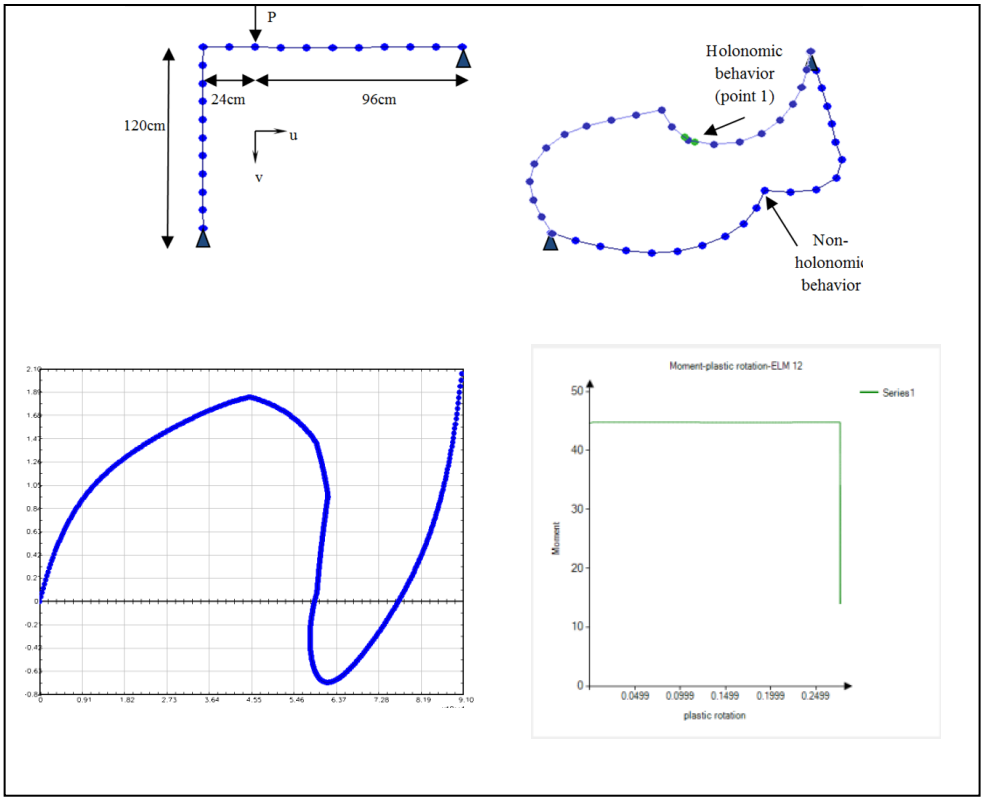


**Supervisor:**
**Professor**
**K.V. SPILIOPOULOS**

ATHENS
JANUARY 2014

## Acknowledgements

I would like to thank professor K.V. Spiliopoulos for his constant guidance, personal attention, endless encouragement and full support during this dissertation. He gave me the opportunity to carry out the current thesis under his supervision, providing all the necessary knowledge and the efforts needed.

I would like to thank the PhD candidates K. Panagiotou and M. Antonini, who as good friends and partners were always willing to help and give their best suggestions.

I would also like to thank my family and my friends. They were always supporting me and encouraging me to attend the current postgraduate program.

# Table of contents

## SUMMARY

It is a well-known fact that an incremental step by step analysis, considering both geometric and materials nonlinearities, provides the most accurate response for every structural system. To achieve this goal, the solution algorithm used, should be both numerically robust and accurate.

Towards this direction, an advanced second order analysis software package is developed, with the following characteristics

- The program simulates 2D-structures, which have been defined by beam-column elements.
- A beam-column based tangent stiffness matrix is used which provides extra information about equilibrium in the deformed configuration and is updated for each iterative loading.
- The equilibrium path is traced by the spherical arc-length method (a displacement control method) , where the radius of the arc determines the value of the load increment.
- The plasticity is implemented, adopting the plastic hinge model. Regarding the yield criterion, the yield surface introduced by AISC is used. The moment plastic rotation laws are used to describe the behavior of the yield surface. All the possible cases of material were taking into account
  - Elastic perfectly plastic material
  - Elastic plastic with isotropic strain hardening behavior
  - Elastic plastic with isotropic strain softening behavior
- Plastic unstressing is implemented by a simple approach, taking into account the current stress state as compared with the plastic incremental deformation
- New computational strategies regarding the plastic hinge formation and the load increment control are proposed.
- The solution algorithm was developed in FORTRAN 2008 , while the graphics interface in visual basic 2008

Some illustrative examples are presented and they are compared with solutions provided by the well-known software SAP2000. It is worth-noting that, some results holding for elastic perfectly plastic materials behavior, has already been presented in [1]

# 1. Introduction

An incremental step by step analysis, considering both geometric and material nonlinearities, provides the most accurate response for every structural system. For this reason, such analyses are used to improve the current limit-state design codes prediction about strength and stability. To achieve this goal, the solution algorithm used should be numerically robust and accurate.

Towards this direction, an advanced second order analysis software package is developed, combining the natural deformation approach with the corotational formulation. The plastic hinge model has been adopted to simulate the inelastic material behavior, which describes the stiffness degradation due to plastification under a continuously varying loading. Three possible materials laws were implemented elastic perfectly plastic, elastic plastic with strain hardening and elastic plastic with strain softening. A beam-column based tangent stiffness matrix is used which provides extra information about equilibrium in the deformed configuration; this has an effect of using less elements for the discretization of the structure. The equilibrium path is traced by the spherical arc-length method, where the radius of the arc determines the value of the load increment.

Plastic unstressing is usually not taken into account, as various numerical problems have been experienced [2]. Nevertheless, especially when large deformations are considered, this phenomenon should not be neglected, as a totally different equilibrium path may be reached. In the present work, plastic unstressing (non-holonomic behavior) is implemented by a simple approach, taking into account the current stress state as compared with the plastic incremental deformation. Additionally, other computational topics are discussed, such as the opening of plastic hinges (P.H.) and the number of them, which are allowed to occur per iteration. These issues are quite important because they determine the stability of the equilibrium path.

## 2. Formulation of the plasticity problem

### 2.1. Governing equations and geometric non-linearity

According to [3] for a frame that consists of nodes and members, let us denote the nodal forces by **U** and the corresponding nodal displacements by **u**, where bold letters are used for vectors and matrices.

Using the natural deformation approach [4], for each individual member there are three independent deformations, two rotational, one at each end, and an extensional deformation. These may all be grouped in the vector $\mathbf{q}_{\mathrm{N}}$. At the same time the nodal displacements of the member, consisting of two translations and one rotation for each end, may be grouped in the vector $\mathbf{q}_{\mathrm{g}}$.

As it is well known, in a large displacement problem, the force-displacement relation is non-linear and therefore the study of such a problem may be accomplished through an incremental procedure where the force is applied in small increments.

At the beginning of an incremental step we may write :

$$\mathrm{d}\mathbf{q}_{\mathrm{N}} = \boldsymbol{\alpha}_{\mathrm{N}} \mathrm{d}\mathbf{q}_{\mathrm{g}} \tag{2.1}$$

where $\boldsymbol{\alpha}_{\mathrm{N}}$ is defined according to the geometry at the beginning of the step ( Figure 2.1) .

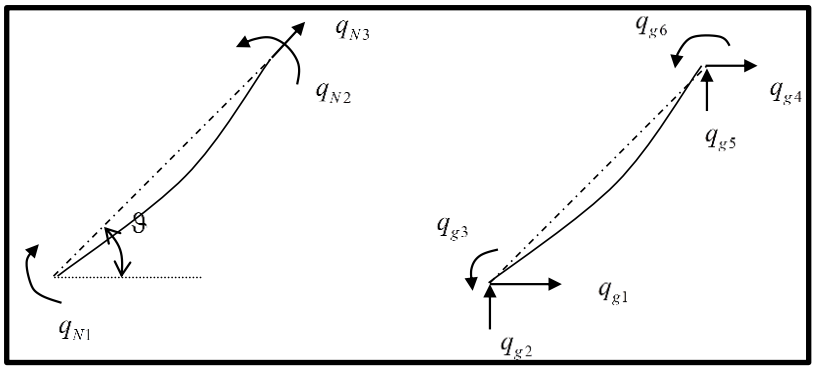


Figure 2.1 The natural and the global deformations

Using the principle of virtual work (P.V.W):

$$(\mathrm{d}\mathbf{q}_{\mathrm{N}})^{\mathrm{T}} \mathbf{Q}_{\mathrm{N}} = (\mathrm{d}\mathbf{q}_{\mathrm{g}})^{\mathrm{T}} \mathbf{Q}_{\mathrm{g}} \tag{2.2}$$

Combining equations (2.1) and (2.2) we get the following relation which expresses the equilibrium between the existing nodal element forces $\mathbf{Q}_g$ and internal element forces $\mathbf{Q}_N$:

$$\mathbf{Q}_g = \boldsymbol{\alpha}_N^T \mathbf{Q}_N \tag{2.3}$$

Using a constitutive material law, expressed through a matrix $\mathbf{k}_N$, the increment $d\mathbf{q}_N$ gives rise to an increment of internal forces $d\mathbf{Q}_N$:

$$d\mathbf{Q}_N = \mathbf{k}_N d\mathbf{q}_N \tag{2.4}$$

At the end of the incremental step, the $\boldsymbol{\alpha}_N$ matrix, as a result of the increment $d\mathbf{q}_g$, also changes, so the compatibility equation changes also to:

$$d\mathbf{q}_N = (\boldsymbol{\alpha}_N + d\boldsymbol{\alpha}_N) d\mathbf{q}_g \tag{2.5}$$

Equilibrium of the element's internal and nodal forces at the end of the step is guaranteed through the P.V.W equation:

$$(d\mathbf{q}_N)^T (\mathbf{Q}_N + d\mathbf{Q}_N) = (d\mathbf{q}_g)^T (\mathbf{Q}_g + d\mathbf{Q}_g) \tag{2.6}$$

By expanding the above equation we get:

$$\mathbf{Q}_g + d\mathbf{Q}_g = [\boldsymbol{\alpha}_N^T + (d\boldsymbol{\alpha}_N)^T](\mathbf{Q}_N + d\mathbf{Q}_N) = \boldsymbol{\alpha}_N^T \mathbf{Q}_N + \boldsymbol{\alpha}_N^T d\mathbf{Q}_N + (d\boldsymbol{\alpha}_N)^T \mathbf{Q}_N + (d\boldsymbol{\alpha}_N)^T d\mathbf{Q}_N \tag{2.7}$$

Using (2.3) and neglecting second order terms the above equation results to:

$$d\mathbf{Q}_g = \boldsymbol{\alpha}_N^T d\mathbf{Q}_N + (d\boldsymbol{\alpha}_N)^T \mathbf{Q}_N \tag{2.8}$$

Using (2.4) and (2.1), equation (2.8) may be finally written as:

$$d\mathbf{Q}_g = (\boldsymbol{\alpha}_N^T \mathbf{k}_N \boldsymbol{\alpha}_N)\, d\mathbf{q}_g + (d\boldsymbol{\alpha}_N)^T \mathbf{Q}_N \tag{2.9}$$

As far as the second term of the right-hand side is concerned, by examining the nature of $\boldsymbol{\alpha}_N$:

$$dq_{Ni} = \boldsymbol{\alpha}_{Ni} d\mathbf{q}_g = \frac{\partial q_{Ni}}{\partial q_{g1}} dq_{g1} + \frac{\partial q_{Ni}}{\partial q_{g2}} dq_{g2} + \ldots + \frac{\partial q_{Ni}}{\partial q_{g6}} dq_{g6} = \frac{\partial q_{Ni}}{\partial \mathbf{q}_g} d\mathbf{q}_g \tag{2.10}$$

where i=1,2,3. From the above expression it may be determined that:

$$\mathbf{a}_{Ni}^{T} = \left\{ \frac{\partial q_{Ni}}{\partial q_{g1}} \quad \frac{\partial q_{Ni}}{\partial q_{g2}} \quad \dots \quad \frac{\partial q_{Ni}}{\partial q_{g6}} \right\} \tag{2.11}$$

is a column vector.

The matrix $(d\boldsymbol{\alpha}_N)^T$ may then be looked at as a composition of column vectors:

$$d\boldsymbol{\alpha}_N^T = \left\{ d\boldsymbol{\alpha}_{N1}^T \quad d\boldsymbol{\alpha}_{N2}^T \quad d\boldsymbol{\alpha}_{N3}^T \right\} \tag{2.12}$$

Expressing these increments with the aid of (2.10) we finally get:

$$(d\boldsymbol{\alpha}_N)^T \mathbf{Q}_N = \sum_{i=1}^{3} d\boldsymbol{\alpha}_{Ni}^T Q_{Ni} = \left\{ \sum_{i=1}^{3} \begin{bmatrix} \frac{\partial^2 q_{Ni}}{\partial q_{g1}^2} & \dots & \frac{\partial^2 q_{Ni}}{\partial q_{g6}^2} \\ \dots & \dots & \dots \\ \frac{\partial^2 q_{Ni}}{\partial q_{g1} \partial q_{g6}} & \dots & \frac{\partial^2 q_{Ni}}{\partial q_{g6}^2} \end{bmatrix} Q_{Ni} \right\} d\mathbf{q}_g = \left\{ \sum_{i=1}^{3} (\boldsymbol{\Lambda}_i Q_{Ni}) \right\} d\mathbf{q}_g \tag{2.13}$$

The term in the bracket is the geometric stiffness matrix of the element $\mathbf{k}_G$.

## 2.2. The corotational formulation and the stiffness matrix

According to the corotational formulation [5], a local coordinate system is attached to each element with its x-axis coinciding with the current element chord. This formulation fits nicely with natural deformation approach. In Figure 2.2 two configurations of the same element are presented. The first configuration referes to a state before the application of a random loading and therefore before deformation, while the one at some stage of subsequent loading and deformation.

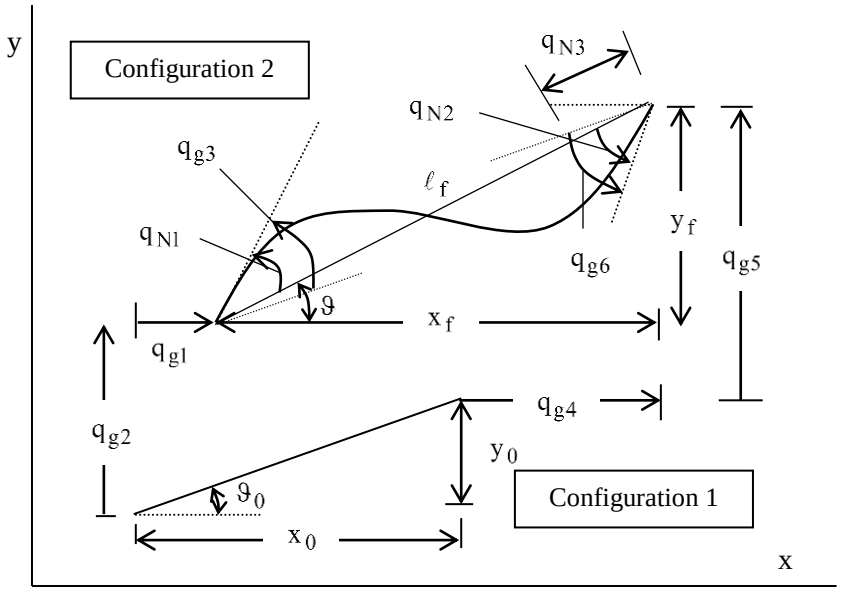


Figure 2.2 Local deformations and global displacements of a beam element

Using the Figure 2.2, the following strain-displacement relationships may be derived:

$$q_{N1} = q_{g3} + \vartheta_0 - \vartheta = \vartheta_0 + q_{g3} - \tan^{-1}\frac{y_f}{x_f}$$

$$q_{N2} = q_{g6} + \vartheta_0 - \vartheta = \vartheta_0 + q_{g6} - \tan^{-1}\frac{y_f}{x_f} \qquad (2.14)$$

$$q_{N3} \approx \ell_f - \ell = \frac{\ell_f^2 - \ell^2}{\ell_f + \ell}$$

It has been pointed out [6] that the use of the difference of squares in the third of the group of equation (2.14) produces more accurate results, especially for large lengths. By carrying out the appropriate differentiations, as suggested by (2.11) and (2.13), the $\boldsymbol{\alpha}_N$ and the $\boldsymbol{\Lambda}_i$ matrices may be established [2]

$$\boldsymbol{\Lambda}_1 = \frac{1}{\ell^2}\begin{bmatrix} 2\cos\vartheta\sin\vartheta & (\sin^2\vartheta - \cos^2\vartheta) & 0 & -2\cos\vartheta\sin\vartheta & -(\sin^2\vartheta - \cos^2\vartheta) & 0 \\ & -2\cos\vartheta\sin\vartheta & 0 & -(\sin^2\vartheta - \cos^2\vartheta) & 2\cos\vartheta\sin\vartheta & 0 \\ & & 0 & 0 & 0 & 0 \\ & & & 2\cos\vartheta\sin\vartheta & (\sin^2\vartheta - \cos^2\vartheta) & 0 \\ & & & & -2\cos\vartheta\sin\vartheta & 0 \\ & & & & & 0 \end{bmatrix}$$

$$\boldsymbol{\Lambda}_2 = -\boldsymbol{\Lambda}_1 \qquad (2.15)$$

$$\boldsymbol{\Lambda}_3 = \frac{1}{\ell^2}\begin{bmatrix} \sin^2\vartheta & -\cos\vartheta\sin\vartheta & 0 & -\sin^2\vartheta & -\cos\vartheta\sin\vartheta & 0 \\ & \cos^2\vartheta & 0 & -\cos\vartheta\sin\vartheta & -\cos^2\vartheta & 0 \\ & & 0 & 0 & 0 & 0 \\ & & & \sin^2\vartheta & -\cos\vartheta\sin\vartheta & 0 \\ & & & & \cos^2\vartheta & 0 \\ & & & & & 0 \end{bmatrix}$$

$$\boldsymbol{\alpha}_N^T = \begin{bmatrix} \frac{\sin\vartheta}{\ell} & -\frac{\sin\vartheta}{\ell} & -\cos\vartheta \\ -\frac{\cos\vartheta}{\ell} & \frac{\cos\vartheta}{\ell} & -\sin\vartheta \\ -1 & 0 & 0 \\ -\frac{\sin\vartheta}{\ell} & \frac{\sin\vartheta}{\ell} & \cos\vartheta \\ \frac{\cos\vartheta}{\ell} & -\frac{\cos\vartheta}{\ell} & \sin\vartheta \\ 0 & 1 & 0 \end{bmatrix} \qquad (2.16)$$

In order to increase the computational efficiency so that less elements and bigger load increments are used, equilibrium in the deformed configuration inside an element is done in a more accurate way by solving the differential equations of the beam-column model. This leads to an enhancement of the matrix $\mathbf{k}_N$ through the use of stability functions. In this notation, the $\mathbf{k}_N$ is established as [2] :

$$\mathbf{k}_N = \frac{EI}{\ell}\begin{bmatrix} S_1 & S_2 & 0 \\ S_2 & S_1 & 0 \\ 0 & 0 & A/I \end{bmatrix} \tag{2.17}$$

where E, I, A, $\ell$ are the modulus of elasticity, moment of inertia, cross-sectional area and length of the element under consideration. $S_1$ and $S_2$ are the stability functions (2.18 and 2.19) which take into account the effect that the axial force has on the equilibrium inside an element.

$$S_1 = \begin{Bmatrix} \dfrac{\rho\sin(\rho) - \rho^2\cos(\rho)}{2 - 2\cos(\rho) - \rho\sin(\rho)} & (Q_{N3} < 0) \\ \dfrac{\rho^2\cosh(\rho) - \rho\sinh(\rho)}{2 - 2\cosh(\rho) + \rho\sinh(\rho)} & (Q_{N3} > 0) \end{Bmatrix} \tag{2.18}$$

$$S_2 = \begin{Bmatrix} \dfrac{\rho^2 - \rho\sin(\rho)}{2 - 2\cos(\rho) - \rho\sin(\rho)} & (Q_{N3} < 0) \\ \dfrac{\rho\sinh(\rho) - \rho^2}{2 - 2\cosh(\rho) + \rho\sinh(\rho)} & (Q_{N3} > 0) \end{Bmatrix} \tag{2.19}$$

Where $\rho = \ell\sqrt{-Q_{N3}/EI}$

## 2.3. Spherical Arc length method

The spherical arc-length method [7] is used to trace the whole load-displacement curve. This method belongs to a class of methods called “continuation methods”. According to these methods the non-linear equilibrium equations are cast in the form:

$$\mathbf{f}(\mathbf{u}, \lambda) = \lambda\mathbf{U} - \mathbf{Q}_N(\mathbf{u}) = \mathbf{0} \tag{2.20}$$

where $\lambda$ is a proportional loading parameter defining the load level.

The non-linear equation (2.20) may be written in an iterative form:

$$\mathbf{K}_T\, d\mathbf{u}^{(i)} = (\lambda_t + \Delta\lambda^{(i)})\mathbf{U} - \mathbf{Q}_{N_{t+\Delta t}}^{(i-1)} \tag{2.21}$$

where subscripts $t$ and $t+\Delta t$ denote entities at the beginning (known quantities) and at the end (sought quantities) of an incremental step, respectively.

At the same time the increments of the forces and the displacements form a vector whose length is equal to a pre-chosen value equal to $\Delta l$:

$$[\Delta\mathbf{u}^{(i-1)} + d\mathbf{u}^{(i)}]^T[\Delta\mathbf{u}^{(i-1)} + d\mathbf{u}^{(i)}] + \psi^2(\Delta\lambda^{(i)}\mathbf{U})^T(\Delta\lambda^{(i)}\mathbf{U}) = \Delta l^2 \tag{2.22}$$

where :

$$\Delta\mathbf{u}^{(i)} = \Delta\mathbf{u}^{(i-1)} + d\mathbf{u}^{(i)} \quad , \text{ with } \Delta\mathbf{u}(0) = \mathbf{0} \tag{2.23}$$

$$\Delta\lambda^{(i)} = \Delta\lambda^{(i-1)} + d\lambda^{(i)} \quad , \text{ with } \Delta\lambda^{(0)} = 0 \tag{2.24}$$

Combining equations (2.21)-(2.24), we may get a quadratic equation with respect to $d\lambda^{(i)}$. If this equation is solved, two roots may be found and therefore a new update for the next iteration. The procedure stops when the external and internal forces coincide within some tolerance and all the entities at the end of the incremental step $(t+\Delta t)$ have now been found. The first two iterations, for an equivalent one-dimensional, may be seen in Fig.2.2.

The efficiency of the numerical procedure highly depends on the magnitude of $\Delta l$ and the next thing to be discussed is how to choose it.

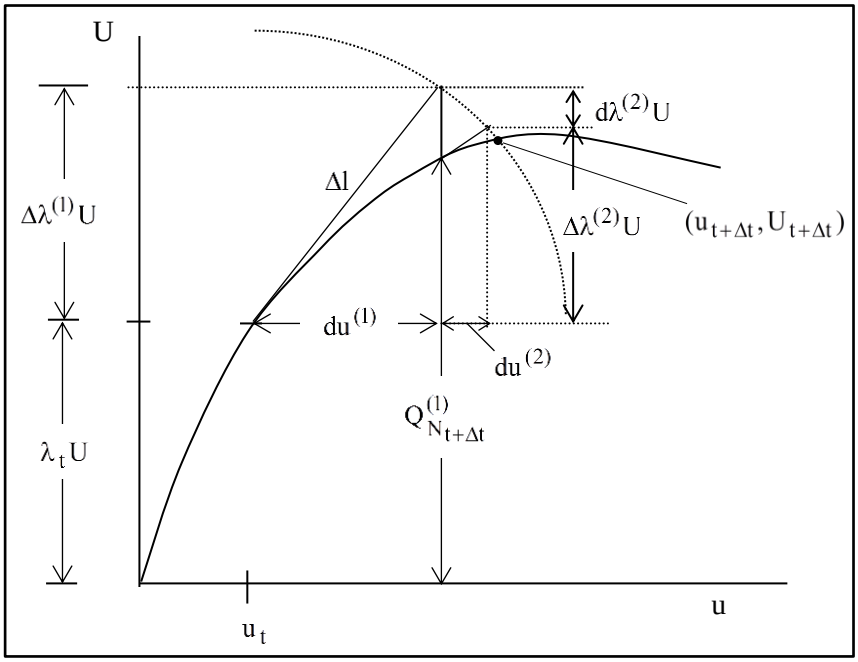


Figure 2.3 The spherical arc length method

## 3. The material non-linearity

In the current work, a lumped plasticity model was used for each member end and the yield moment is defined by a yield surface criterion. This criterion is the one proposed by the AISC [8] for steel profile sections (Figure 3.1)

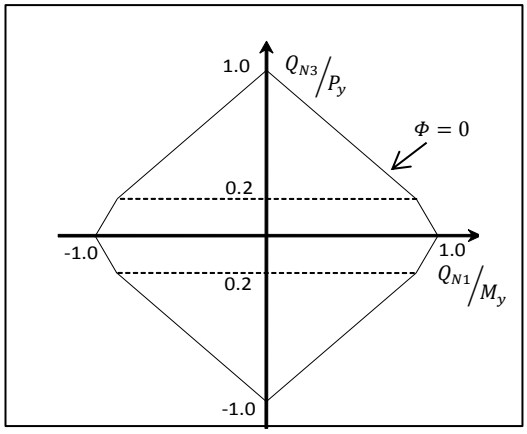


Figure 3.1 AISC proposed yield surface

It is pointed out that the force point where plastic hinge occurs is decided by combination the axial force and the bending moment. As presented in (Figure 3.1) the first quadrant of the yield surface is expressed by the following relations

- For the first branch

$$\frac{Q_{N3}}{P_y} + \frac{8}{9}\frac{Q_{N1,2}}{M_p} = 1.0 \qquad \text{when} \qquad \frac{Q_{N3}}{P_y} \geq 0.2 \tag{3.1}$$

- For the second branch

$$\frac{Q_{N3}}{2P_y} + \frac{Q_{N1,2}}{M_p} = 1.0 \qquad \text{when} \qquad \frac{Q_{N3}}{P_y} < 0.2 \tag{3.2}$$

Considering the hardening/softening effect, it is expressed by the change of the initial yield surface in shape or size. This condition is discussed thoroughly in the next sections, where the differences in approaching the elastic-perfectly plastic problem and the elastic-plastic with strain-hardening/softening problem are pointed out. Regarding the material laws that are considered in the current computer program, the following options are available

- Elastic perfectly plastic :The initial yield surface does not change in shape or size after the yield occurs
- Elastic plastic material with isotropic hardening : The initial yield surface expands in shape and size in a uniform manner
- Elastic plastic material with isotropic softening : The initial yield surface shrinks in a uniform manner

## 3.1. Elastic Perfectly plastic material

In case of elastic perfectly plastic material, the adopted plastic hinge model allows only plastic rotation and no plastic axial deformation. Supposing an initial elastic trial step the increments of the internal forces (point A in Figure 3.2) are given by:

$$\begin{bmatrix} dQ_{N1} \\ dQ_{N2} \\ dQ_{N3} \end{bmatrix} = \mathbf{k}_N d\mathbf{q}_N^{el} = \frac{EI}{\ell} \begin{bmatrix} S_1 & S_2 & 0 \\ S_2 & S_1 & 0 \\ 0 & 0 & A/I \end{bmatrix} \begin{bmatrix} dq_{N1}^{el} \\ dq_{N2}^{el} \\ dq_{N3}^{el} \end{bmatrix} \tag{3.3}$$

Let us suppose that applying the next load increment, the left end of an element develops a plastic hinge. Then the force point moves from point A to point B ( Figure 3.2 ). However, due to the elastic-perfectly plastic material law, the force point must lie on the initial yield surface. Thus a correction takes place and finally the point C is selected. Although there is no correction in the axial force, this procedure provides satisfactory results when specific conditions are met. These conditions are presented in section 4.1.

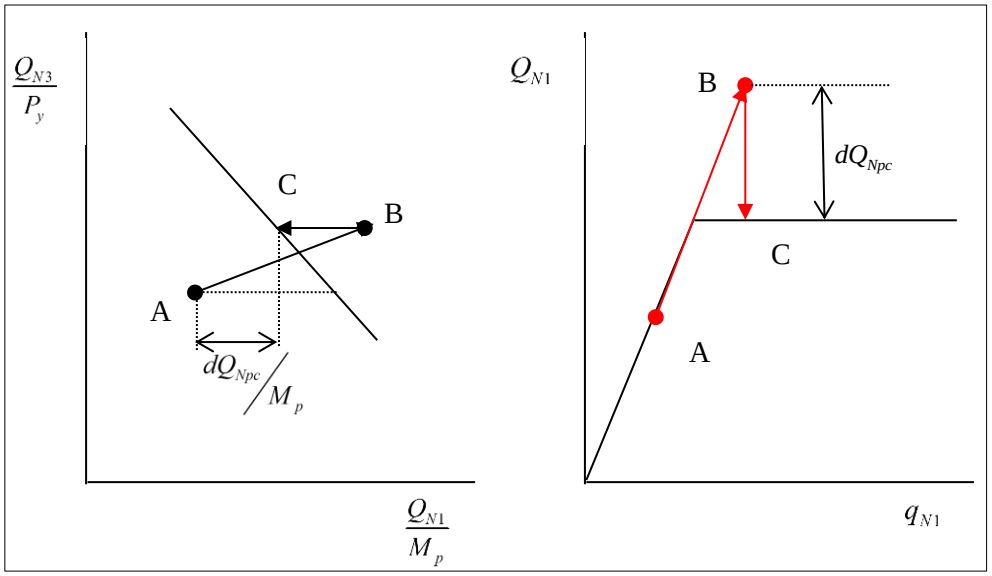


Figure 3.2 The force point movement when plastic hinge occurs

At point C (Figure 3.2), the total deformation at this end is split into an elastic and an inelastic part:

$$\mathrm{dq_{N1}} = \mathrm{dq_{N1}^{el}} + \mathrm{dq_{N1}^{pl}} \tag{3.4}$$

If we combine (3.3) and (3.4) the plastic displacement is equal to

$$\begin{aligned} dQ_{N1} &= \frac{EI}{\ell}(S_1(dq_{N1} - dq_{N1}^{pl}) + S_2 dq_{N2}^{el}) = dQ_{N1}^{pl} \\ dq_{N1}^{pl} &= dq_{N1} + (S_2 / S_1)dq_{N2}^{el} - \frac{\ell}{\ell EIS_1} dQ_{N1}^{pl} \end{aligned} \tag{3.5}$$

The incremental internal force $dQ_{N2}$ according to (3.3) and (3.5)

$$\begin{aligned} dQ_{N2} &= \frac{EI}{\ell}(S_2(dq_{N1} - dq_{N1}^{pl}) + S_1 dq_{N2}^{el}) \\ dQ_{N2} &= (S_2 / S_1) * dQ_{Npc1} - \frac{EI}{\ell}(\frac{S_2^2 - S_1^2}{S_1}) dq_{N2}^{el} \end{aligned} \tag{3.6}$$

Finally we get a modification of the $\mathbf{k}_N$ matrix:

$$\begin{bmatrix} dQ_{N1} \\ dQ_{N2} \\ dQ_{N3} \end{bmatrix} = \frac{EI}{\ell} \begin{bmatrix} 0 & 0 & 0 \\ 0 & \frac{S_1^2 - S_2^2}{S_1} & 0 \\ 0 & 0 & A/I \end{bmatrix} \begin{bmatrix} dq_{N1} \\ dq_{N2}^{el} \\ dq_{N3}^{el} \end{bmatrix} + \begin{bmatrix} 1 \\ \frac{S_2}{S_1} \\ 0 \end{bmatrix} dQ_{Npc1} \tag{3.7}$$

where the correction quantity $\mathrm{dQ_{Npc}}$ is shown in Figure 3.2

Following the same procedure, analogous equations come up when a plastic hinge forms :

- at the right end of the member

$$\begin{bmatrix} dQ_{N1} \\ dQ_{N2} \\ dQ_{N3} \end{bmatrix} = \frac{EI}{\ell} \begin{bmatrix} \frac{S_1^2 - S_2^2}{S_1} & 0 & 0 \\ 0 & 0 & 0 \\ 0 & 0 & A/I \end{bmatrix} \begin{bmatrix} dq_{N1}^{el} \\ dq_{N2} \\ dq_{N3}^{el} \end{bmatrix} + \begin{bmatrix} \frac{S_2}{S_1} \\ 1 \\ 0 \end{bmatrix} dQ_{Npc2} \tag{3.8}$$

- at both ends if the member

$$\begin{bmatrix} dQ_{N1} \\ dQ_{N2} \\ dQ_{N3} \end{bmatrix} = \frac{EI}{\ell} \begin{bmatrix} 0 & 0 & 0 \\ 0 & 0 & 0 \\ 0 & 0 & A/I \end{bmatrix} \begin{bmatrix} dq_{N1}^{pl} \\ dq_{N2}^{pl} \\ dq_{N3}^{el} \end{bmatrix} + \begin{bmatrix} dQ_{Npc1} \\ dQ_{Npc2} \\ 0 \end{bmatrix} \tag{3.9}$$

In all these cases, therefore, we may write:

$$\mathrm{d}\mathbf{Q}_{\mathrm{N}} = \mathbf{k}_{\mathrm{N}}^{\mathrm{ep}} \mathrm{d}\mathbf{q}_{\mathrm{N}} + \mathrm{d}\mathbf{Q}_{\mathrm{Npc}} \tag{3.10}$$

Combining this equation with (2.8) we may finally get the following equation:

$$\mathrm{d}\mathbf{Q}_{\mathrm{g}} = (\mathbf{k}_{\mathrm{g}}^{\mathrm{ep}} + \mathbf{k}_{\mathrm{G}})\, \mathrm{d}\mathbf{q}_{\mathrm{g}} + \boldsymbol{\alpha}_{\mathrm{N}}{}^{\mathrm{T}} \mathrm{d}\mathbf{Q}_{\mathrm{Npc}} \tag{3.11}$$

Results are then transferred from the element level to the structural level and equation (3.11) may be used to form the structure's stiffness matrix $\mathbf{K}_{\mathrm{T}}$ with the aid of which the structural displacement increments d**u** may be evaluated with known force increments d**U**.

## 3.2. Material with hardening/softening

### 3.2.1. Theoretical background

The hardening behavior expresses how the elastic regime expands, when the initial yield has occurred. Towards this direction, the well-known laws of isotropic and kinematic hardening have been established. In case of pure isotropic hardening, the initial yield surface expands in a uniform manner (Figure 3.3), whereas considering a pure kinematic assumption it translates (Figure 3.4).

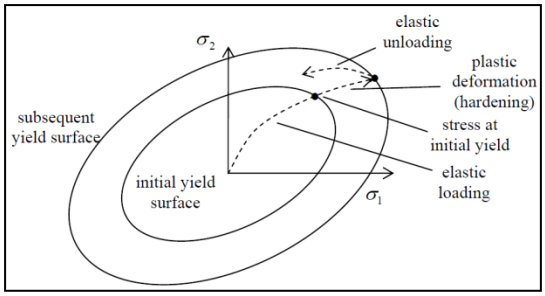


Figure 3.3 Isotropic hardening

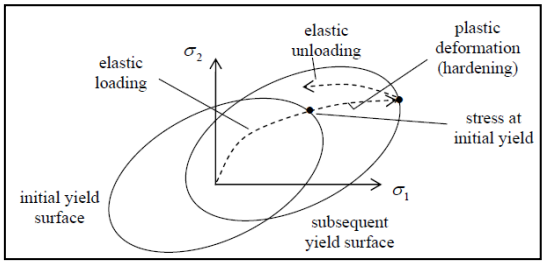


Figure 3.4 kinematic hardening

In the present work, the model of isotropic hardening was adopted because of its simplicity to be implemented in a computer code. However it is pointed out that, in case of cycling loading, these two models provide accurate predictions only for the first cycle of loading [9]. This behavior of metals, subjected to cyclic loading, can be represented by two limit states, the virgin and the saturated one [10]. The virgin state represents the initial yield surface which corresponds to strength and hardening properties of the material for the first half-cycle of inelastic loading. The saturated state represents the strength and the hardening properties of the material when it reaches the steady-state cyclic behavior. The connection between the virgin and the saturated situation is established by a variable field model proposed by Mosaddad and Powel [11]. According to their model, the transition from the virgin to the fully saturated state is controlled by a weighting function, which is based on the accumulated plastic strain.

### 3.2.2. Governing equations for isotropic hardening/softening

Regarding the implementation of the hardening law into a computer program, special consideration should be taken for the calculation of the elasto-plastic stiffness matrix and the incremental plastic deformations. Let an equilibrium point which is characterized by a force point A on the initial yield surface (plastic hinge has formed) (Figure 3.5). The next load increment will force point A to move towards an outer yield surface (point B), due to the existence of hardening phenomenon. This transition

from A to B is determined by an updated elastoplastic stiffness matrix which is adopted when the plastic hinge opens (point A). This stiffness matrix is determined by

- The shape of the yield surface, where the force point A lies ( Figure 3.5),
- the hardening moduli q (Figure 3.5)
- the flow rule

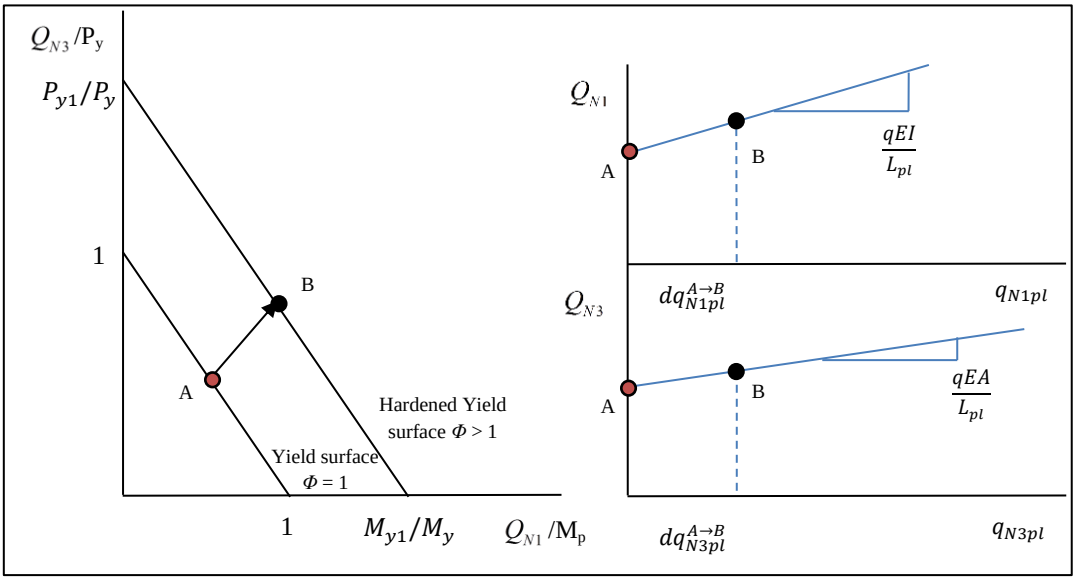


Figure 3.5 Expansion of yield surface due to hardening when plastic hinge forms at the left end (left), moment-plastic rotation and axial force plastic-plastic axial displacement diagrams (right)

As presented in Figure 3.6, during the transition from point A to point B both the axial capacity and the moment capacity increase. In the computer code developed, it was supposed that both the axial force capacity $Q_{N3}$ and the moment capacity $Q_{N1}$ increase with the same hardening modulus q (Figure 3.5). Towards the same direction with the elastic perfectly plastic material, during the transition from point A to point B, the incremental displacement component ($d\boldsymbol{q_N}$) , consists of an elastic and a plastic part because of the hardening behavior [12] ,as shown in Figure 3.6.

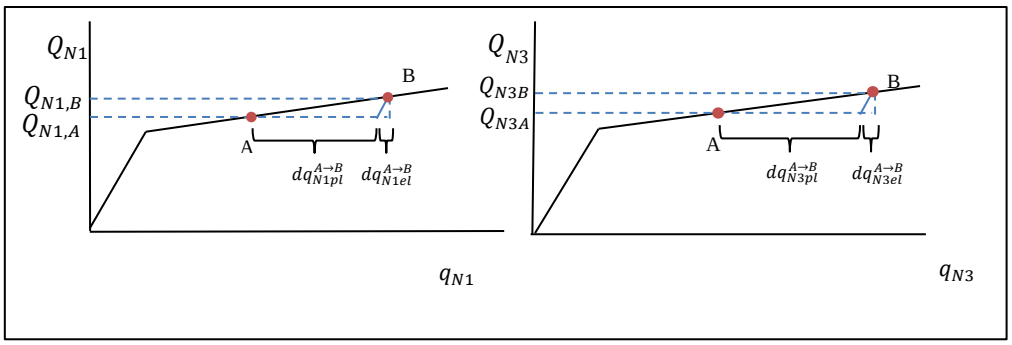


Figure 3.6 Tracing the force point between two yield surfaces

Thus, one may write

$$dq_{N_1} = dq_{N_1}^{el} + dq_{N_1}^{pl}$$
$$dq_{N_3} = dq_{N_3}^{el} + dq_{N_3}^{pl} \quad (3.12)$$

The previously described procedure refers to a plastic hinge at the left end of an element. At this point, one should take into the consideration all the possible plastic hinges which can occur in an element. These cases are the following:

- ***Case 1.1 : Plastic hinge at both ends*** $(\boldsymbol{Q_{N3}/P_Y > 0.2})$ 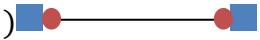

In this case both ends have been plastified and the corresponding force points lie in the first branch of the yield surface, where $Q_{N3}/P_Y > 0.2$ (Figure 3.7) .

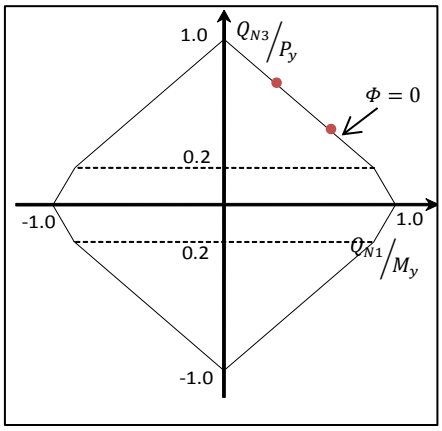


Figure 3.7 Force points of the plastic hinges lying in the first branch of the yield surface

Then, the incremental plastic deformations $dq_{N_i}^{pl}$ for each hinge are determined by the yield functions $f_1(dq_{N_1}, dq_{N_3}), f_2(dq_{N_2}, dq_{N_3})$ and the flow potentials $g_1(dq_{N_1}, dq_{N_3})$, $g_2(dq_{N_2}, dq_{N_3})$. The gradients of these functions, can be easily expressed in terms of natural forces $d\boldsymbol{Q_{N_i}}$ and combined in the following two by three matrices eq.(3.13)

$$\boldsymbol{F} = \begin{bmatrix} \frac{\partial f_1}{\partial Q_{N_1}} & \frac{\partial f_1}{\partial Q_{N_2}} & \frac{\partial f_1}{\partial Q_{N_3}} \\ \frac{\partial f_2}{\partial Q_{N_1}} & \frac{\partial f_2}{\partial Q_{N_2}} & \frac{\partial f_2}{\partial Q_{N_3}} \end{bmatrix}, \boldsymbol{G} = \begin{bmatrix} \frac{\partial g_1}{\partial Q_{N_1}} & \frac{\partial g_1}{\partial Q_{N_2}} & \frac{\partial g_1}{\partial Q_{N_3}} \\ \frac{\partial g_2}{\partial Q_{N_1}} & \frac{\partial g_2}{\partial Q_{N_2}} & \frac{\partial g_2}{\partial Q_{N_3}} \end{bmatrix} \quad (3.13)$$

However, taking into consideration that, the yield functions are in the first branch of the yield surface are (equation (3.1))

- For the right end : $\frac{8}{9} * \frac{Q_{N_1}}{M_y} + \frac{Q_{N_3}}{P_y} < 1.0$
- For the left end : $\frac{8}{9} * \frac{Q_{N_2}}{M_y} + \frac{Q_{N_3}}{P_y} < 1.0$

The equation (3.13) is transformed into

$$\boldsymbol{F} = \begin{bmatrix} \frac{\partial f_1}{\partial Q_{N_1}} & 0 & \frac{\partial f_1}{\partial Q_{N_3}} \\ 0 & \frac{\partial f_2}{\partial Q_{N_2}} & \frac{\partial f_2}{\partial Q_{N_3}} \end{bmatrix}, \boldsymbol{G} = \begin{bmatrix} \frac{\partial g_1}{\partial Q_{N_1}} & \frac{\partial g_1}{\partial Q_{N_2}} & \frac{\partial g_1}{\partial Q_{N_3}} \\ \frac{\partial g_2}{\partial Q_{N_1}} & \frac{\partial g_2}{\partial Q_{N_2}} & \frac{\partial g_2}{\partial Q_{N_3}} \end{bmatrix} \quad (3.14)$$

However, according to the associated flow rule, the plastic potential $g$ coincides with the yield function $f$, so the equation (3.14) turns to

$$\boldsymbol{F} = \begin{bmatrix} \frac{8}{9M_{y1}} & 0 & \frac{1}{P_{y1}} \\ 0 & \frac{8}{9M_{y2}} & \frac{1}{P_{y2}} \end{bmatrix} \quad and \quad \boldsymbol{G} = \begin{bmatrix} \frac{8}{9M_{y1}} & 0 & \frac{1}{P_{y1}} \\ 0 & \frac{8}{9M_{y2}} & \frac{1}{P_{y2}} \end{bmatrix} \quad (3.15)$$

In this notation the incremental plastic deformation is given by

$$d\boldsymbol{q}_{\boldsymbol{N}}^{\boldsymbol{pl}} = \boldsymbol{G}^T * \begin{bmatrix} \lambda_1 \\ \lambda_2 \end{bmatrix} \quad (3.16)$$

Where the plastic multipliers for active plastic hinges are denoted as $\lambda_1$and $\lambda_2$. The equilibrium force increment via elastic deformation increment is expressed as

$$d\boldsymbol{Q}_{\boldsymbol{N}} = \boldsymbol{K}_{\boldsymbol{N}}^{\boldsymbol{el}} * d\boldsymbol{q}_{\boldsymbol{N}}^{\boldsymbol{el}} \xrightarrow{eq.\ 3.12} d\boldsymbol{Q}_{\boldsymbol{N}} = \boldsymbol{K}_{\boldsymbol{N}}^{\boldsymbol{el}}\left(d\boldsymbol{q}_{\boldsymbol{N}} - d\boldsymbol{q}_{\boldsymbol{N}}^{\boldsymbol{pl}}\right) \xrightarrow{eq.\ 3.16}$$

$$d\boldsymbol{Q}_{\boldsymbol{N}} = \boldsymbol{K}_{\boldsymbol{N}}^{\boldsymbol{el}}(d\boldsymbol{q}_{\boldsymbol{N}} - \boldsymbol{G}^T * \begin{bmatrix} \lambda_1 \\ \lambda_2 \end{bmatrix}) \quad (3.17)$$

According to the consistency condition, on the new yield surfaces

$$f_1 + df_1 = 0 \xrightarrow{f_1=0} df_1 = 0 \rightarrow \frac{\partial f_1}{\partial \boldsymbol{Q}_{\boldsymbol{N}}} * d\boldsymbol{Q}_{\boldsymbol{N}} + \frac{\partial f_1}{\partial \boldsymbol{q}_{\boldsymbol{N,pl}}} * d\boldsymbol{q}_{\boldsymbol{N,pl}} = 0 \quad (3.18)$$

$$f_2 + df_2 = 0 \xrightarrow{f_2=0} df_2 = 0 \rightarrow \frac{\partial f_2}{\partial \boldsymbol{Q}_{\boldsymbol{N}}} * d\boldsymbol{Q}_{\boldsymbol{N}} + \frac{\partial f_2}{\partial \boldsymbol{q}_{\boldsymbol{N,pl}}} * d\boldsymbol{q}_{\boldsymbol{N,pl}} = 0 \quad (3.19)$$

Grouping equations (3.18) and (3.19), it turns out

$$\boldsymbol{F} * d\boldsymbol{Q_N} - \boldsymbol{H} * \begin{bmatrix}\lambda_1\\ \lambda_2\end{bmatrix} = \boldsymbol{0} \tag{3.20}$$

Where **H** is the diagonal matrix expressing the hardening law

$$\boldsymbol{H} = \begin{bmatrix}H_1 & 0\\ 0 & H_2\end{bmatrix} = \begin{bmatrix}\dfrac{\partial f_1}{\partial \lambda_1} & 0\\ 0 & \dfrac{\partial f_2}{\partial \lambda_2}\end{bmatrix} \tag{3.21}$$

For the left end, the incremental forces $d\boldsymbol{Q_N}$ is equal to

$$d\boldsymbol{Q_{Ni}} = \begin{bmatrix}qEI & 0\\ 0 & qEA\end{bmatrix} * \frac{d\boldsymbol{q_{Ni,pl}}}{l_{pl}}, i = 1{,}3 \tag{3.22}$$

The value of $H_1$ corresponds to the left end, according to [12] are calculated as follows

$$H_1 = \frac{1}{l_{pl}} * \begin{bmatrix}\dfrac{\partial f_1}{\partial Q_{N_1}} & \dfrac{\partial f_1}{\partial Q_{N_3}}\end{bmatrix} * \begin{bmatrix}qEI & 0\\ 0 & qEA\end{bmatrix} * \begin{bmatrix}\dfrac{\partial g_1}{\partial Q_{N_1}} & \dfrac{\partial g_1}{\partial Q_{N_3}}\end{bmatrix}^T \overset{eq\ 3.15}{\Longrightarrow}$$

$$H_1 = \frac{\dfrac{64\mathrm{EIq}}{81M_{Y1}^2} + \dfrac{\mathrm{AEq}}{P_{Y1}^2}}{l_{pl}} \tag{3.23}$$

Supposing that, the two ends have the same hardening modulus, an analogous procedure can be applied for the right end

$$d\boldsymbol{Q_{Ni}} = \begin{bmatrix}qEI & 0\\ 0 & qEA\end{bmatrix} * \frac{d\boldsymbol{q_{Ni,pl}}}{l_{pl}}, i = 2{,}3 \tag{3.24}$$

The value of $H_2$ corresponds to the right end, according to [12] are calculated as follows

$$H_2 = \frac{1}{l_{pl}} * \begin{bmatrix}\dfrac{\partial f_2}{\partial Q_{N_2}} & \dfrac{\partial f_2}{\partial Q_{N_3}}\end{bmatrix} * \begin{bmatrix}qEI & 0\\ 0 & qEA\end{bmatrix} * \begin{bmatrix}\dfrac{\partial g_2}{\partial Q_2} & \dfrac{\partial g_2}{\partial Q_{N_3}}\end{bmatrix}^T \overset{eq\ 3.15}{\Longrightarrow}$$

$$H_2 = \frac{\dfrac{64\mathrm{EIq}}{81M_{Y2}^2} + \dfrac{\mathrm{AEq}}{P_{Y2}^2}}{l_{pl}} \tag{3.25}$$

Where

- $l_{pl}$ corresponds to the length of the plastic hinge (in the current work is assumed equal to the 1% of the initial element's length)
- $q$ is the hardening modulus
- $M_{Y2}$ ,$M_{Y1}$, $P_{Y1}$and $P_{Y2}$ are the values of the moment of the yield surface corners (point A in Figure 3.5)

As a result the hardening matrix **H** can be written as

$$\boldsymbol{H} = \begin{bmatrix} \dfrac{\dfrac{64\mathrm{EIq}}{81M_{Y1}^2} + \dfrac{\mathrm{AEq}}{P_{Y1}^2}}{l_{pl}} & 0 \\ 0 & \dfrac{\dfrac{64\mathrm{EIq}}{81M_{Y2}^2} + \dfrac{\mathrm{AEq}}{P_{Y2}^2}}{l_{pl}} \end{bmatrix} \tag{3.26}$$

Additionally, combining the equations (3.17) and (3.20) the following block matrix equation appears

$$\begin{bmatrix} \boldsymbol{K_N^{el}}^{-1} & \boldsymbol{G}^T \\ \boldsymbol{F} & -\boldsymbol{H} \end{bmatrix} * \begin{bmatrix} d\boldsymbol{Q_N} \\ d\boldsymbol{\lambda} \end{bmatrix} = \begin{bmatrix} d\boldsymbol{q_N} \\ 0 \end{bmatrix} \tag{3.27}$$

Solving the equation (3.27), the $d\boldsymbol{\lambda}$ arises

$$\begin{bmatrix} \lambda_1 \\ \lambda_2 \end{bmatrix} = \left(\boldsymbol{H} + \boldsymbol{F}\boldsymbol{K_N^{el}}\boldsymbol{G^T}\right)^{-1}\boldsymbol{F}\boldsymbol{K_N^{el}}d\boldsymbol{q_N} \tag{3.28}$$

Due to the last equation(3.28), the relation (3.17) turns to

$$d\boldsymbol{Q_N} = \boldsymbol{K_N^{el}}\left(d\boldsymbol{q_N} - \boldsymbol{G}^T * \left(\boldsymbol{H} + \boldsymbol{F}\boldsymbol{K_N^{el}}\boldsymbol{G^T}\right)^{-1}\boldsymbol{F}\boldsymbol{K_N^{el}}d\boldsymbol{q_N}\right)$$

$$d\boldsymbol{Q_N} = \left(\boldsymbol{K_N^{el}} - \boldsymbol{K_N^{el}}\boldsymbol{G}^T * \left(\boldsymbol{H} + \boldsymbol{F}\boldsymbol{K_N^{el}}\boldsymbol{G^T}\right)^{-1}\boldsymbol{F}\boldsymbol{K_N^{el}}\right)d\boldsymbol{q_N} \tag{3.29}$$

The equation (3.29) reveals the elastoplastic stiffness because $\boldsymbol{K_N^{ep}} = \left(\boldsymbol{K_N^{el}} - \boldsymbol{K_N^{el}}\boldsymbol{G}^T * \left(\boldsymbol{H} + \boldsymbol{F}\boldsymbol{K_N^{el}}\boldsymbol{G^T}\right)^{-1}\boldsymbol{F}\boldsymbol{K_N^{el}}\right)$ and in this case is equal with

$$K_N^{ep}(1,1) = \frac{\begin{array}{c} EI(6561A^2Lq(Lq+2L_{\mathrm{pl}})M_{\mathrm{Y1}}^2M_{\mathrm{Y2}}^2S_1 + 4096LqI^2P_{\mathrm{Y1}}^2P_{\mathrm{Y2}}^2((Lq+L_{\mathrm{pl}})S_1^2 - L_{\mathrm{pl}}S_2^2) + \cdots \\ 5184AI(Lq+L_{\mathrm{pl}})(LqS_1(M_{\mathrm{Y2}}^2P_{\mathrm{Y1}}^2 + M_{\mathrm{Y1}}^2P_{\mathrm{Y2}}^2S_1) + L_{\mathrm{pl}}M_{\mathrm{Y1}}^2P_{\mathrm{Y2}}^2(S_1-S_2)(S_1+S_2))) \end{array}}{\begin{array}{c} L(6561A^2Lq(Lq+2L_{\mathrm{pl}})M_{\mathrm{Y1}}^2M_{\mathrm{Y2}}^2 + 5184AI(\left(Lq+L_{\mathrm{pl}}\right)\left(L_{\mathrm{pl}}(M_{\mathrm{Y2}}^2P_{\mathrm{Y1}}^2 + M_{\mathrm{Y1}}^2P_{\mathrm{Y2}}^2)S_1 + Lq(M_{\mathrm{Y2}}^2P_{\mathrm{Y1}}^2 + M_{\mathrm{Y1}}^2P_{\mathrm{Y2}}^2S_1)\right) - \cdots \\ 2L_{\mathrm{pl}}^2M_{\mathrm{Y1}}M_{\mathrm{Y2}}P_{\mathrm{Y1}}P_{\mathrm{Y2}}S_2) + 4096I^2P_{\mathrm{Y1}}^2P_{\mathrm{Y2}}^2((Lq+L_{\mathrm{pl}})S_1(Lq+L_{\mathrm{pl}}S_1) - L_{\mathrm{pl}}^2S_2^2)) \end{array}} \tag{3.30}$$

$$K_N^{ep}(1,2) = \frac{\begin{array}{c} EI(6561A^2Lq(Lq+2L_{\mathrm{pl}})M_{\mathrm{Y1}}^2M_{\mathrm{Y2}}^2S_2 + 4096L^2q^2I^2P_{\mathrm{Y1}}^2P_{\mathrm{Y2}}^2S_1S_2 + 5184AI(L_{\mathrm{pl}}^2M_{\mathrm{Y1}}M_{\mathrm{Y2}}P_{\mathrm{Y1}}P_{\mathrm{Y2}}S_1^2 + \cdots \\ Lq(Lq+L_{\mathrm{pl}})(M_{\mathrm{Y2}}^2P_{\mathrm{Y1}}^2 + M_{\mathrm{Y1}}^2P_{\mathrm{Y2}}^2S_1)S_2 - L_{\mathrm{pl}}^2M_{\mathrm{Y1}}M_{\mathrm{Y2}}P_{\mathrm{Y1}}P_{\mathrm{Y2}}S_2^2)) \end{array}}{\begin{array}{c} L(6561A^2Lq(Lq+2L_{\mathrm{pl}})M_{\mathrm{Y1}}^2M_{\mathrm{Y2}}^2 + 5184AI((Lq+L_{\mathrm{pl}})(L_{\mathrm{pl}}(M_{\mathrm{Y2}}^2P_{\mathrm{Y1}}^2 + M_{\mathrm{Y1}}^2P_{\mathrm{Y2}}^2)S_1 + Lq(M_{\mathrm{Y2}}^2P_{\mathrm{Y1}}^2 + M_{\mathrm{Y1}}^2P_{\mathrm{Y2}}^2S_1)) - \cdots \\ 2L_{\mathrm{pl}}^2M_{\mathrm{Y1}}M_{\mathrm{Y2}}P_{\mathrm{Y1}}P_{\mathrm{Y2}}S_2) + 4096I^2P_{\mathrm{Y1}}^2P_{\mathrm{Y2}}^2((Lq+L_{\mathrm{pl}})S_1(Lq+L_{\mathrm{pl}}S_1) - L_{\mathrm{pl}}^2S_2^2)) \end{array}} \tag{3.31}$$

$$K_N^{ep}(1,3) = -\frac{\begin{array}{c} 72AEIL_{\mathrm{pl}}(81ALqM_{\mathrm{Y1}}M_{\mathrm{Y2}}(M_{\mathrm{Y2}}P_{\mathrm{Y1}}S_1 + M_{\mathrm{Y1}}P_{\mathrm{Y2}}S_2) + 64IP_{\mathrm{Y1}}P_{\mathrm{Y2}}((Lq+\cdots \\ L_{\mathrm{pl}})M_{\mathrm{Y1}}P_{\mathrm{Y2}}S_1^2 + LqM_{\mathrm{Y2}}P_{\mathrm{Y1}}S_2 - L_{\mathrm{pl}}M_{\mathrm{Y1}}P_{\mathrm{Y2}}S_2^2)) \end{array}}{\begin{array}{c} L(6561A^2Lq(Lq+2L_{\mathrm{pl}})M_{\mathrm{Y1}}^2M_{\mathrm{Y2}}^2 + 5184AI((Lq+L_{\mathrm{pl}})(L_{\mathrm{pl}}(M_{\mathrm{Y2}}^2P_{\mathrm{Y1}}^2 + M_{\mathrm{Y1}}^2P_{\mathrm{Y2}}^2)S_1 + Lq(M_{\mathrm{Y2}}^2P_{\mathrm{Y1}}^2 + \cdots \\ M_{\mathrm{Y1}}^2P_{\mathrm{Y2}}^2S_1)) - 2L_{\mathrm{pl}}^2M_{\mathrm{Y1}}M_{\mathrm{Y2}}P_{\mathrm{Y1}}P_{\mathrm{Y2}}S_2) + 4096I^2P_{\mathrm{Y1}}^2P_{\mathrm{Y2}}^2((Lq+L_{\mathrm{pl}})S_1(Lq+L_{\mathrm{pl}}S_1) - L_{\mathrm{pl}}^2S_2^2)) \end{array}} \tag{3.32}$$

$$K_N^{ep}(2,2) = \frac{\begin{array}{c} EI(6561A^2Lq(Lq+2L_{\mathrm{pl}})M_{\mathrm{Y1}}^2M_{\mathrm{Y2}}^2S_1 + 4096LqI^2P_{\mathrm{Y1}}^2P_{\mathrm{Y2}}^2S_1(LqS_1 + L_{\mathrm{pl}}(S_1-S_2)(S_1+S_2)) + \cdots \\ 5184AI(Lq+L_{\mathrm{pl}})(LqS_1(M_{\mathrm{Y2}}^2P_{\mathrm{Y1}}^2 + M_{\mathrm{Y1}}^2P_{\mathrm{Y2}}^2S_1) + L_{\mathrm{pl}}M_{\mathrm{Y2}}^2P_{\mathrm{Y1}}^2(S_1-S_2)(S_1+S_2))) \end{array}}{\begin{array}{c} L(6561A^2Lq(Lq+2L_{\mathrm{pl}})M_{\mathrm{Y1}}^2M_{\mathrm{Y2}}^2 + 5184AI((Lq+L_{\mathrm{pl}})(L_{\mathrm{pl}}(M_{\mathrm{Y2}}^2P_{\mathrm{Y1}}^2 + M_{\mathrm{Y1}}^2P_{\mathrm{Y2}}^2)S_1 + \cdots \\ Lq(M_{\mathrm{Y2}}^2P_{\mathrm{Y1}}^2 + M_{\mathrm{Y1}}^2P_{\mathrm{Y2}}^2S_1)) - 2L_{\mathrm{pl}}^2M_{\mathrm{Y1}}M_{\mathrm{Y2}}P_{\mathrm{Y1}}P_{\mathrm{Y2}}S_2) + 4096I^2P_{\mathrm{Y1}}^2P_{\mathrm{Y2}}^2((Lq+L_{\mathrm{pl}})S_1(Lq+L_{\mathrm{pl}}S_1) - L_{\mathrm{pl}}^2S_2^2)) \end{array}} \tag{3.33}$$

$$K_N^{ep}(2,3) = -\frac{\begin{array}{c} 72AEIL_{\mathrm{pl}}(81ALqM_{\mathrm{Y1}}M_{\mathrm{Y2}}(M_{\mathrm{Y1}}P_{\mathrm{Y2}}S_1 + M_{\mathrm{Y2}}P_{\mathrm{Y1}}S_2) + \cdots \\ 64IP_{\mathrm{Y1}}P_{\mathrm{Y2}}(L_{\mathrm{pl}}M_{\mathrm{Y2}}P_{\mathrm{Y1}}(S_1-S_2)(S_1+S_2) + LqS_1(M_{\mathrm{Y2}}P_{\mathrm{Y1}} + M_{\mathrm{Y1}}P_{\mathrm{Y2}}S_2))) \end{array}}{\begin{array}{c} L(6561A^2Lq(Lq+2L_{\mathrm{pl}})M_{\mathrm{Y1}}^2M_{\mathrm{Y2}}^2 + 5184AI((Lq+L_{\mathrm{pl}})(L_{\mathrm{pl}}(M_{\mathrm{Y2}}^2P_{\mathrm{Y1}}^2 + M_{\mathrm{Y1}}^2P_{\mathrm{Y2}}^2)S_1 + \cdots \\ Lq(M_{\mathrm{Y2}}^2P_{\mathrm{Y1}}^2 + M_{\mathrm{Y1}}^2P_{\mathrm{Y2}}^2S_1)) - 2L_{\mathrm{pl}}^2M_{\mathrm{Y1}}M_{\mathrm{Y2}}P_{\mathrm{Y1}}P_{\mathrm{Y2}}S_2) + 4096I^2P_{\mathrm{Y1}}^2P_{\mathrm{Y2}}^2((Lq+L_{\mathrm{pl}})S_1(Lq+L_{\mathrm{pl}}S_1) - L_{\mathrm{pl}}^2S_2^2)) \end{array}} \tag{3.34}$$

$$K_N^{ep}(3,3) = \frac{\begin{array}{c} AE(6561A^2L^2q^2M_{Y1}^2M_{Y2}^2 + 5184ALqI(L_{pl}(M_{Y2}^2P_{Y1}^2 + M_{Y1}^2P_{Y2}^2)S_1 + \cdots \\ Lq(M_{Y2}^2P_{Y1}^2 + M_{Y1}^2P_{Y2}^2S_1)) + 4096I^2P_{Y1}^2P_{Y2}^2((Lq + L_{pl})S_1(Lq + L_{pl}S_1) - L_{pl}^2S_2^2)) \end{array}}{\begin{array}{c} L(6561A^2Lq(Lq + 2L_{pl})M_{Y1}^2M_{Y2}^2 + 5184AI((Lq + L_{pl})(L_{pl}(M_{Y2}^2P_{Y1}^2 + M_{Y1}^2P_{Y2}^2)S_1 + \cdots \\ Lq(M_{Y2}^2P_{Y1}^2 + M_{Y1}^2P_{Y2}^2S_1)) - 2L_{pl}^2M_{Y1}M_{Y2}P_{Y1}P_{Y2}S_2) + 4096I^2P_{Y1}^2P_{Y2}^2((Lq + L_{pl})S_1(Lq + L_{pl}S_1) - L_{pl}^2S_2^2)) \end{array}} \tag{3.35}$$

Regarding the incremental plastic deformations combining the equations (3.16) and (3.28)

$$dq_{N1}^{pl} = \frac{\begin{array}{c} 8L_{pl}P_{Y1}(9AM_{Y1}(81A\text{dqN3}LqM_{Y2}^2 + 64\text{dqN3}I(Lq + L_{pl})P_{Y2}^2S_1 - 72IL_{pl}M_{Y2}P_{Y2}(\text{dqN2}S_1 + \text{dqN1}S_2)) + 8IP_{Y1}(-72A\text{dqN3}L_{pl}M_{Y2}P_{Y2}S_2 + \cdots \\ 81A(Lq + L_{pl})M_{Y2}^2(\text{dqN1}S_1 + \text{dqN2}S_2) + 64IP_{Y2}^2(\text{dqN1}(Lq + L_{pl})S_1^2 + \text{dqN2}LqS_1S_2 - \text{dqN1}L_{pl}S_2^2))) \end{array}}{\begin{array}{c} 81AM_{Y1}^2\left(81ALq(Lq + 2L_{pl})M_{Y2}^2 + 64I(Lq + L_{pl})^2P_{Y2}^2S_1\right) - 10368AIL_{pl}^2M_{Y1}M_{Y2}P_{Y1}P_{Y2}S_264IP_{Y1}^2((Lq + \cdots \\ L_{pl})(Lq + L_{pl}S_1)(81AM_{Y2}^2 + 64IP_{Y2}^2S_1) - 64IL_{pl}^2P_{Y2}^2S_2^2) \end{array}}$$

$$dq_{n2}^{pl} = \frac{\begin{array}{c} 8L_{pl}P_{Y2}(64IP_{Y1}^2((Lq + L_{pl}S_1)(9A\text{dqN3}M_{Y2} + 8\text{dqN2}IP_{Y2}S_1) + 8\text{dqN1}LqIP_{Y2}S_2 - 8\text{dqN2}IL_{pl}P_{Y2}S_2^2) + \cdots \\ 81AM_{Y1}^2(9A\text{dqN3}LqM_{Y2} + 8I(Lq + L_{pl})P_{Y2}(\text{dqN2}S_1 + \text{dqN1}S_2)) - 72AIL_{pl}M_{Y1}P_{Y1}(8\text{dqN3}P_{Y2}S_2 + 9M_{Y2}(\text{dqN1}S_1 + \text{dqN2}S_2))) \end{array}}{\begin{array}{c} 81AM_{Y1}^2\left(81ALq(Lq + 2L_{pl})M_{Y2}^2 + 64I(Lq + L_{pl})^2P_{Y2}^2S_1\right) - 10368AIL_{pl}^2M_{Y1}M_{Y2}P_{Y1}P_{Y2}S_2 + \cdots \\ 64IP_{Y1}^2((Lq + L_{pl})(Lq + L_{pl}S_1)(81AM_{Y2}^2 + 64IP_{Y2}^2S_1) - 64IL_{pl}^2P_{Y2}^2S_2^2) \end{array}} \tag{3.37}$$

$$dq_{n3}^{pl} = \frac{\begin{array}{c} 18L_{pl}(32IM_{Y2}P_{Y1}^2((Lq+L_{pl}S_1)(9A\text{dqN3}M_{Y2}+8\text{dqN2}IP_{Y2}S_1)+8\text{dqN1}LqIP_{Y2}S_2-8\text{dqN2}IL_{pl}P_{Y2}S_2^2)+9AM_{Y1}^2(81A\text{dqN3}LqM_{Y2}^2+\cdots \\ 32\text{dqN3}I(Lq+L_{pl})P_{Y2}^2S_1+36LqIM_{Y2}P_{Y2}(\text{dqN2}S_1+\text{dqN1}S_2))+4IM_{Y1}P_{Y1}(-144A\text{dqN3}L_{pl}M_{Y2}P_{Y2}S_2+81ALqM_{Y2}^2(\text{dqN1}S_1+\text{dqN2}S_2)+\cdots \\ 64IP_{Y2}^2(\text{dqN1}(Lq+L_{pl})S_1^2+\text{dqN2}LqS_1S_2-\text{dqN1}L_{pl}S_2^2))) \end{array}}{\begin{array}{c} 81AM_{Y1}^2(81ALq(Lq+2L_{pl})M_{Y2}^2+64I(Lq+L_{pl})^2P_{Y2}^2S_1)-10368AIL_{pl}^2M_{Y1}M_{Y2}P_{Y1}P_{Y2}S_2+.64IP_{Y1}^2((Lq+\cdots \\ L_{pl})(Lq+L_{pl}S_1)(81AM_{Y2}^2+64IP_{Y2}^2S_1)-64IL_{pl}^2P_{Y2}^2S_2^2) \end{array}} \tag{3.38}$$

- ***Case 1.2 : Plastic hinge at both ends*** $(\boldsymbol{Q_{N3}/P_Y < 0.2})$

In this case both ends have been plastified and the corresponding force points lie in the second branch of the yield surface, where $Q_{N3}/P_Y < 0.2$ (Figure 3.8) .

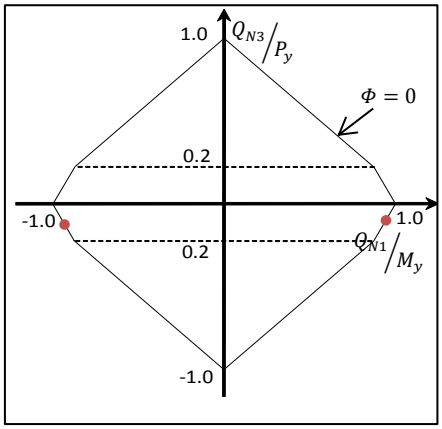


Figure 3.8 Force points of the plastic hinges lying in the second branch of the yield surface

Assuming, the force point lies on the second branch of the yield surface, the previous relations from (3.13) to (3.29) change in the following direction

$$\boldsymbol{F} = \begin{bmatrix} \frac{1}{M_y} & 0 & \frac{1}{2 * P_y} \\ 0 & \frac{1}{M_y} & \frac{1}{2 * P_y} \end{bmatrix} \quad and \quad \boldsymbol{G} = \begin{bmatrix} \frac{1}{M_y} & 0 & \frac{1}{2 * P_y} \\ 0 & \frac{1}{M_y} & \frac{1}{2 * P_y} \end{bmatrix} \tag{3.39}$$

$$\boldsymbol{H} = \begin{bmatrix} \frac{\frac{EIq}{M_{Y1}^2} + \frac{AEq}{4P_{Y1}^2}}{l_{pl}} & 0 \\ 0 & \frac{\frac{EIq}{M_{Y2}^2} + \frac{AEq}{4P_{Y2}^2}}{l_{pl}} \end{bmatrix} \tag{3.40}$$

The resulting for the elastoplastic stiffness matrix $\boldsymbol{K_N^{ep}}$ and the incremental plastic deformations, turn out to be

$$K_N^{ep}(1,1) = \frac{EI(A^2Lq(Lq+2L_{\mathrm{pl}})M_{\mathrm{Y1}}^2M_{\mathrm{Y2}}^2S_1 + 16LqI^2P_{\mathrm{Y1}}^2P_{\mathrm{Y2}}^2(LqS_1 + L_{\mathrm{pl}}(S_1 - \cdots \\ S_2)(S_1+S_2)) + 4AI(Lq+L_{\mathrm{pl}})(Lq(M_{\mathrm{Y2}}^2P_{\mathrm{Y1}}^2 + M_{\mathrm{Y1}}^2P_{\mathrm{Y2}}^2)S_1 + L_{\mathrm{pl}}M_{\mathrm{Y1}}^2P_{\mathrm{Y2}}^2(S_1-S_2)(S_1+S_2)))}{L(A^2Lq(Lq+2L_{\mathrm{pl}})M_{\mathrm{Y1}}^2M_{\mathrm{Y2}}^2 + 4AI((Lq+L_{\mathrm{pl}})(M_{\mathrm{Y2}}^2P_{\mathrm{Y1}}^2 + M_{\mathrm{Y1}}^2P_{\mathrm{Y2}}^2)(Lq+\cdots \\ L_{\mathrm{pl}}S_1) - 2L_{\mathrm{pl}}^2M_{\mathrm{Y1}}M_{\mathrm{Y2}}P_{\mathrm{Y1}}P_{\mathrm{Y2}}S_2) + 16I^2P_{\mathrm{Y1}}^2P_{\mathrm{Y2}}^2((Lq+L_{\mathrm{pl}}S_1)^2 - L_{\mathrm{pl}}^2S_2^2))} \tag{3.41}$$

$$K_N^{ep}(1,2) = \frac{EI(4AIL_{\mathrm{pl}}^2M_{\mathrm{Y1}}M_{\mathrm{Y2}}P_{\mathrm{Y1}}P_{\mathrm{Y2}}S_1^2 + Lq(A^2(Lq+2L_{\mathrm{pl}})M_{\mathrm{Y1}}^2M_{\mathrm{Y2}}^2 + 16LqI^2P_{\mathrm{Y1}}^2P_{\mathrm{Y2}}^2 + \cdots \\ 4AI(Lq+L_{\mathrm{pl}})(M_{\mathrm{Y2}}^2P_{\mathrm{Y1}}^2 + M_{\mathrm{Y1}}^2P_{\mathrm{Y2}}^2))S_2 - 4AIL_{\mathrm{pl}}^2M_{\mathrm{Y1}}M_{\mathrm{Y2}}P_{\mathrm{Y1}}P_{\mathrm{Y2}}S_2^2)}{L(A^2Lq(Lq+2L_{\mathrm{pl}})M_{\mathrm{Y1}}^2M_{\mathrm{Y2}}^2 + 4AI((Lq+L_{\mathrm{pl}})(M_{\mathrm{Y2}}^2P_{\mathrm{Y1}}^2 + M_{\mathrm{Y1}}^2P_{\mathrm{Y2}}^2)(Lq+\cdots \\ L_{\mathrm{pl}}S_1) - 2L_{\mathrm{pl}}^2M_{\mathrm{Y1}}M_{\mathrm{Y2}}P_{\mathrm{Y1}}P_{\mathrm{Y2}}S_2) + 16I^2P_{\mathrm{Y1}}^2P_{\mathrm{Y2}}^2((Lq+L_{\mathrm{pl}}S_1)^2 - L_{\mathrm{pl}}^2S_2^2))} \tag{3.42}$$

$$K_N^{ep}(1,3) = -\frac{2AEIL_{\mathrm{pl}}(ALqM_{\mathrm{Y1}}M_{\mathrm{Y2}}(M_{\mathrm{Y2}}P_{\mathrm{Y1}}S_1 + M_{\mathrm{Y1}}P_{\mathrm{Y2}}S_2) + \cdots \\ 4IP_{\mathrm{Y1}}P_{\mathrm{Y2}}(L_{\mathrm{pl}}M_{\mathrm{Y1}}P_{\mathrm{Y2}}(S_1-S_2)(S_1+S_2) + Lq(M_{\mathrm{Y1}}P_{\mathrm{Y2}}S_1 + M_{\mathrm{Y2}}P_{\mathrm{Y1}}S_2)))}{L(A^2Lq(Lq+2L_{\mathrm{pl}})M_{\mathrm{Y1}}^2M_{\mathrm{Y2}}^2 + 4AI((Lq+L_{\mathrm{pl}})(M_{\mathrm{Y2}}^2P_{\mathrm{Y1}}^2 + M_{\mathrm{Y1}}^2P_{\mathrm{Y2}}^2)(Lq+\cdots \\ L_{\mathrm{pl}}S_1) - 2L_{\mathrm{pl}}^2M_{\mathrm{Y1}}M_{\mathrm{Y2}}P_{\mathrm{Y1}}P_{\mathrm{Y2}}S_2) + 16I^2P_{\mathrm{Y1}}^2P_{\mathrm{Y2}}^2((Lq+L_{\mathrm{pl}}S_1)^2 - L_{\mathrm{pl}}^2S_2^2))} \tag{3.43}$$

$$K_N^{ep}(2,2) = \frac{EI(A^2Lq(Lq+2L_{\mathrm{pl}})M_{\mathrm{Y1}}^2M_{\mathrm{Y2}}^2S_1 + 16LqI^2P_{\mathrm{Y1}}^2P_{\mathrm{Y2}}^2(LqS_1 + L_{\mathrm{pl}}(S_1 - S_2)(S_1 + \cdots \\ S_2)) + 4AI(Lq+L_{\mathrm{pl}})(Lq(M_{\mathrm{Y2}}^2P_{\mathrm{Y1}}^2 + M_{\mathrm{Y1}}^2P_{\mathrm{Y2}}^2)S_1 + L_{\mathrm{pl}}M_{\mathrm{Y2}}^2P_{\mathrm{Y1}}^2(S_1-S_2)(S_1+S_2)))}{L(A^2Lq(Lq+2L_{\mathrm{pl}})M_{\mathrm{Y1}}^2M_{\mathrm{Y2}}^2 + 4AI((Lq+L_{\mathrm{pl}})(M_{\mathrm{Y2}}^2P_{\mathrm{Y1}}^2 + M_{\mathrm{Y1}}^2P_{\mathrm{Y2}}^2)(Lq+\cdots \\ L_{\mathrm{pl}}S_1) - 2L_{\mathrm{pl}}^2M_{\mathrm{Y1}}M_{\mathrm{Y2}}P_{\mathrm{Y1}}P_{\mathrm{Y2}}S_2) + 16I^2P_{\mathrm{Y1}}^2P_{\mathrm{Y2}}^2((Lq+L_{\mathrm{pl}}S_1)^2 - L_{\mathrm{pl}}^2S_2^2))} \tag{3.44}$$

$$K_N^{ep}(2,3) = -\frac{2AEIL_{\mathrm{pl}}(ALqM_{\mathrm{Y1}}M_{\mathrm{Y2}}(M_{\mathrm{Y1}}P_{\mathrm{Y2}}S_1 + M_{\mathrm{Y2}}P_{\mathrm{Y1}}S_2) + \cdots \\ 4IP_{\mathrm{Y1}}P_{\mathrm{Y2}}(L_{\mathrm{pl}}M_{\mathrm{Y2}}P_{\mathrm{Y1}}(S_1-S_2)(S_1+S_2) + Lq(M_{\mathrm{Y2}}P_{\mathrm{Y1}}S_1 + M_{\mathrm{Y1}}P_{\mathrm{Y2}}S_2)))}{L(A^2Lq(Lq+2L_{\mathrm{pl}})M_{\mathrm{Y1}}^2M_{\mathrm{Y2}}^2 + 4AI((Lq+L_{\mathrm{pl}})(M_{\mathrm{Y2}}^2P_{\mathrm{Y1}}^2 + M_{\mathrm{Y1}}^2P_{\mathrm{Y2}}^2)(Lq+\cdots \\ L_{\mathrm{pl}}S_1) - 2L_{\mathrm{pl}}^2M_{\mathrm{Y1}}M_{\mathrm{Y2}}P_{\mathrm{Y1}}P_{\mathrm{Y2}}S_2) + 16I^2P_{\mathrm{Y1}}^2P_{\mathrm{Y2}}^2((Lq+L_{\mathrm{pl}}S_1)^2 - L_{\mathrm{pl}}^2S_2^2))} \tag{3.45}$$

$$K_N^{ep}(3,3) = \frac{\begin{array}{c} AE(A^2L^2q^2M_{\mathrm{Y}1}^2M_{\mathrm{Y}2}^2 + 4ALqI(M_{\mathrm{Y}2}^2P_{\mathrm{Y}1}^2 + M_{\mathrm{Y}1}^2P_{\mathrm{Y}2}^2)(Lq + \cdots \\ L_{\mathrm{pl}}S_1) + 16I^2P_{\mathrm{Y}1}^2P_{\mathrm{Y}2}^2((Lq + L_{\mathrm{pl}}S_1)^2 - L_{\mathrm{pl}}^2S_2^2)) \end{array}}{\begin{array}{c} L(A^2Lq(Lq + 2L_{\mathrm{pl}})M_{\mathrm{Y}1}^2M_{\mathrm{Y}2}^2 + 4AI((Lq + L_{\mathrm{pl}})(M_{\mathrm{Y}2}^2P_{\mathrm{Y}1}^2 + M_{\mathrm{Y}1}^2P_{\mathrm{Y}2}^2)(Lq + \cdots \\ L_{\mathrm{pl}}S_1) - 2L_{\mathrm{pl}}^2M_{\mathrm{Y}1}M_{\mathrm{Y}2}P_{\mathrm{Y}1}P_{\mathrm{Y}2}S_2) + 16I^2P_{\mathrm{Y}1}^2P_{\mathrm{Y}2}^2((Lq + L_{\mathrm{pl}}S_1)^2 - L_{\mathrm{pl}}^2S_2^2)) \end{array}} \tag{3.46}$$

Regarding the incremental plastic deformations

$$dq_{N1}^{pl} = \frac{\begin{array}{c} 2L_{\mathrm{pl}}P_{\mathrm{Y}1}(A^2\mathrm{dqN3}LqM_{\mathrm{Y}1}M_{\mathrm{Y}2}^2 + 8I^2P_{\mathrm{Y}1}P_{\mathrm{Y}2}^2(\mathrm{dqN1}S_1(Lq + L_{\mathrm{pl}}S_1) + \mathrm{dqN2}LqS_2 - \mathrm{dqN1}L_{\mathrm{pl}}S_2^2) + 2AI(2\mathrm{dqN3}P_{\mathrm{Y}2}(LqM_{\mathrm{Y}1}P_{\mathrm{Y}2} + \cdots \\ L_{\mathrm{pl}}M_{\mathrm{Y}1}P_{\mathrm{Y}2}S_1 - L_{\mathrm{pl}}M_{\mathrm{Y}2}P_{\mathrm{Y}1}S_2) + M_{\mathrm{Y}2}(\mathrm{dqN1}(Lq + L_{\mathrm{pl}})M_{\mathrm{Y}2}P_{\mathrm{Y}1}S_1 - \mathrm{dqN2}L_{\mathrm{pl}}M_{\mathrm{Y}1}P_{\mathrm{Y}2}S_1 + \mathrm{dqN2}(Lq + L_{\mathrm{pl}})M_{\mathrm{Y}2}P_{\mathrm{Y}1}S_2 - \mathrm{dqN1}L_{\mathrm{pl}}M_{\mathrm{Y}1}P_{\mathrm{Y}2}S_2))) \end{array}}{\begin{array}{c} A^2Lq(Lq + 2L_{\mathrm{pl}})M_{\mathrm{Y}1}^2M_{\mathrm{Y}2}^2 + 4AI((Lq + L_{\mathrm{pl}})(M_{\mathrm{Y}2}^2P_{\mathrm{Y}1}^2 + M_{\mathrm{Y}1}^2P_{\mathrm{Y}2}^2)(Lq + L_{\mathrm{pl}}S_1) - \cdots \\ 2L_{\mathrm{pl}}^2M_{\mathrm{Y}1}M_{\mathrm{Y}2}P_{\mathrm{Y}1}P_{\mathrm{Y}2}S_2) + 16I^2P_{\mathrm{Y}1}^2P_{\mathrm{Y}2}^2((Lq + L_{\mathrm{pl}}S_1)^2 - L_{\mathrm{pl}}^2S_2^2) \end{array}} \tag{3.47}$$

$$dq_{N2}^{pl} = \frac{\begin{array}{c} 2L_{\mathrm{pl}}P_{\mathrm{Y}2}(A^2\mathrm{dqN3}LqM_{\mathrm{Y}1}^2M_{\mathrm{Y}2} + 8I^2P_{\mathrm{Y}1}^2P_{\mathrm{Y}2}(\mathrm{dqN2}S_1(Lq + L_{\mathrm{pl}}S_1) + \mathrm{dqN1}LqS_2 - \mathrm{dqN2}L_{\mathrm{pl}}S_2^2) + \cdots \\ 2AI(2\mathrm{dqN3}P_{\mathrm{Y}1}(LqM_{\mathrm{Y}2}P_{\mathrm{Y}1} + L_{\mathrm{pl}}M_{\mathrm{Y}2}P_{\mathrm{Y}1}S_1 - L_{\mathrm{pl}}M_{\mathrm{Y}1}P_{\mathrm{Y}2}S_2) + M_{\mathrm{Y}1}(-\mathrm{dqN1}L_{\mathrm{pl}}M_{\mathrm{Y}2}P_{\mathrm{Y}1}S_1 + \mathrm{dqN2}(Lq + L_{\mathrm{pl}})M_{\mathrm{Y}1}P_{\mathrm{Y}2}S_1 - \cdots \\ \mathrm{dqN2}L_{\mathrm{pl}}M_{\mathrm{Y}2}P_{\mathrm{Y}1}S_2 + \mathrm{dqN1}(Lq + L_{\mathrm{pl}})M_{\mathrm{Y}1}P_{\mathrm{Y}2}S_2))) \end{array}}{\begin{array}{c} A^2Lq(Lq + 2L_{\mathrm{pl}})M_{\mathrm{Y}1}^2M_{\mathrm{Y}2}^2 + 4AI((Lq + L_{\mathrm{pl}})(M_{\mathrm{Y}2}^2P_{\mathrm{Y}1}^2 + M_{\mathrm{Y}1}^2P_{\mathrm{Y}2}^2)(Lq + L_{\mathrm{pl}}S_1) - \cdots \\ 2L_{\mathrm{pl}}^2M_{\mathrm{Y}1}M_{\mathrm{Y}2}P_{\mathrm{Y}1}P_{\mathrm{Y}2}S_2) + 16I^2P_{\mathrm{Y}1}^2P_{\mathrm{Y}2}^2((Lq + L_{\mathrm{pl}}S_1)^2 - L_{\mathrm{pl}}^2S_2^2) \end{array}} \tag{3.48}$$

$$dq_{N3}^{pl} = \frac{\begin{array}{c} 2L_{\mathrm{pl}}(A^2\mathrm{dqN3}LqM_{\mathrm{Y}1}^2M_{\mathrm{Y}2}^2 + 4I^2P_{\mathrm{Y}1}P_{\mathrm{Y}2}((\mathrm{dqN2}M_{\mathrm{Y}2}P_{\mathrm{Y}1} + \mathrm{dqN1}M_{\mathrm{Y}1}P_{\mathrm{Y}2})S_1(Lq + L_{\mathrm{pl}}S_1) + Lq(\mathrm{dqN1}M_{\mathrm{Y}2}P_{\mathrm{Y}1} + \mathrm{dqN2}M_{\mathrm{Y}1}P_{\mathrm{Y}2})S_2 - \cdots \\ L_{\mathrm{pl}}(\mathrm{dqN2}M_{\mathrm{Y}2}P_{\mathrm{Y}1} + \mathrm{dqN1}M_{\mathrm{Y}1}P_{\mathrm{Y}2})S_2^2) + AI(2\mathrm{dqN3}(M_{\mathrm{Y}2}^2P_{\mathrm{Y}1}^2 + M_{\mathrm{Y}1}^2P_{\mathrm{Y}2}^2)(Lq + L_{\mathrm{pl}}S_1) - 4\mathrm{dqN3}L_{\mathrm{pl}}M_{\mathrm{Y}1}M_{\mathrm{Y}2}P_{\mathrm{Y}1}P_{\mathrm{Y}2}S_2 + \cdots \\ LqM_{\mathrm{Y}1}M_{\mathrm{Y}2}(\mathrm{dqN1}M_{\mathrm{Y}2}P_{\mathrm{Y}1}S_1 + \mathrm{dqN2}M_{\mathrm{Y}1}P_{\mathrm{Y}2}S_1 + \mathrm{dqN2}M_{\mathrm{Y}2}P_{\mathrm{Y}1}S_2 + \mathrm{dqN1}M_{\mathrm{Y}1}P_{\mathrm{Y}2}S_2))) \end{array}}{\begin{array}{c} A^2Lq(Lq + 2L_{\mathrm{pl}})M_{\mathrm{Y}1}^2M_{\mathrm{Y}2}^2 + 4AI((Lq + L_{\mathrm{pl}})(M_{\mathrm{Y}2}^2P_{\mathrm{Y}1}^2 + M_{\mathrm{Y}1}^2P_{\mathrm{Y}2}^2)(Lq + L_{\mathrm{pl}}S_1) - \cdots \\ 2L_{\mathrm{pl}}^2M_{\mathrm{Y}1}M_{\mathrm{Y}2}P_{\mathrm{Y}1}P_{\mathrm{Y}2}S_2) + 16I^2P_{\mathrm{Y}1}^2P_{\mathrm{Y}2}^2((Lq + L_{\mathrm{pl}}S_1)^2 - L_{\mathrm{pl}}^2S_2^2) \end{array}} \tag{3.49}$$

- ***Case 2.1 : Plastic hinge at left end*** $(\boldsymbol{Q_{N3}/P_Y < 0.2})$

Assuming that one plastic hinge has occurred at the left end and the force point lies on the second branch of the yield surface, the previous relations from (3.13) to (3.29) change in the following direction

$$\boldsymbol{F} = \begin{bmatrix} \frac{1}{M_y} & 0 & \frac{1}{2 * P_y} \\ 0 & 0 & 0 \end{bmatrix} \quad and \quad \boldsymbol{G} = \begin{bmatrix} \frac{1}{M_y} & 0 & \frac{1}{2 * P_y} \\ 0 & 0 & 0 \end{bmatrix} \tag{3.50}$$

$$d\boldsymbol{Q_N} = \boldsymbol{K_N^{el}}(d\boldsymbol{q_N} - \boldsymbol{G}^T * \begin{bmatrix} \lambda_1 \\ 0 \end{bmatrix}) \tag{3.51}$$

$$\boldsymbol{H} = \begin{bmatrix} H_1 & 0 \\ 0 & 0 \end{bmatrix} \tag{3.52}$$

$$\boldsymbol{H} = \begin{bmatrix} \frac{\mathrm{EIq}}{M_{Y1}^2} + \frac{\mathrm{AEq}}{4P_{Y1}^2} & 0 \\ \frac{}{l_{pl}} & \\ 0 & 0 \end{bmatrix} \tag{3.53}$$

The resulting for the elastoplastic stiffness matrix $\boldsymbol{K_N^{ep}}$ turns out to be

$$\begin{bmatrix} \frac{EI(A(Lq+L_{\mathrm{pl}})M_{\mathrm{Y1}}^2+4LqIP_{\mathrm{Y1}}^2)S_1}{L(A(Lq+L_{\mathrm{pl}})M_{\mathrm{Y1}}^2+4IP_{\mathrm{Y1}}^2(Lq+L_{\mathrm{pl}}S_1))} & \frac{EI(A(Lq+L_{\mathrm{pl}})M_{\mathrm{Y1}}^2+4LqIP_{\mathrm{Y1}}^2)S_2}{L(A(Lq+L_{\mathrm{pl}})M_{\mathrm{Y1}}^2+4IP_{\mathrm{Y1}}^2(Lq+L_{\mathrm{pl}}S_1))} & -\frac{2AEIL_{\mathrm{pl}}M_{\mathrm{Y1}}P_{\mathrm{Y1}}S_1}{L(A(Lq+L_{\mathrm{pl}})M_{\mathrm{Y1}}^2+4IP_{\mathrm{Y1}}^2(Lq+L_{\mathrm{pl}}S_1))} \\ \frac{EI(A(Lq+L_{\mathrm{pl}})M_{\mathrm{Y1}}^2+4LqIP_{\mathrm{Y1}}^2)S_2}{L(A(Lq+L_{\mathrm{pl}})M_{\mathrm{Y1}}^2+4IP_{\mathrm{Y1}}^2(Lq+L_{\mathrm{pl}}S_1))} & \frac{EI(S_1-\frac{4IL_{\mathrm{pl}}P_{\mathrm{Y1}}^2S_2^2}{A(Lq+L_{\mathrm{pl}})M_{\mathrm{Y1}}^2+4IP_{\mathrm{Y1}}^2(Lq+L_{\mathrm{pl}}S_1)})}{L} & -\frac{2AEIL_{\mathrm{pl}}M_{\mathrm{Y1}}P_{\mathrm{Y1}}S_2}{L(A(Lq+L_{\mathrm{pl}})M_{\mathrm{Y1}}^2+4IP_{\mathrm{Y1}}^2(Lq+L_{\mathrm{pl}}S_1))} \\ -\frac{2AEIL_{\mathrm{pl}}M_{\mathrm{Y1}}P_{\mathrm{Y1}}S_1}{L(A(Lq+L_{\mathrm{pl}})M_{\mathrm{Y1}}^2+4IP_{\mathrm{Y1}}^2(Lq+L_{\mathrm{pl}}S_1))} & -\frac{2AEIL_{\mathrm{pl}}M_{\mathrm{Y1}}P_{\mathrm{Y1}}S_2}{L(A(Lq+L_{\mathrm{pl}})M_{\mathrm{Y1}}^2+4IP_{\mathrm{Y1}}^2(Lq+L_{\mathrm{pl}}S_1))} & \frac{AE(ALqM_{\mathrm{Y1}}^2+4IP_{\mathrm{Y1}}^2(Lq+L_{\mathrm{pl}}S_1))}{L(A(Lq+L_{\mathrm{pl}})M_{\mathrm{Y1}}^2+4IP_{\mathrm{Y1}}^2(Lq+L_{\mathrm{pl}}S_1))} \end{bmatrix} \tag{3.54}$$

Regarding the incremental plastic deformations

$$dq_N^{pl} = \begin{bmatrix} \frac{2L_{\mathrm{pl}}P_{\mathrm{Y1}}(A\mathrm{dqN3}M_{\mathrm{Y1}} + 2IP_{\mathrm{Y1}}(\mathrm{dqN1}S_1 + \mathrm{dqN2}S_2))}{A(Lq + L_{\mathrm{pl}})M_{\mathrm{Y1}}^2 + 4IP_{\mathrm{Y1}}^2(Lq + L_{\mathrm{pl}}S_1)} \\ 0 \\ \frac{L_{\mathrm{pl}}M_{\mathrm{Y1}}(A\mathrm{dqN3}M_{\mathrm{Y1}} + 2IP_{\mathrm{Y1}}(\mathrm{dqN1}S_1 + \mathrm{dqN2}S_2))}{A(Lq + L_{\mathrm{pl}})M_{\mathrm{Y1}}^2 + 4IP_{\mathrm{Y1}}^2(Lq + L_{\mathrm{pl}}S_1)} \end{bmatrix} \tag{3.55}$$

- ***Case 2.2 : Plastic hinge at right ends*** $(\boldsymbol{Q_{N3}/P_Y > 0.2})$

Assuming that one plastic hinge has occurred at the left end and the force point lies on the first branch of the yield surface, the previous relations from (3.13) to (3.29) change in the following direction

$$\boldsymbol{F} = \begin{bmatrix} \frac{8}{9M_y} & 0 & \frac{1}{P_y} \\ 0 & 0 & 0 \end{bmatrix} \quad and \quad \boldsymbol{G} = \begin{bmatrix} \frac{8}{9M_y} & 0 & \frac{1}{P_y} \\ 0 & 0 & 0 \end{bmatrix} \tag{3.56}$$

$$d\boldsymbol{Q_N} = \boldsymbol{K_N^{el}}(d\boldsymbol{q_N} - \boldsymbol{G}^T * \begin{bmatrix} \lambda_1 \\ 0 \end{bmatrix}) \tag{3.57}$$

$$\boldsymbol{H} = \begin{bmatrix} H_1 & 0 \\ 0 & 0 \end{bmatrix} \tag{3.58}$$

$$\boldsymbol{H} = \begin{bmatrix} \frac{64\mathrm{EIq}}{81M_{Y1}^2} + \frac{\mathrm{AEq}}{P_{Y1}^2} & 0 \\ \frac{l_{pl}}{0} & 0 \end{bmatrix} \tag{3.59}$$

The resulting for the elastoplastic stiffness matrix $\boldsymbol{K_N^{ep}}$ turns out to be

$$\begin{bmatrix} \frac{EI(81A(Lq+L_{\mathrm{pl}})M_{\mathrm{Y1}}^2+64LqIP_{\mathrm{Y1}}^2)S_1}{L(81A(Lq+L_{\mathrm{pl}})M_{\mathrm{Y1}}^2+64IP_{\mathrm{Y1}}^2(Lq+L_{\mathrm{pl}}S_1))} & \frac{EI(81A(Lq+L_{\mathrm{pl}})M_{\mathrm{Y1}}^2+64LqIP_{\mathrm{Y1}}^2)S_2}{L(81A(Lq+L_{\mathrm{pl}})M_{\mathrm{Y1}}^2+64IP_{\mathrm{Y1}}^2(Lq+L_{\mathrm{pl}}S_1))} & -\frac{72AEIL_{\mathrm{pl}}M_{\mathrm{Y1}}P_{\mathrm{Y1}}S_1}{L(81A(Lq+L_{\mathrm{pl}})M_{\mathrm{Y1}}^2+64IP_{\mathrm{Y1}}^2(Lq+L_{\mathrm{pl}}S_1))} \\ \frac{EI(81A(Lq+L_{\mathrm{pl}})M_{\mathrm{Y1}}^2+64LqIP_{\mathrm{Y1}}^2)S_2}{L(81A(Lq+L_{\mathrm{pl}})M_{\mathrm{Y1}}^2+64IP_{\mathrm{Y1}}^2(Lq+L_{\mathrm{pl}}S_1))} & \frac{EI(S_1-\frac{64IL_{\mathrm{pl}}P_{\mathrm{Y1}}^2S_2^2}{81A(Lq+L_{\mathrm{pl}})M_{\mathrm{Y1}}^2+64IP_{\mathrm{Y1}}^2(Lq+L_{\mathrm{pl}}S_1)})}{L} & -\frac{72AEIL_{\mathrm{pl}}M_{\mathrm{Y1}}P_{\mathrm{Y1}}S_2}{L(81A(Lq+L_{\mathrm{pl}})M_{\mathrm{Y1}}^2+64IP_{\mathrm{Y1}}^2(Lq+L_{\mathrm{pl}}S_1))} \\ -\frac{72AEIL_{\mathrm{pl}}M_{\mathrm{Y1}}P_{\mathrm{Y1}}S_1}{L(81A(Lq+L_{\mathrm{pl}})M_{\mathrm{Y1}}^2+64IP_{\mathrm{Y1}}^2(Lq+L_{\mathrm{pl}}S_1))} & -\frac{72AEIL_{\mathrm{pl}}M_{\mathrm{Y1}}P_{\mathrm{Y1}}S_2}{L(81A(Lq+L_{\mathrm{pl}})M_{\mathrm{Y1}}^2+64IP_{\mathrm{Y1}}^2(Lq+L_{\mathrm{pl}}S_1))} & \frac{AE(81ALqM_{\mathrm{Y1}}^2+64IP_{\mathrm{Y1}}^2(Lq+L_{\mathrm{pl}}S_1))}{L(81A(Lq+L_{\mathrm{pl}})M_{\mathrm{Y1}}^2+64IP_{\mathrm{Y1}}^2(Lq+L_{\mathrm{pl}}S_1))} \end{bmatrix} \tag{3.60}$$

Regarding the incremental plastic deformations

$$dq_N^{pl} = \begin{bmatrix} \frac{8L_{\mathrm{pl}}P_{\mathrm{Y1}}(9A\mathrm{dqN3}M_{\mathrm{Y1}} + 8IP_{\mathrm{Y1}}(\mathrm{dqN1}S_1 + \mathrm{dqN2}S_2))}{81A(Lq + L_{\mathrm{pl}})M_{\mathrm{Y1}}^2 + 64IP_{\mathrm{Y1}}^2(Lq + L_{\mathrm{pl}}S_1)} \\ 0 \\ \frac{9L_{\mathrm{pl}}M_{\mathrm{Y1}}(9A\mathrm{dqN3}M_{\mathrm{Y1}} + 8IP_{\mathrm{Y1}}(\mathrm{dqN1}S_1 + \mathrm{dqN2}S_2))}{81A(Lq + L_{\mathrm{pl}})M_{\mathrm{Y1}}^2 + 64IP_{\mathrm{Y1}}^2(Lq + L_{\mathrm{pl}}S_1)} \end{bmatrix} \tag{3.61}$$

- ***Case 3.1 : Plastic hinge at right ends*** $(\boldsymbol{Q_{N3}/P_Y < 0.2})$

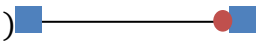

Assuming that one plastic hinge has occurred at the right end and the force point lies on the second branch of the yield surface, the previous relations from (3.13) to (3.29) change in the following direction

$$\boldsymbol{F} = \begin{bmatrix} 0 & 0 & 0 \\ 0 & \dfrac{1}{M_y} & \dfrac{1}{2 * P_y} \end{bmatrix} \quad and \quad \boldsymbol{G} = \begin{bmatrix} 0 & 0 & 0 \\ \dfrac{1}{M_y} & 0 & \dfrac{1}{2 * P_y} \end{bmatrix} \tag{3.62}$$

$$d\boldsymbol{Q_N} = \boldsymbol{K_N^{el}}(d\boldsymbol{q_N} - \boldsymbol{G}^T * \begin{bmatrix} 0 \\ \lambda_2 \end{bmatrix}) \tag{3.63}$$

$$\boldsymbol{H} = \begin{bmatrix} 0 & 0 \\ 0 & H_2 \end{bmatrix} \tag{3.64}$$

$$\boldsymbol{H} = \begin{bmatrix} 0 & 0 \\ 0 & \dfrac{\mathrm{EIq}}{M_{Y2}^2} + \dfrac{\mathrm{AEq}}{4P_{Y2}^2} \\ & l_{pl} \end{bmatrix} \tag{3.65}$$

The resulting for the elastoplastic stiffness matrix $\boldsymbol{K_N^{ep}}$ turns out to be

$$\begin{bmatrix} \dfrac{EI(S_1 - \frac{4IL_{\mathrm{pl}}P_{\mathrm{Y2}}^2S_2^2}{A(Lq+L_{\mathrm{pl}})M_{\mathrm{Y2}}^2+4IP_{\mathrm{Y2}}^2(Lq+L_{\mathrm{pl}}S_1)})}{L} & \dfrac{EI(A(Lq+L_{\mathrm{pl}})M_{\mathrm{Y2}}^2+4LqIP_{\mathrm{Y2}}^2)S_2}{L(A(Lq+L_{\mathrm{pl}})M_{\mathrm{Y2}}^2+4IP_{\mathrm{Y2}}^2(Lq+L_{\mathrm{pl}}S_1))} & -\dfrac{2AEIL_{\mathrm{pl}}M_{\mathrm{Y2}}P_{\mathrm{Y2}}S_2}{L(A(Lq+L_{\mathrm{pl}})M_{\mathrm{Y2}}^2+4IP_{\mathrm{Y2}}^2(Lq+L_{\mathrm{pl}}S_1))} \\ \dfrac{EI(A(Lq+L_{\mathrm{pl}})M_{\mathrm{Y2}}^2+4LqIP_{\mathrm{Y2}}^2)S_2}{L(A(Lq+L_{\mathrm{pl}})M_{\mathrm{Y2}}^2+4IP_{\mathrm{Y2}}^2(Lq+L_{\mathrm{pl}}S_1))} & \dfrac{EI(A(Lq+L_{\mathrm{pl}})M_{\mathrm{Y2}}^2+4LqIP_{\mathrm{Y2}}^2)S_1}{L(A(Lq+L_{\mathrm{pl}})M_{\mathrm{Y2}}^2+4IP_{\mathrm{Y2}}^2(Lq+L_{\mathrm{pl}}S_1))} & -\dfrac{2AEIL_{\mathrm{pl}}M_{\mathrm{Y2}}P_{\mathrm{Y2}}S_1}{L(A(Lq+L_{\mathrm{pl}})M_{\mathrm{Y2}}^2+4IP_{\mathrm{Y2}}^2(Lq+L_{\mathrm{pl}}S_1))} \\ -\dfrac{2AEIL_{\mathrm{pl}}M_{\mathrm{Y2}}P_{\mathrm{Y2}}S_2}{L(A(Lq+L_{\mathrm{pl}})M_{\mathrm{Y2}}^2+4IP_{\mathrm{Y2}}^2(Lq+L_{\mathrm{pl}}S_1))} & -\dfrac{2AEIL_{\mathrm{pl}}M_{\mathrm{Y2}}P_{\mathrm{Y2}}S_1}{L(A(Lq+L_{\mathrm{pl}})M_{\mathrm{Y2}}^2+4IP_{\mathrm{Y2}}^2(Lq+L_{\mathrm{pl}}S_1))} & \dfrac{AE(ALqM_{\mathrm{Y2}}^2+4IP_{\mathrm{Y2}}^2(Lq+L_{\mathrm{pl}}S_1))}{L(A(Lq+L_{\mathrm{pl}})M_{\mathrm{Y2}}^2+4IP_{\mathrm{Y2}}^2(Lq+L_{\mathrm{pl}}S_1))} \end{bmatrix} \tag{3.66}$$

Regarding the incremental plastic deformations

$$dq_N^{pl} = \begin{bmatrix} 0 \\ \dfrac{2L_{\mathrm{pl}}P_{\mathrm{Y2}}(A\mathrm{dqN3}M_{\mathrm{Y2}} + 2IP_{\mathrm{Y2}}(\mathrm{dqN2}S_1 + \mathrm{dqN1}S_2))}{A(Lq + L_{\mathrm{pl}})M_{\mathrm{Y2}}^2 + 4IP_{\mathrm{Y2}}^2(Lq + L_{\mathrm{pl}}S_1)} \\ \dfrac{L_{\mathrm{pl}}M_{\mathrm{Y2}}(A\mathrm{dqN3}M_{\mathrm{Y2}} + 2IP_{\mathrm{Y2}}(\mathrm{dqN2}S_1 + \mathrm{dqN1}S_2))}{A(Lq + L_{\mathrm{pl}})M_{\mathrm{Y2}}^2 + 4IP_{\mathrm{Y2}}^2(Lq + L_{\mathrm{pl}}S_1)} \end{bmatrix} \tag{3.67}$$

- ***Case 3.2 : Plastic hinge at both ends*** $(\boldsymbol{Q_{N3}/P_Y > 0.2})$

Assuming that one plastic hinge has occurred at the right end and the force point lies on the first branch of the yield surface, the previous relations from (3.13) to (3.29) change in the following direction.

$$\boldsymbol{F} = \begin{bmatrix} 0 & 0 & 0 \\ 0 & \dfrac{8}{9M_y} & \dfrac{1}{P_y} \end{bmatrix} \quad and \quad \boldsymbol{G} = \begin{bmatrix} 0 & 0 & 0 \\ 0 & \dfrac{8}{9M_y} & \dfrac{1}{P_y} \end{bmatrix} \tag{3.68}$$

$$d\boldsymbol{Q_N} = \boldsymbol{K_N^{el}}(d\boldsymbol{q_N} - \boldsymbol{G}^T * \begin{bmatrix} \boldsymbol{0} \\ \lambda_2 \end{bmatrix}) \tag{3.69}$$

$$\boldsymbol{H} = \begin{bmatrix} 0 & 0 \\ 0 & H_2 \end{bmatrix} \tag{3.70}$$

$$\boldsymbol{H} = \begin{bmatrix} 0 & 0 \\ 0 & \dfrac{\dfrac{64\mathrm{EIq}}{81M_{Y1}^2} + \dfrac{\mathrm{AEq}}{P_{Y1}^2}}{l_{pl}} \end{bmatrix} \tag{3.71}$$

The resulting for the elastoplastic stiffness matrix $\boldsymbol{K_N^{ep}}$ turns out to be

$$\begin{bmatrix} \dfrac{EI\left(S_1 - \dfrac{64IL_{\mathrm{pl}}P_{\mathrm{Y2}}^2S_2^2}{81A(Lq+L_{\mathrm{pl}})M_{\mathrm{Y2}}^2+64IP_{\mathrm{Y2}}^2(Lq+L_{\mathrm{pl}}S_1)}\right)}{L} & \dfrac{EI(81A(Lq+L_{\mathrm{pl}})M_{\mathrm{Y2}}^2+64LqIP_{\mathrm{Y2}}^2)S_2}{L(81A(Lq+L_{\mathrm{pl}})M_{\mathrm{Y2}}^2+64IP_{\mathrm{Y2}}^2(Lq+L_{\mathrm{pl}}S_1))} & -\dfrac{72AEIL_{\mathrm{pl}}M_{\mathrm{Y2}}P_{\mathrm{Y2}}S_2}{L(81A(Lq+L_{\mathrm{pl}})M_{\mathrm{Y2}}^2+64IP_{\mathrm{Y2}}^2(Lq+L_{\mathrm{pl}}S_1))} \\ \dfrac{EI(81A(Lq+L_{\mathrm{pl}})M_{\mathrm{Y2}}^2+64LqIP_{\mathrm{Y2}}^2)S_2}{L(81A(Lq+L_{\mathrm{pl}})M_{\mathrm{Y2}}^2+64IP_{\mathrm{Y2}}^2(Lq+L_{\mathrm{pl}}S_1))} & \dfrac{EI(81A(Lq+L_{\mathrm{pl}})M_{\mathrm{Y2}}^2+64LqIP_{\mathrm{Y2}}^2)S_1}{L(81A(Lq+L_{\mathrm{pl}})M_{\mathrm{Y2}}^2+64IP_{\mathrm{Y2}}^2(Lq+L_{\mathrm{pl}}S_1))} & -\dfrac{72AEIL_{\mathrm{pl}}M_{\mathrm{Y2}}P_{\mathrm{Y2}}S_1}{L(81A(Lq+L_{\mathrm{pl}})M_{\mathrm{Y2}}^2+64IP_{\mathrm{Y2}}^2(Lq+L_{\mathrm{pl}}S_1))} \\ -\dfrac{72AEIL_{\mathrm{pl}}M_{\mathrm{Y2}}P_{\mathrm{Y2}}S_2}{L(81A(Lq+L_{\mathrm{pl}})M_{\mathrm{Y2}}^2+64IP_{\mathrm{Y2}}^2(Lq+L_{\mathrm{pl}}S_1))} & -\dfrac{72AEIL_{\mathrm{pl}}M_{\mathrm{Y2}}P_{\mathrm{Y2}}S_1}{L(81A(Lq+L_{\mathrm{pl}})M_{\mathrm{Y2}}^2+64IP_{\mathrm{Y2}}^2(Lq+L_{\mathrm{pl}}S_1))} & \dfrac{AE(81ALqM_{\mathrm{Y2}}^2+64IP_{\mathrm{Y2}}^2(Lq+L_{\mathrm{pl}}S_1))}{L(81A(Lq+L_{\mathrm{pl}})M_{\mathrm{Y2}}^2+64IP_{\mathrm{Y2}}^2(Lq+L_{\mathrm{pl}}S_1))} \end{bmatrix} \tag{3.72}$$

Regarding the incremental plastic deformations

$$dq_N^{pl} = \begin{bmatrix} 0 \\ \dfrac{8L_{\mathrm{pl}}P_{\mathrm{Y2}}(9A\mathrm{dqN3}M_{\mathrm{Y2}} + 8IP_{\mathrm{Y2}}(\mathrm{dqN2}S_1 + \mathrm{dqN1}S_2))}{81A(Lq+L_{\mathrm{pl}})M_{\mathrm{Y2}}^2 + 64IP_{\mathrm{Y2}}^2(Lq+L_{\mathrm{pl}}S_1)} \\ \dfrac{9L_{\mathrm{pl}}M_{\mathrm{Y2}}(9A\mathrm{dqN3}M_{\mathrm{Y2}} + 8IP_{\mathrm{Y2}}(\mathrm{dqN2}S_1 + \mathrm{dqN1}S_2))}{81A(Lq+L_{\mathrm{pl}})M_{\mathrm{Y2}}^2 + 64IP_{\mathrm{Y2}}^2(Lq+L_{\mathrm{pl}}S_1)} \end{bmatrix} \tag{3.73}$$

# 4. Numerical strategies for analysis

Significant numerical issues raised while the current computer code was developed. Towards this direction the return mapping algorithms were combined with the hardening/softening behavior.

## 4.1. Load increment control and new plastic hinge formation

In case a force point has exceeded the yield surface (line A-C-B), a correction must take place. This may be done in a direction parallel to the bending moment axis [2] (Figure 4.1(a)). Alternatively, it has been suggested [13] that the analysis should restart from the last equilibrium step (point A) and converge to point C using repeatedly the bisection method (Figure 4.1(b)).

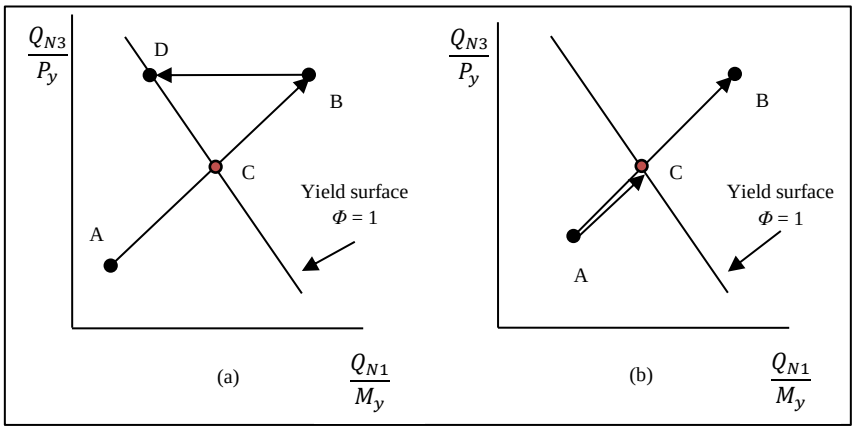


Figure 4.1 Alternative corrections back on the yield surface

The first strategy is less accurate than the second one, but is more efficient, especially when two or more new plastic hinges open in the same iteration. Thus the first strategy was implemented in the present work. If B is located close to C, the discrepancy of choosing D instead of C can be accepted, as long as, an overshooting tolerance around 1% is used. If point B is not located near C the analysis restarts from the equilibrium point A with a new $\Delta l$. In this case, the $\Delta l$ value is multiplied by the fraction (AC)/(AB). If the value of this fraction is greater than 0.9, meaning that points C and B are close to each other, the value of $\Delta l$ is multiplied by 0.01. This methodology avoids unnecessary iterations and proves to be very stable, even in cases where more than one plastic hinges form in the same iteration.

Although in an incremental inelastic analysis, only one plastic hinge should occur per iteration, in practice this condition may not always be met. In the present work, a

plastic tolerance of about 0.5%, as an acceptance area, is allowed. All plastic hinges should lie inside this area. If this condition is not satisfied, the analysis will restart with a decreased $\Delta l$. For example, let us suppose that three plastic hinges open together and all force points are located outside the acceptance area (Figure 4.2). Then the following procedure is followed

- The plastic hinge, with the greater value (AC), is selected (P.H.3 in Figure 4.2)
- The corresponding ratio (AC)/(AB) is calculated for the selected hinge
- The $\Delta l$ value is updated through its multiplication by this ratio
- The analysis restarts form the last equilibrium point with updated $\Delta l$ value and the analysis restarts from the last saved step.

As a result, the P.H.3 does not open. As long as the other two plastic hinges do open, a similar procedure is repeated, so that only one plastic hinge finally remains. A possible scenario for the formation of plastic hinge after each restart is described in Figure 4.2

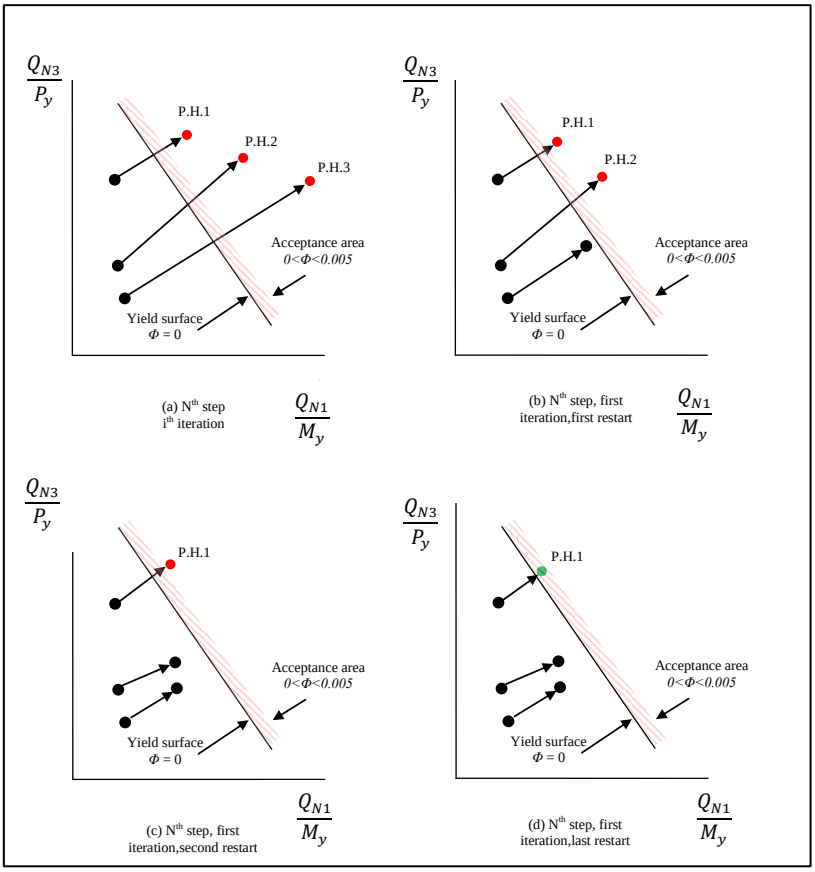


Figure 4.2 Treatment of plastic hinges

## 4.2. Corrections for elastic perfectly plastic material

As presented in the previous section, when plastic hinge occurs ,the force point should lie on the yield surface (Figure 4.3(a)). This correction is also needed, when an already formed plastic hinge continues rotating. Thus, the correction takes place also parallel to the bending moment axis (point C) (Figure 4.3(b) ).

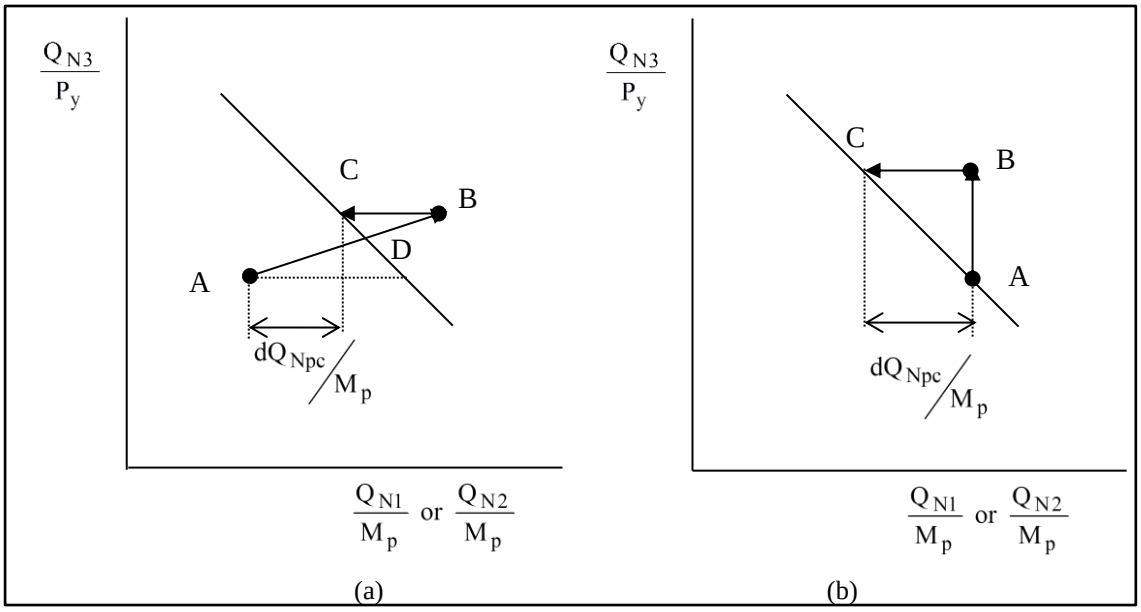


Figure 4.3 Correction back on the yield surface (a) from an elastic point, (b) from an already yielded point. $P_y$ and $M_p$ are the ultimate axial and bending moment capacities of the cross section

## 4.3. Corrections with hardening/softening effect

Similar problems arise when the hardening phenomenon is considered. In this case the required corrections are the following

- **Correction back to the initial yield surface:** When a plastic hinge opens, the force point moves from the elastic domain to the inelastic one. Thus before applying the equations of hardening, one has to return this point on the initial yield surface which has been exceeded. This return takes place as presented in section 4.1.
- **Correction back to the expanded yield surface:** Let an already formed plastic hinge, which is expressed by a force point located at point A (Figure 4.4). Applying an incremental load, the force point moves to point B. In this increment both plastic axial deformation and plastic rotation are developed (see section 3.2.2). The internal forces should obey the material's constitutive laws regarding moment-plastic rotations and axial force-axial plastic

deformation. Thus a correction is needed towards this direction as described in Figure 4.4. As a result, the internal forces decrease, the force point finally lies on C and the new yield surface is calculated.

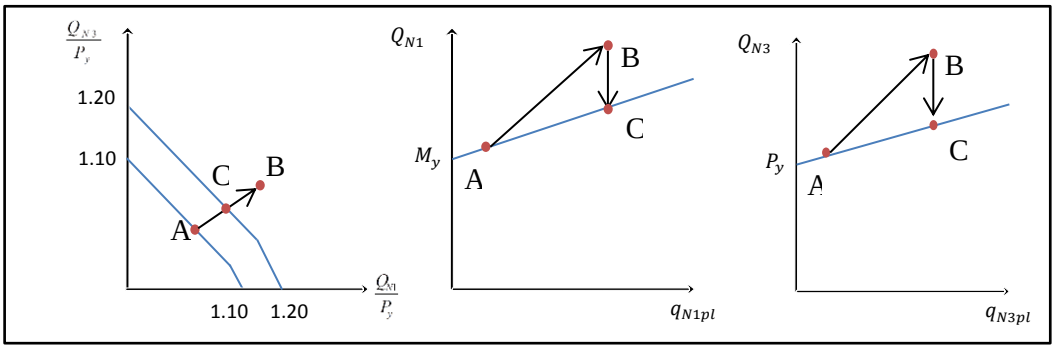


Figure 4.4 Correction back to expanded yield surface, due to large displacements

- **<u>Calculation of the expanded yield surface limits:</u>** Continuing from the procedure described above (point C in Figure 4.4), the new yield surface limits are calculated. Initially, it is identified whether the force point C remains on the same branch of the yield surface or not. A simple algorithm is used for this purpose :
  - The line O-D is defined (Figure 4.5), which is given by the function

$$Q_{N3,OD}(Q_{N1}) = a * Q_{N1} \tag{4.1}$$

  - The value $Q_{N1,C}$ is already known, so the value $Q_{N3,OD}(Q_{N1,C})$ is calculated (4.1).
  - Compare the two values
    - if $Q_{N3,OD}(Q_{N1,C}) > Q_{N3,C}$ the point C is located at the lower branch
    - if $Q_{N3,OD}(Q_{N1,C}) < Q_{N3,C}$ the point C is located at the upper branch

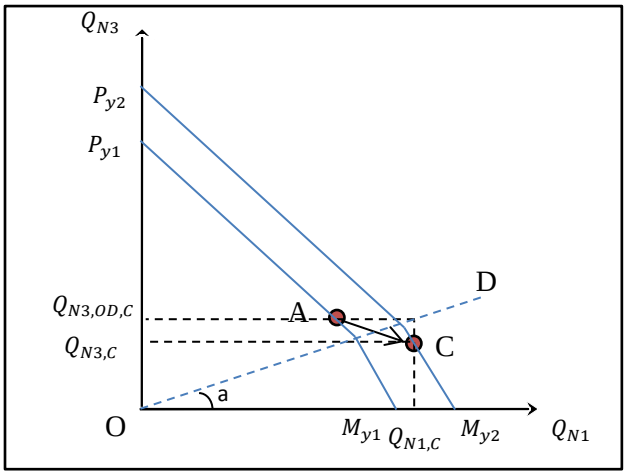


Figure 4.5 Moving form yield surface to another

In case point C is located in the upper branch, the next steps are proposed (Figure 4.6) .

- The line that includes point C, is drawn parallel to the previous yield surface
- The value $P_{cy}$ is thus calculated
- The other branch is drawn, knowing $M_{yc} = \frac{P_{cy}}{P_{y1}} * M_{y1}$

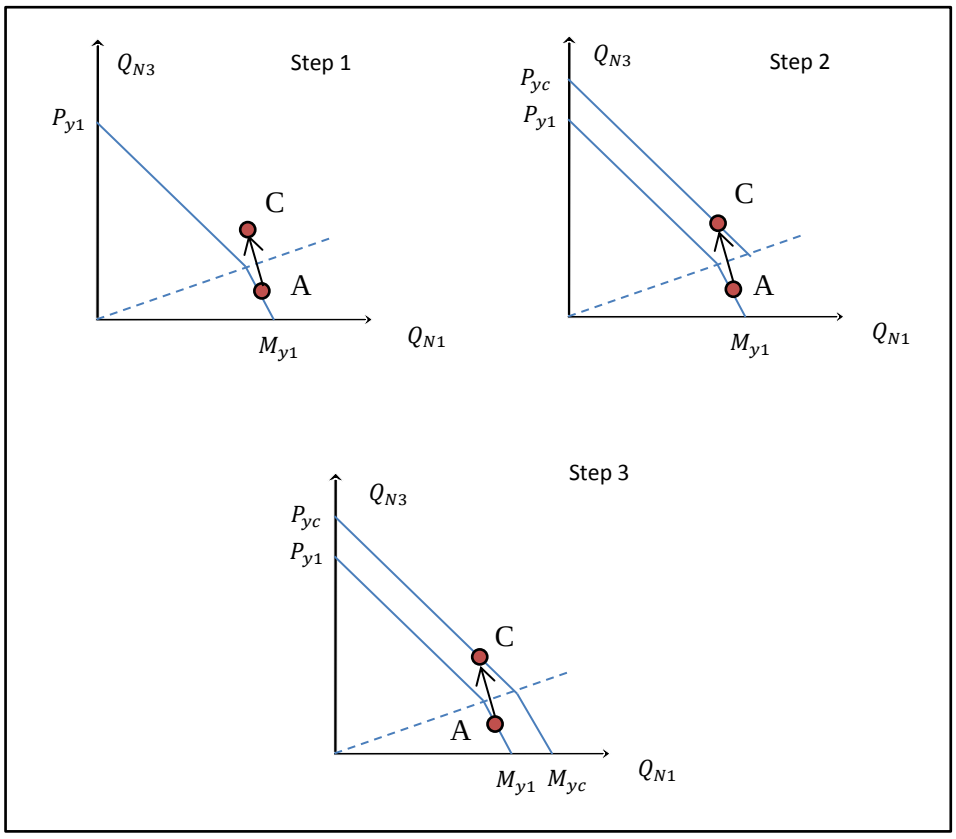


Figure 4.6 Calculation of the expanded yield surface (case 1)

In a similar way, if point C is found in the lower branch as shown in the (Figure 4.7), the previous steps are modified.

- The branch that includes point C, is drawn parallel to the previous yield surface
- The value $M_{cy}$ is calculated
- The other branch is drawn, knowing $P_{cy} = \frac{M_{cy}}{M_{y1}} * P_{y1}$

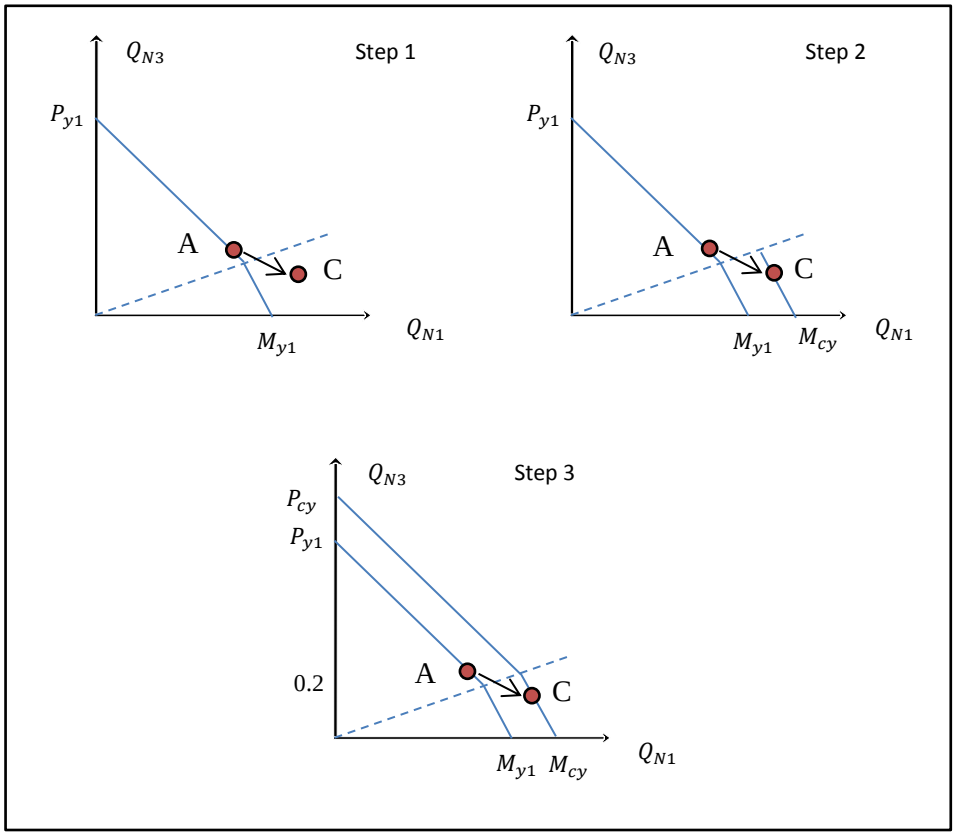


Figure 4.7 Calculation of the expanded yield surface (case 2)

The above described strategy could be briefly presented in the following flowchart

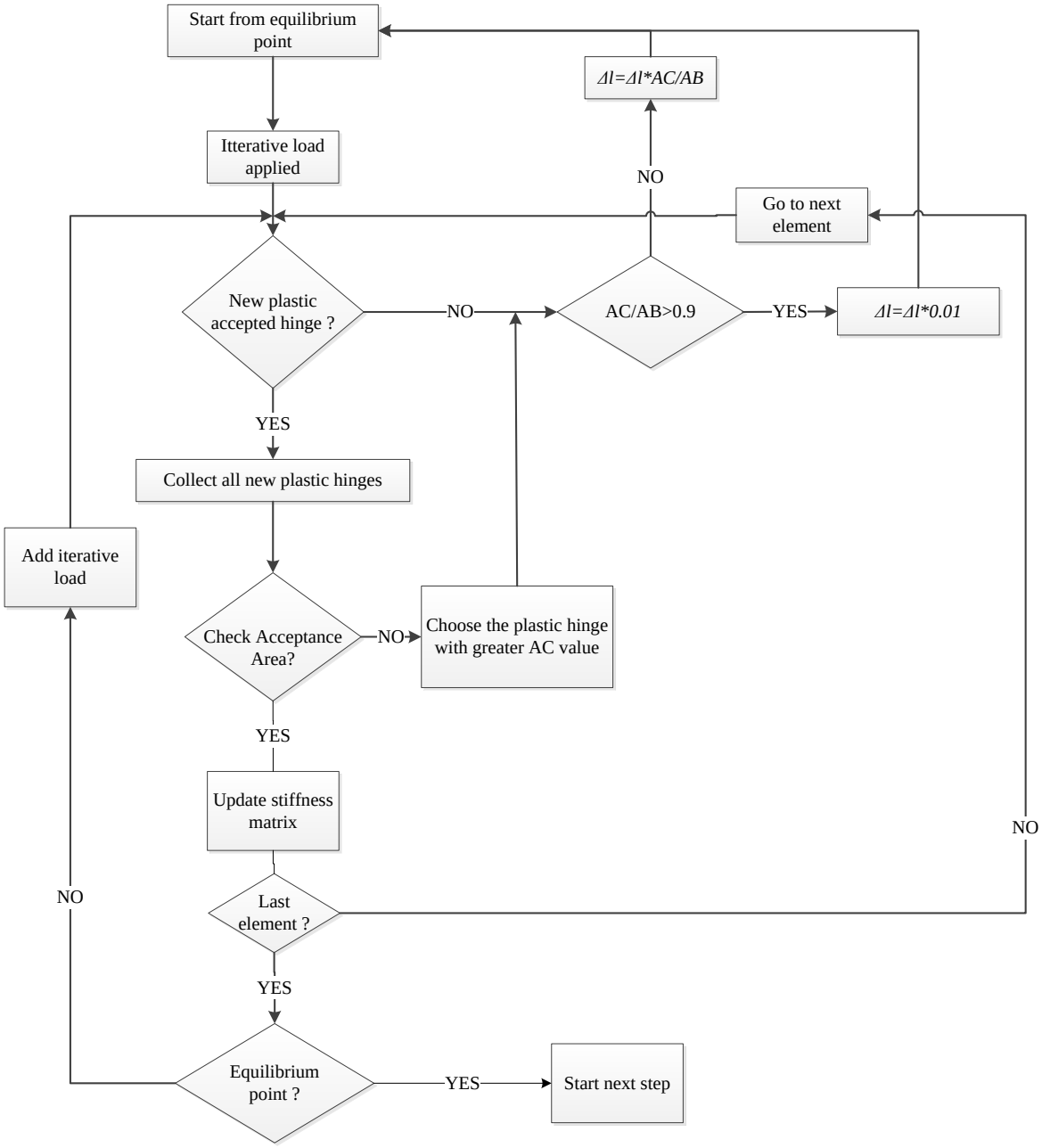


Figure 4.8 Strategy for the acceptance of new plastic hinges, these steps are followed form all elements

Regarding the procedure that takes place when an already formed plastic hinge continues rotating, the next flowchart describes shortly how the code is written.

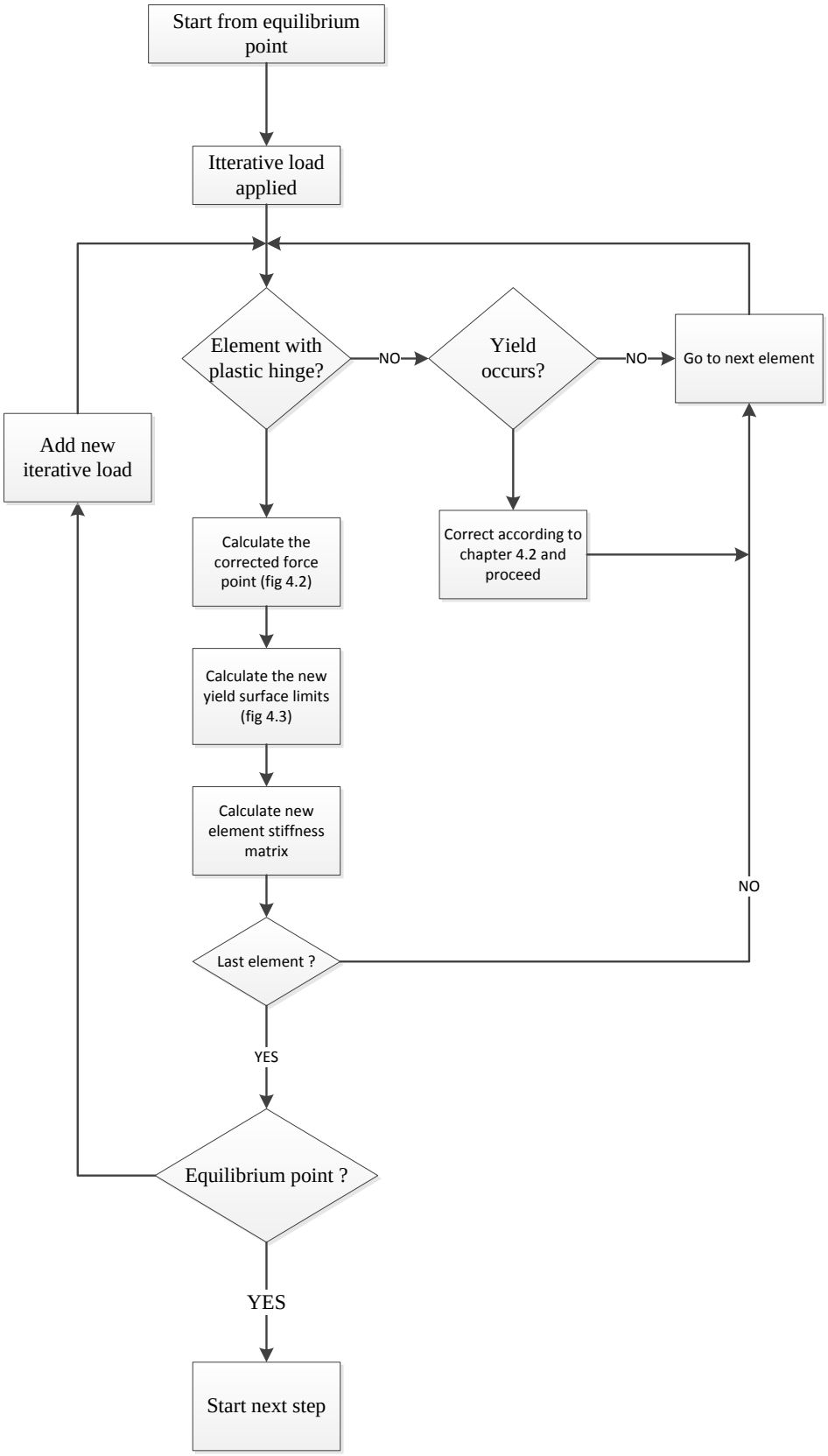


Figure 4.9 Flowchart for the considering of hardening/softening effect

## 4.3 Plastic hinges at common node

Another important issue, is the formation of plastic hinges at common node (Figure 4.10). Plastic hinges may occur at a common node, adjoining two or more elements. If all possible plastic hinges form around a node, its rotational stiffness will drop to zero. As a result, when assembling the global stiffness matrix in an upper triangular form, the column, associated with the specific rotational degree of freedom, will have zero elements. So the stiffness matrix cannot be inverted and the analysis will stop. This may be avoided, by condensing the rotational degrees of freedom of the adjoining elements. However, following this technique requires a continuous monitoring of the active degrees of freedom, something which is computationally cumbersome. Instead, we fix the rotational degree of freedom of the node, by giving a large value to the zero diagonal element of the global stiffness matrix (one hundred times the largest element of the stiffness matrix proves sufficient).

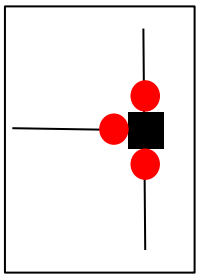

Figure 4.10 Plastic hinges at common node

## 5. Non-holonomic behavior

As already mentioned, an incremental large displacement inelastic analysis represents the more realistic response of a structure. Such an analysis should take into consideration the existence of non-holonomic behavior; otherwise, the traced equilibrium path is totally different from the expected one. Non-holonomic behavior refers to whether an already formed plastic hinge will become elastic (plastic unstressing).

In case of elastic perfectly plastic material, it is expressed by the product of the incremental plastic rotation with the current moment. If this product is negative, the two vectors will not have the same direction and the hinge will unload.

$$dq_{Ni}^{pl} * Q_{Ni} < 0, \qquad i = 1,2 \tag{5.1}$$

In case of elastic plastic material with softening/hardening effect, one should take into account both the axial plastic deformation and the plastic rotation. As a result the plastic unstressing condition should be modified :

- For plastic hinge at the left end

$$dq_{N1}^{pl} * Q_{N1} + dq_{N3}^{pl} * Q_{N3} < 0 \tag{5.2}$$

- For plastic hinge at the right end

$$dq_{N2}^{pl} * Q_2 + dq_{N3}^{pl} * Q_{N3} < 0 \tag{5.3}$$

If this phenomenon is neglected, the analysis traces a totally different equilibrium path which ends up to a wrong limit state. In order to take into account the non-holonomic behaviour, in the end of each iterative step a simple check is required. For each element the product of equation (5.1) is calculated and is decided whether the hinge closes or not. In case it does, the stiffness local matrix is transformed to its elastic formulation (equation 2.17) and the iterative plastic rotation is equal to zero.

The exact way unloading occurs in case of elastic perfectly plastic material, is presented in the following flowcharts.

- For an element with one plastic hinge at the left end 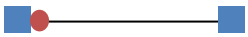

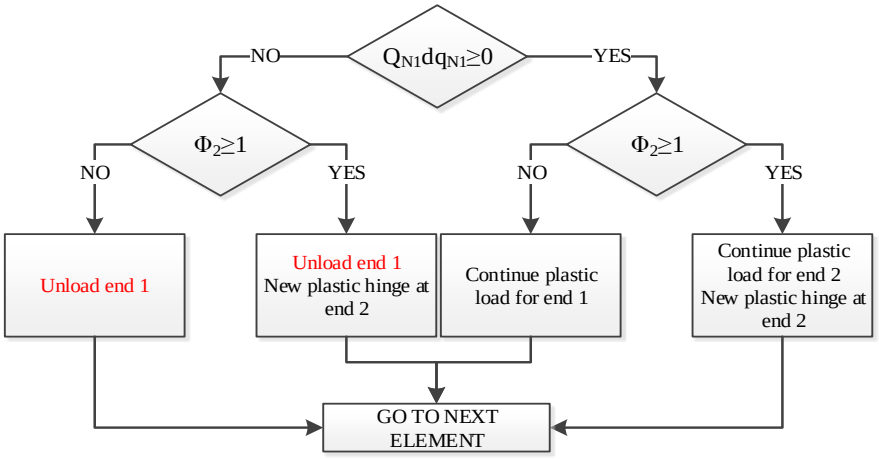


Figure 5.1 : Flow chart of unloading, for an element with one plastic hinge at the left end

- For an element with one plastic hinge at the right end 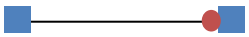

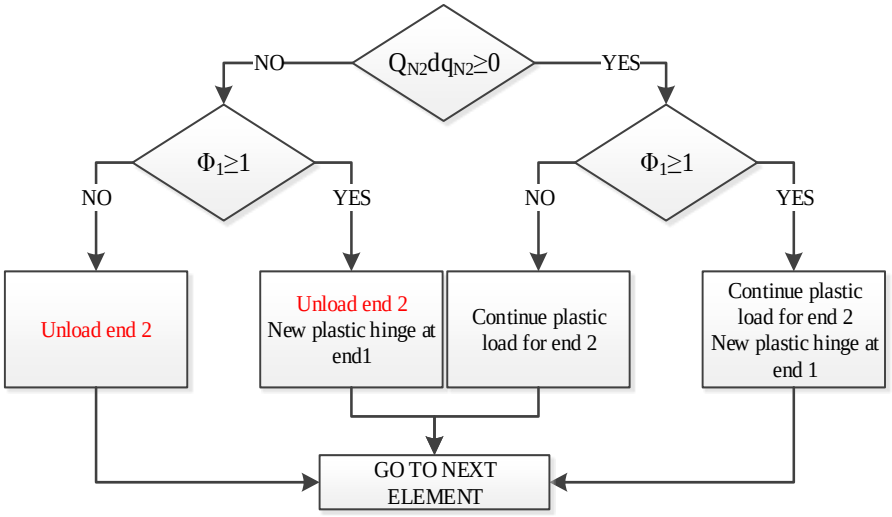


Figure 5.2 : Flow chart of unloading, for an element with one plastic hinge at the right end

- For an element with two plastic hinges 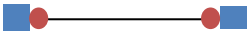

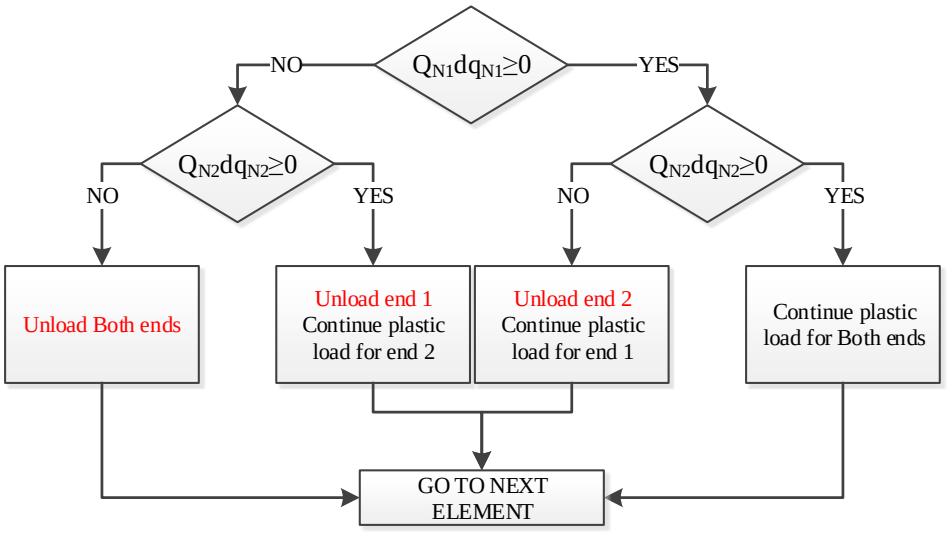


Figure 5.3 Flow chart of unloading, for an element with one plastic hinge at both ends

Regarding all the flowcharts presented, the Φ value corresponds to the yield function for the specific node. As far as the hardening effect, the procedure may be modified as follows

- For an element with one plastic hinge at the left end 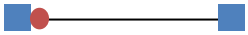

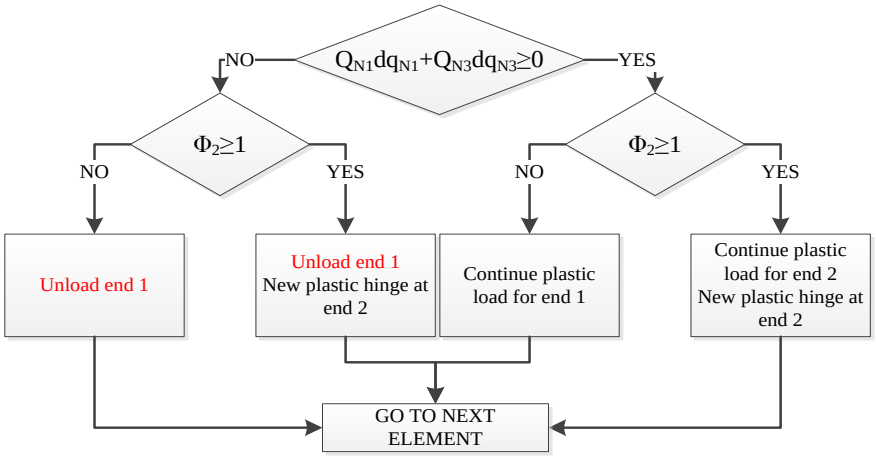


Figure 5.4 : Flow chart of unloading, for an element with one plastic hinge at the left end

- For an element with one plastic hinge at the right end 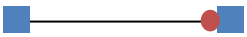

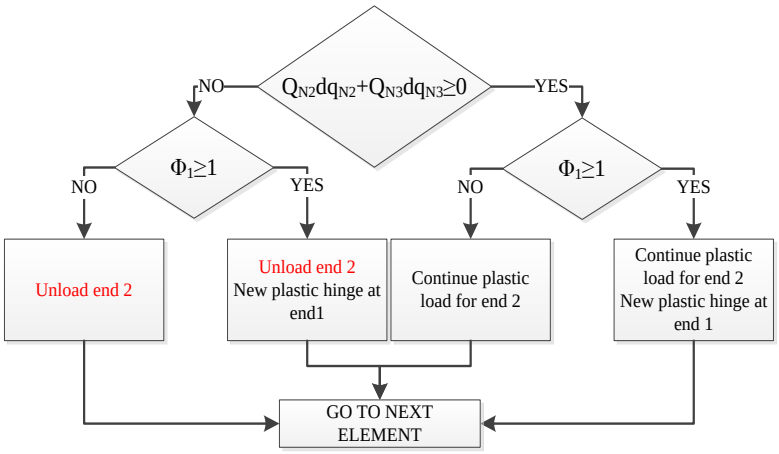


Figure 5.5 : Flow chart of unloading, for an element with one plastic hinge at the right end

- For an element with two plastic hinges 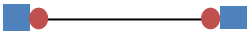

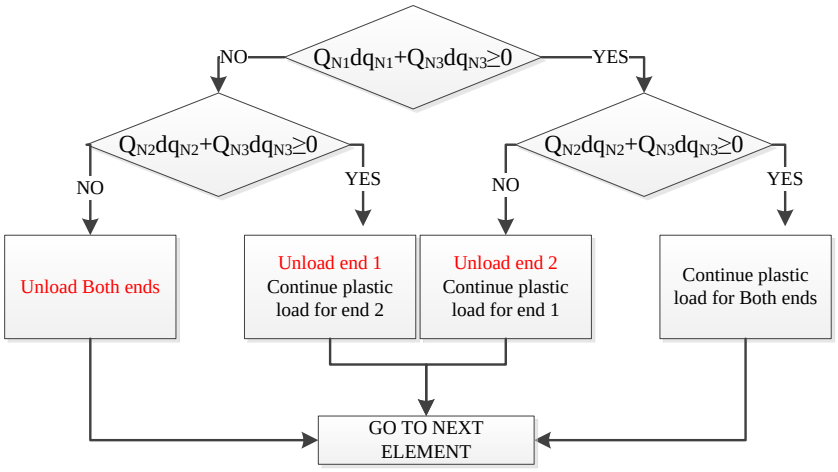


Figure 5.6 Flow chart of unloading, for an element with one plastic hinge at both ends

# 6. Graphics Interface

Apart from the main program that was developed in Fortran 2008, it turned out that the development of a second software, playing the role of graphics interface, could be very useful. Thus another program developed in visual basic 2008, which performs the following functions

- Creates/Loads input files
- Calls the solver
- Displays the result

## 6.1. Create the structure

By double clicking the shortcut on the desktop the following image arises

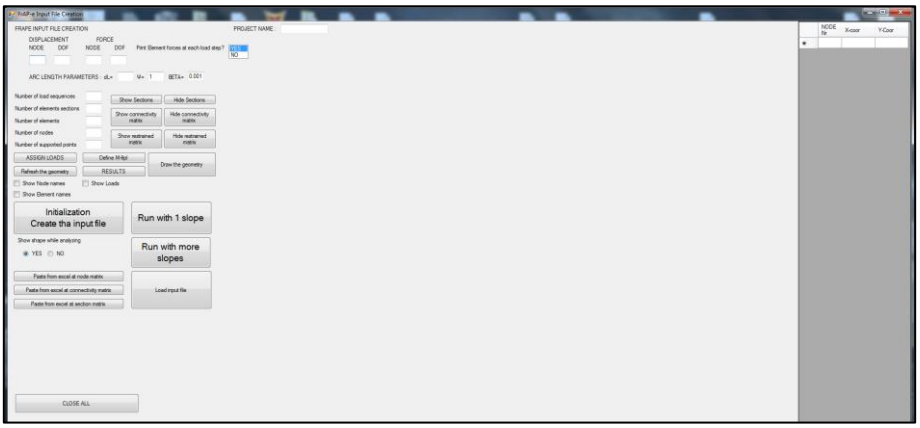


Figure 6.1 Main window

The problem may be defined as follows

1. Using the table ,which is located in the upper right corner, the coordinated of the nodes are defined. For example, let the problem 6.3 (Figure 6.2)

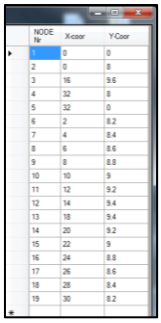


Figure 6.2 Node coordinates matrix

2. Click on the “Show sections” and the section definition matrix arises

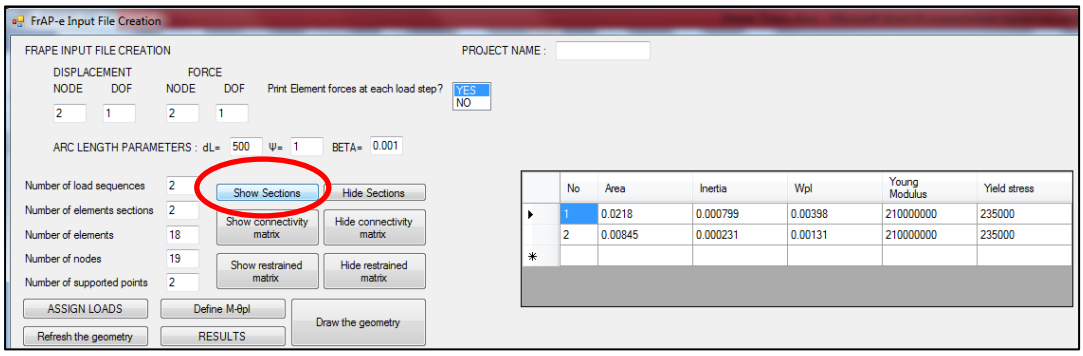


Figure 6.3 Section Definition matrix

3. Click on the “Draw the geometry” and another form appears. The nodes are then drawn and the user

   - Selects the proper section from the defined ones
   - Draws the connectivity from node to node

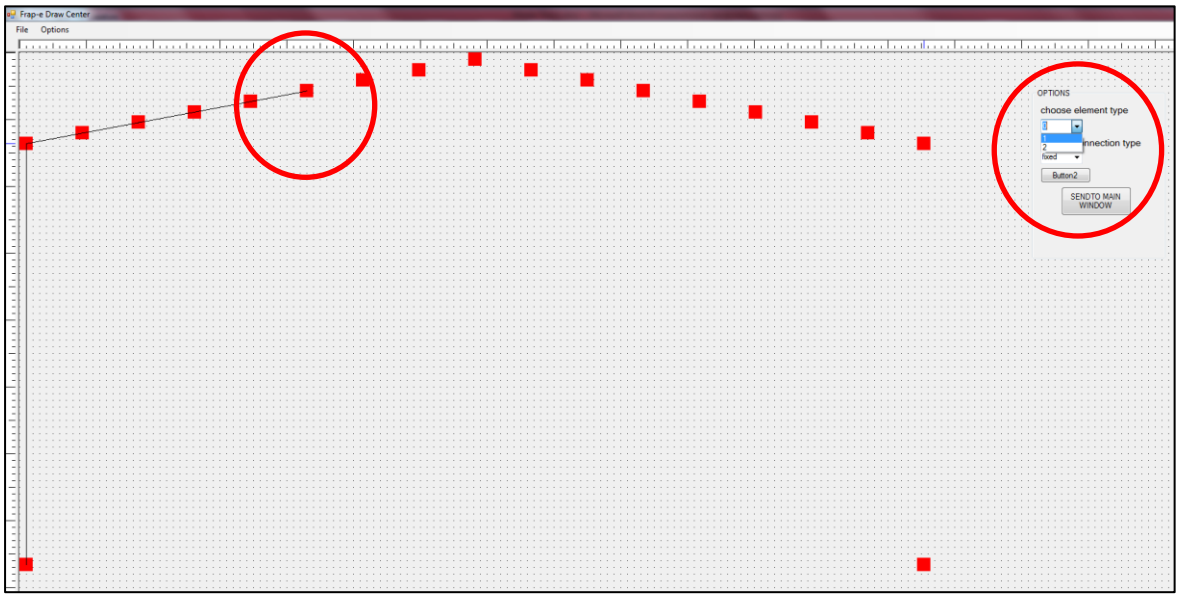


Figure 6.4 Draw of geometry

The options “1” or “2” in the connection type menu, correspond to the fixed or pinned connections respectively. However, instead of using this drawing menu, the user can define the connectivity, clicking the “connectivity matrix”. It is pointed out that, the last columns in connectivity matrix define the slope value for the moment-plastic rotation curve.

4. The textboxes presented in the upper left corner of the screen, should be filled according to the problem at hand

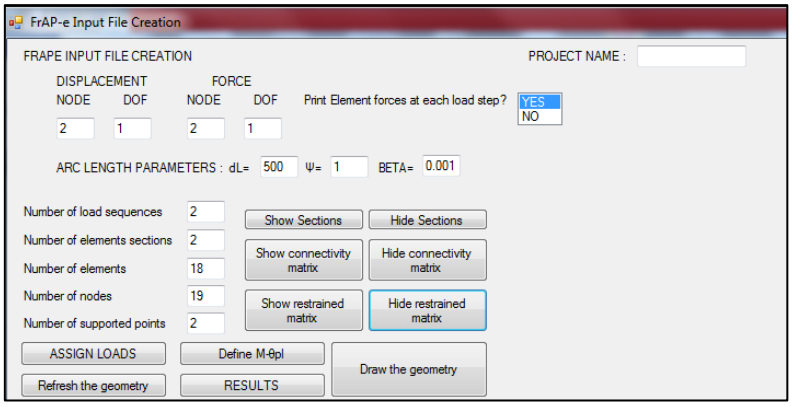


Figure 6.5 Necessary data for the problem

The required fields are the following

- The control nodes for tracing the displacement and the force values
- The number of load sequences
- The number of elements
- The number of nodes
- The number of supports

5. Define the supports using the button “Show restrained matrix”. The column “RNODES” contains the restricted nodes, while the column “RDOFS” is completed as follows
    - Fixed condition “111”
    - Pinned condition “110”
    - Roller condition in Y-axis “010”
    - Roller condition in X-axis “100”

    Regarding the interpretation of the numbers mentioned above, “1” corresponds to fixed DOF, while “0” corresponds to free DOF. The first digit refers to the translational DOF in X-axis, the second to the translational DOF in the Y-axis, and the third to the rotational degree of freedom

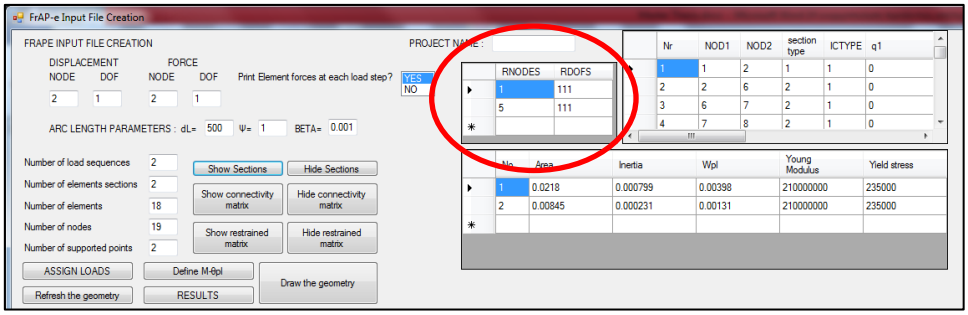


Figure 6.6 Defining the restraints

6. Assign the loads, using the button "ASSIGN LOAD" and saves the form with the "hide" button

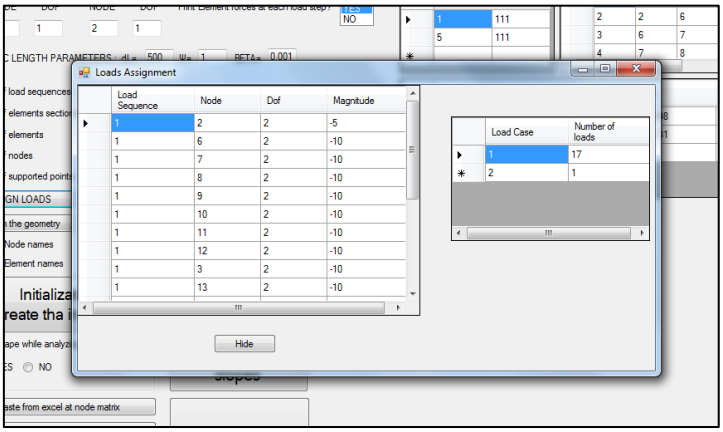


Figure 6.7 Load assignment

The two matrices should be completed as described in Figure 6.7

7. User can control all the data that has imported, using the "Refresh the geometry" button, in cooperation with the options shown below

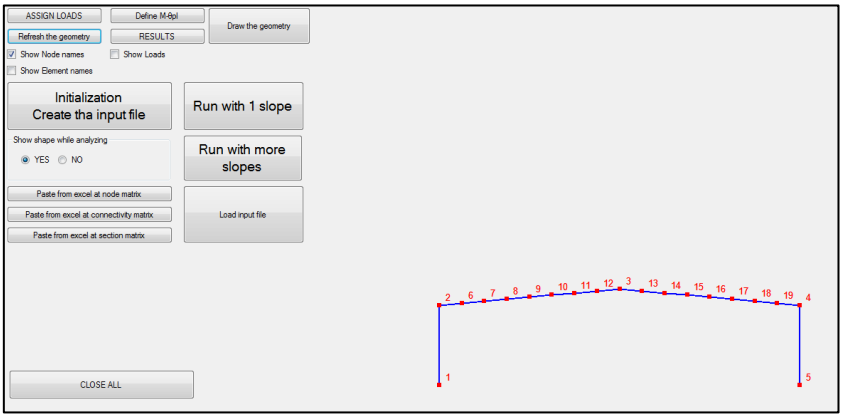


Figure 6.8 "Refresh the geometry" with node names

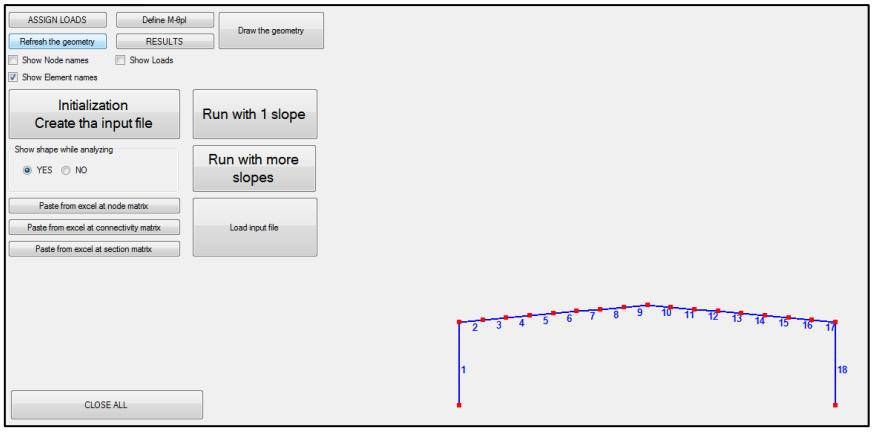


Figure 6.9 "Refresh the geometry" with element names

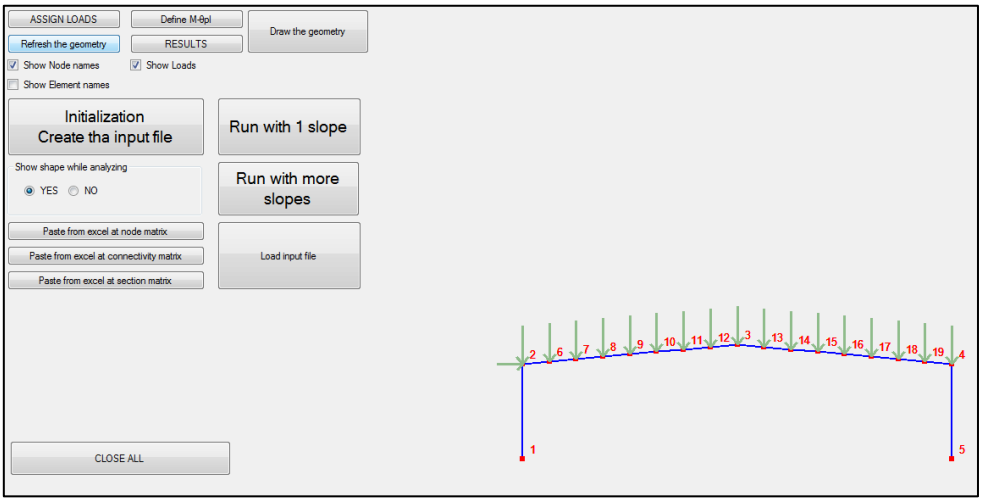


Figure 6.10 "Refresh the geometry" with loads and node names

8. The “initialization” button, creates the input file needed in order to execute the program
9. User decides whether, the deformed shape of each equilibrium point should be plotted during the analysis part using the menu “Show shape while analyzing”

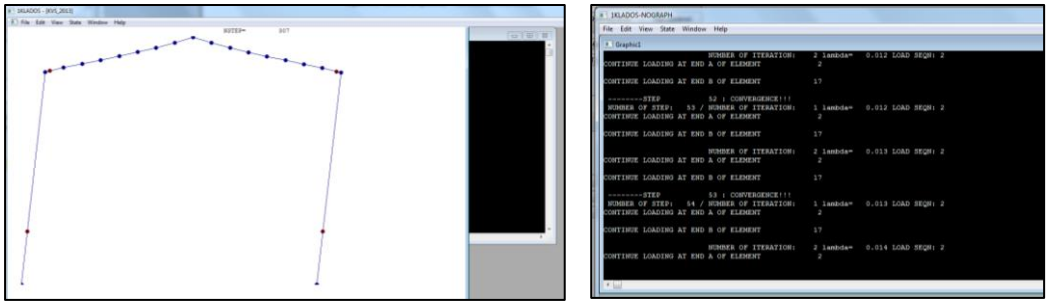

Figure 6.11 Computer screen when analyzing (a) with deformed shape plotted (b) without deformed shape plotted

## 6.2. Results presentation

The results can be presented by clicking on the “RESULTS” button Figure 6.12

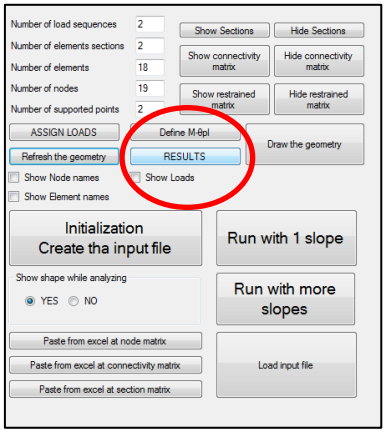


Figure 6.12 Results presentation

Then a new screen appears Figure 6.13

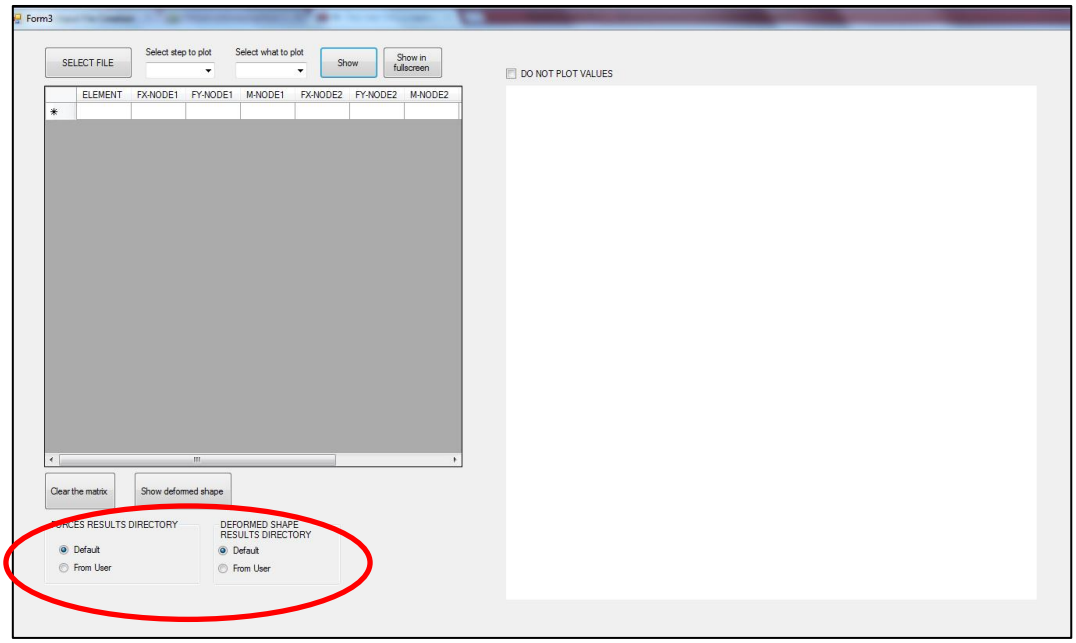


Figure 6.13 Results screen

This menu gives the opportunity to plot for a specific equilibrium step

- The deformed configuration ,in real scale
- The bending moments diagrams
- The global forces Fx diagram
- The global forces Fy diagram

It is pointed out that, all the results information are collected in the files

- “OUTEF.txt” , the internal forces results and the plastic deformations
- “OUTLD.txt”, the nodes’ displacements

The current software reads all the information needed, and then plots the results. Thus, in case the user wants to load another solved problem:

1. Change the “Deformed shape results directory” from “default” to “From user” (Figure 5.13)
2. Select the directory where the deformed shape pictures have been saved.
3. Change “Forces results directory” from “default” to “From user” (Figure 5.13)

As far as the deformed configurations, they are presented as follows:

1. The user clicks the “Select File” button, and wait
2. The message “Forces loaded” appears

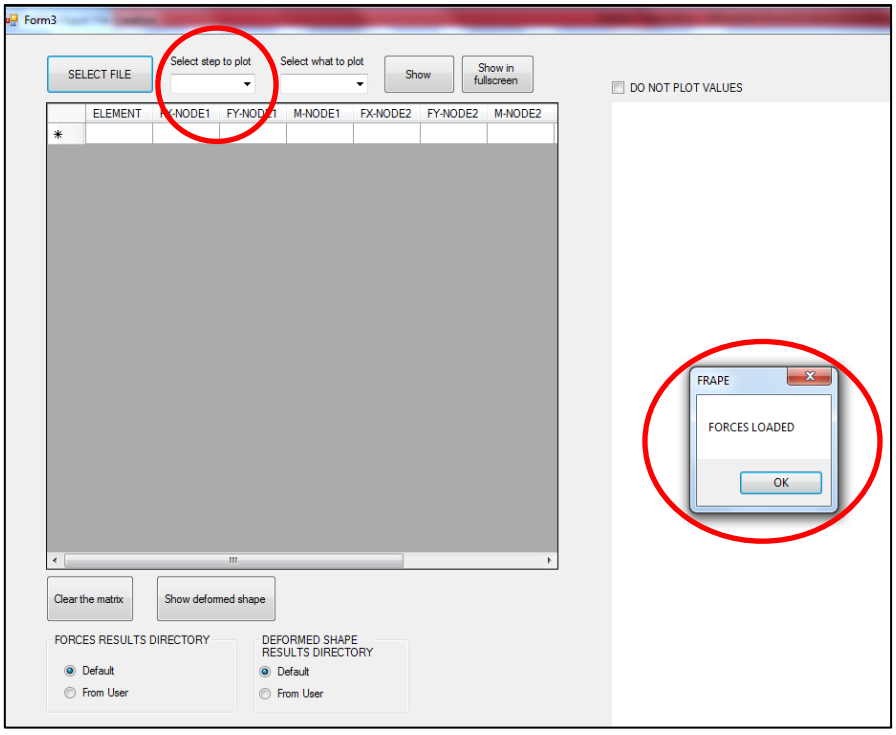


Figure 6.14 show deformed shape

3. The user selects one specific equilibrium step and presses the “Show deformed shape” button

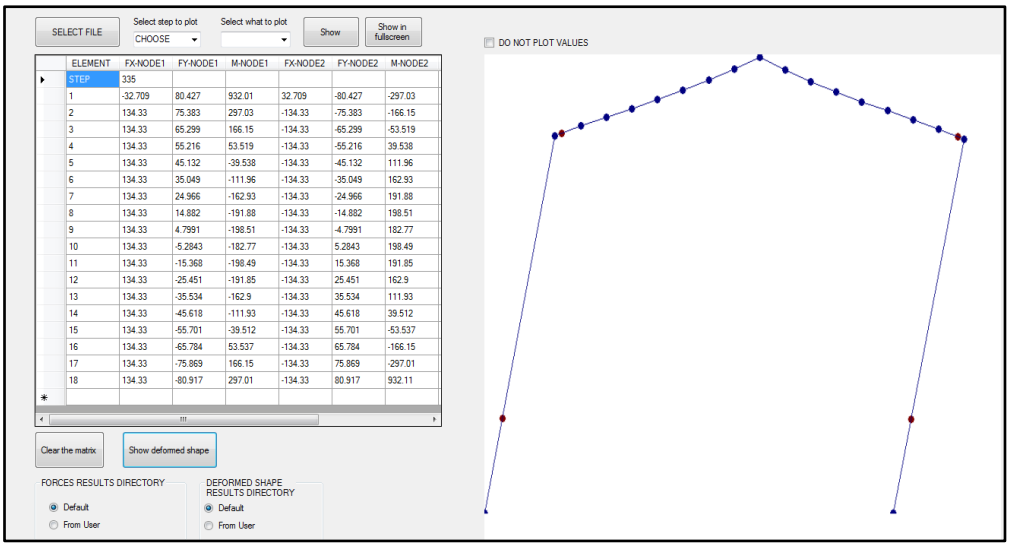


| ELEMENT | FX-NODE1 | FY-NODE1 | M-NODE1 | FX-NODE2 | FY-NODE2 | M-NODE2 |
|---|---|---|---|---|---|---|
| STEP | 335 | | | | | |
| 1 | -32.709 | 80.427 | 932.01 | 32.709 | -80.427 | -297.03 |
| 2 | 134.33 | 75.383 | 297.03 | -134.33 | -75.383 | -166.15 |
| 3 | 134.33 | 65.299 | 166.15 | -134.33 | -65.299 | -53.519 |
| 4 | 134.33 | 55.216 | 53.519 | -134.33 | -55.216 | 39.538 |
| 5 | 134.33 | 45.132 | -39.538 | -134.33 | -45.132 | 111.96 |
| 6 | 134.33 | 35.049 | -111.96 | -134.33 | -35.049 | 162.93 |
| 7 | 134.33 | 24.966 | -162.93 | -134.33 | -24.966 | 191.88 |
| 8 | 134.33 | 14.882 | -191.88 | -134.33 | -14.882 | 198.51 |
| 9 | 134.33 | 4.7991 | -198.51 | -134.33 | -4.7991 | 182.77 |
| 10 | 134.33 | -5.2843 | -182.77 | -134.33 | 5.2843 | 198.49 |
| 11 | 134.33 | -15.368 | -198.49 | -134.33 | 15.368 | 191.85 |
| 12 | 134.33 | -25.451 | -191.85 | -134.33 | 25.451 | 162.9 |
| 13 | 134.33 | -35.534 | -162.9 | -134.33 | 35.534 | 111.93 |
| 14 | 134.33 | -45.618 | -111.93 | -134.33 | 45.618 | 39.512 |
| 15 | 134.33 | -55.701 | -39.512 | -134.33 | 55.701 | -53.537 |
| 16 | 134.33 | -65.784 | 53.537 | -134.33 | 65.784 | -166.15 |
| 17 | 134.33 | -75.869 | 166.15 | -134.33 | 75.869 | -297.01 |
| 18 | 134.33 | -80.917 | 297.01 | -134.33 | 80.917 | 932.11 |

Figure 6.15 Deformed shape presentation

4. The user also selects one specific equilibrium step and presses the “select what to plot” button and then the “Show” button

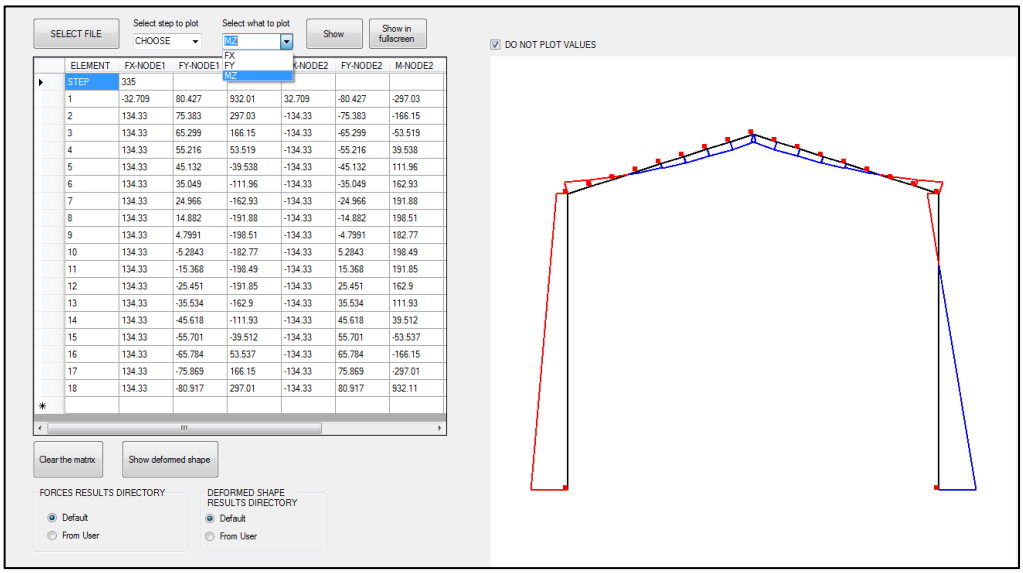


| ELEMENT | FX-NODE1 | FY-NODE1 | M-NODE1 | FX-NODE2 | FY-NODE2 | M-NODE2 |
|---|---|---|---|---|---|---|
| STEP | 335 | | | | | |
| 1 | -32.709 | 80.427 | 932.01 | 32.709 | -80.427 | -297.03 |
| 2 | 134.33 | 75.383 | 297.03 | -134.33 | -75.383 | -166.15 |
| 3 | 134.33 | 65.299 | 166.15 | -134.33 | -65.299 | -53.519 |
| 4 | 134.33 | 55.216 | 53.519 | -134.33 | -55.216 | 39.538 |
| 5 | 134.33 | 45.132 | -39.538 | -134.33 | -45.132 | 111.96 |
| 6 | 134.33 | 35.049 | -111.96 | -134.33 | -35.049 | 162.93 |
| 7 | 134.33 | 24.966 | -162.93 | -134.33 | -24.966 | 191.88 |
| 8 | 134.33 | 14.882 | -191.88 | -134.33 | -14.882 | 198.51 |
| 9 | 134.33 | 4.7991 | -198.51 | -134.33 | -4.7991 | 182.77 |
| 10 | 134.33 | -5.2843 | -182.77 | -134.33 | 5.2843 | 198.49 |
| 11 | 134.33 | -15.368 | -198.49 | -134.33 | 15.368 | 191.85 |
| 12 | 134.33 | -25.451 | -191.85 | -134.33 | 25.451 | 162.9 |
| 13 | 134.33 | -35.534 | -162.9 | -134.33 | 35.534 | 111.93 |
| 14 | 134.33 | -45.618 | -111.93 | -134.33 | 45.618 | 39.512 |
| 15 | 134.33 | -55.701 | -39.512 | -134.33 | 55.701 | -53.537 |
| 16 | 134.33 | -65.784 | 53.537 | -134.33 | 65.784 | -166.15 |
| 17 | 134.33 | -75.869 | 166.15 | -134.33 | 75.869 | -297.01 |
| 18 | 134.33 | -80.917 | 297.01 | -134.33 | 80.917 | 932.11 |

Figure 6.16 Bending moment diagram

# 7. Illustrative examples

In this chapter characteristic examples in inelastic analysis with large displacements are presented. All the analyses are carried out with incremental analysis, considering both geometric and material non-linearity. The plastic unstressing is considered only in the case of perfectly plastic material.

## 7.1. Lee's frame

As a first example of application, the Lee's frame [1], [5] shown in Figure 7.1, is considered. All beam elements have the same cross sectional properties: A=6.00 $cm^2$ and I=2.00 $cm^4$. The assumed material properties are: Young's elastic modulus E=7200 $KN/cm^2$, yield stress σy=100 $KN/cm^2$ and plastic modulus 4.50 $cm^3$.

Twenty elements are used to discretize the structure (Figure 7.1(a)). A purely elastic analysis was performed first and an inelastic one followed, considering elastic-perfectly plastic material. The initial value of Δl was estimated, as corresponding to 1% of the final load value. The load-displacement curves for the loaded node, are shown in Figure 7.2

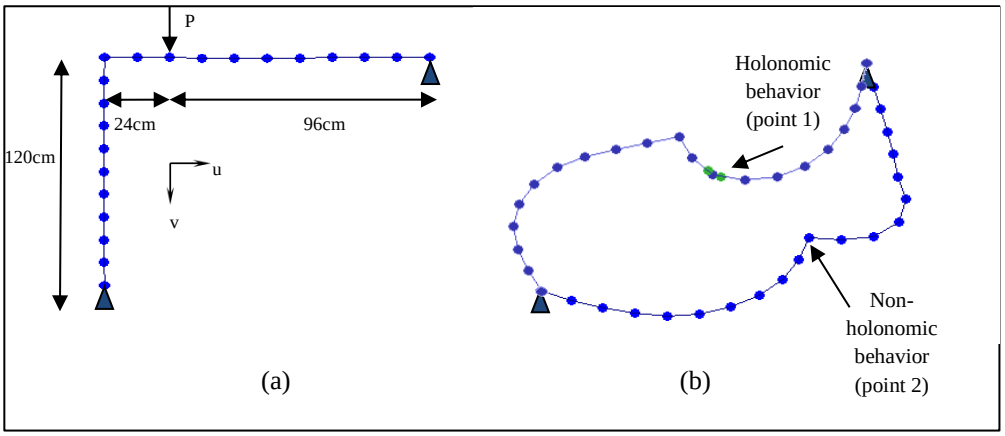


Figure 7.1 (a) Lee's frame in undeformed configuration, (b) Deformed shape configuration (point 2-nonholonomic behavior) and (point 1-holonomic behavior)

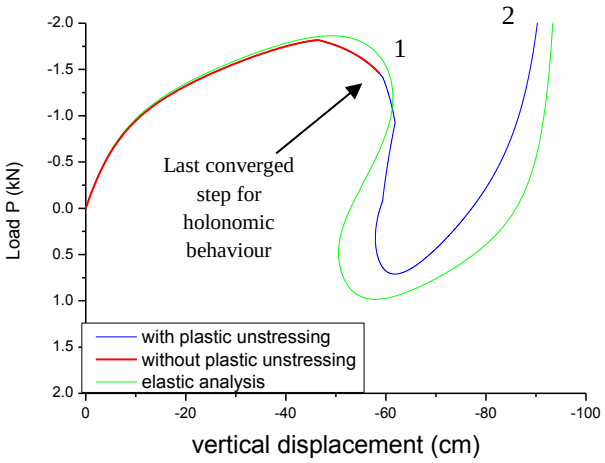


Figure 7.2 Load-displacement curves for elastic and inelastic analysis for the node where the external force is applied

When holonomic behavior is considered, the analysis cannot trace the whole equilibrium path (Figure 7.2) and stops at point 1, due to lack of convergence.

On the other hand, should plastic unstressing take place, the analysis continuous and eventually both these plastic hinges unload, new plastic hinges form in nearby places which unload too. The final deformed shape is shown in Figure 7.1(b)(point 2). It is clearly seen that, the equilibrium curve differs with the one of the purely elastic analysis.

Additionally, it is observed that, in the unstable equilibrium path the analysis is very sensitive and depends on the size of the increments (Figure 7.3). The stability of the algorithm is obvious since the same load displacement curves are produced for a wide range of values of Δl; certainly, a lower value of Δl will always produce more accurate results at the expense of computing time.

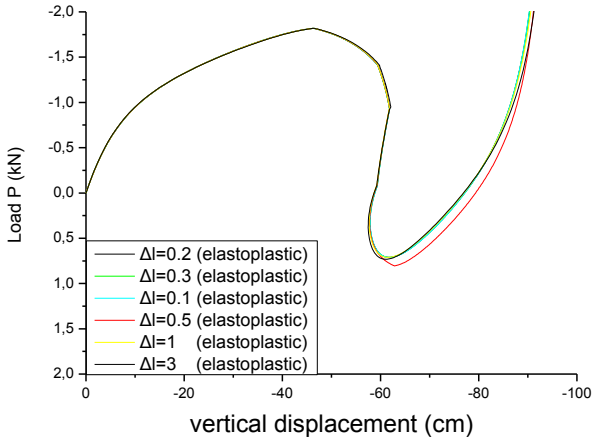


Figure 7.3 Vertical displacement in elastoplastic analysis for different Δl values for the same node

## 7.2. Yarimci's frames

Two frames A and B tested by Yarimci [1], [14] (Figure 7.4(a) and Figure 7.4(b)) are solved as a second example. The assumed material properties are: Young's elastic modulus E=200 GPa, yield stress σy=248 MPa, material elastic perfectly plastic. The vertical loads are applied first up to their final values, shown in Figure 7.4(a) and Figure 7.4(b). The horizontal loads H are applied next. The difference of the two frames is marked by the different cross-sections used for the beams and columns (Table 1). The frames were discretized by 90 elements as shown in the respective figures.

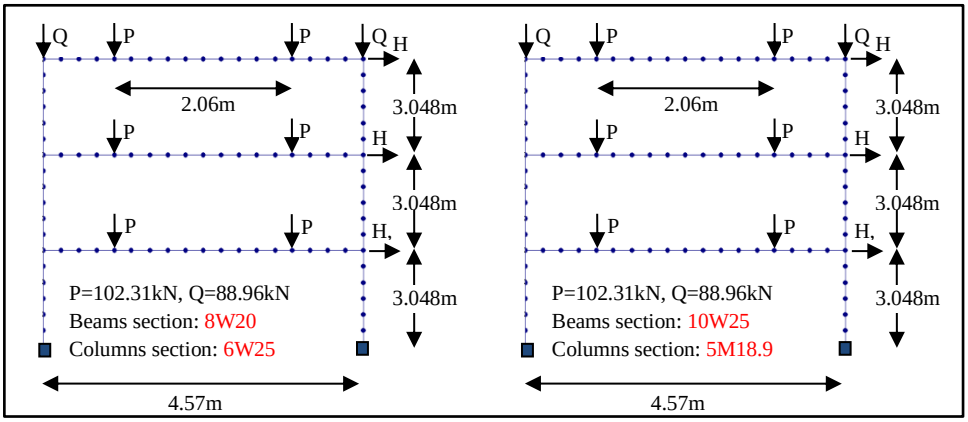


Figure 7.4 (a) Yarimci's frame A ,(b) Yarimci's frame B

| A/A | **A ($10^{-3}m^2$)** | **I ($10^{-5}m^4$)** | **Z ($10^{-4}m^3$)** | A/A | **A ($10^{-3}m^2$)** | **I ($10^{-5}m^4$)** | **Z ($10^{-4}m^3$)** |
|---|---|---|---|---|---|---|---|
| **8W20** | 3,974 | 3,13 | 3,34 | **10W25** | 4,91 | 5,99 | 5,13 |
| **6W25** | 4,75 | 2,22 | 3,1 | **5M18.9** | 3,58 | 1 | 1,8 |

Table 7.1 Properties of beams and columns sections

The responses of the frames are the following:

- Frame A

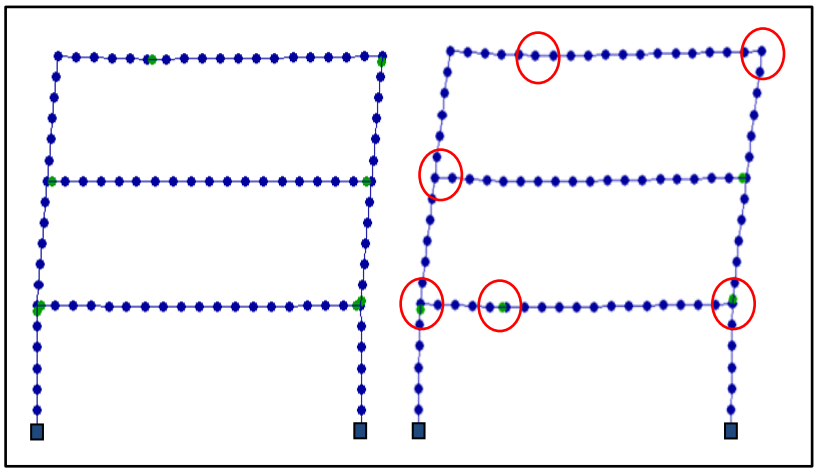

Figure 7.5 (a) Final deformed shape without plastic unstressing,(b) Final deformed shape with plastic unstressing, where the non-common plastic hinges are indicated

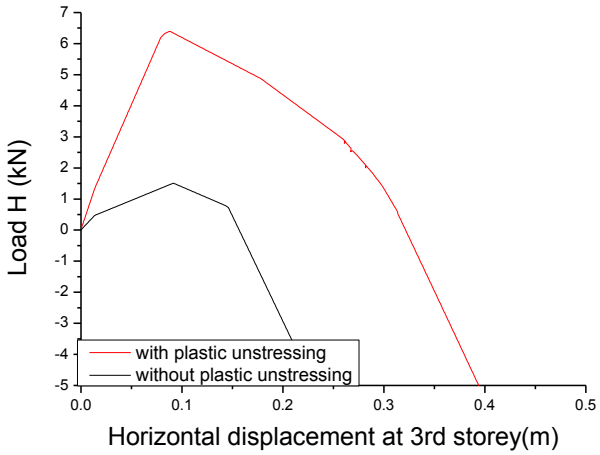


Figure 7.6 Load displacement curves with and without non holonomic behavior

- Frame B

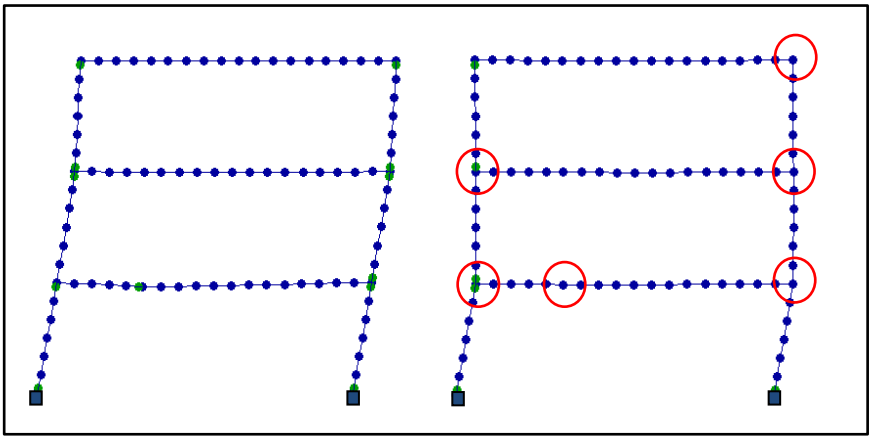

Figure 7.7 (a) Final deformed shape without plastic unstressing,(b) Final deformed shape with plastic unstressing, where the non-common plastic hinges are indicated

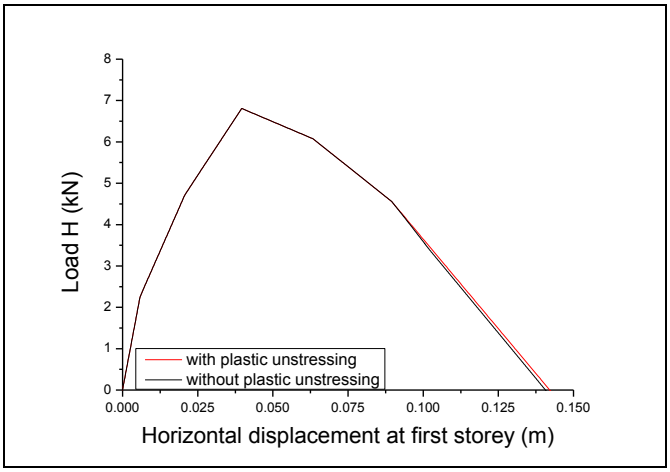


Figure 7.8 Load displacement curves with plastic unstressing and without plastic unstressing

It is interesting to observe, the difference of the response of the two frames while considering unloading or not. Also the sequence of the plastic hinges is totally different. Especially for the frame A, the equilibrium path is shown to be much higher when considering plastic unstressing. One may argue that, the non-consideration of plastic unstressing leads to more conservative results. This may hold for the present example, but it cannot be generalized. On the other hand, non-holonomic behavior is the more realistic behavior of a structure and this is the one that should be followed.

In regard to frame B, one may compare the present numerical solution with the experimental work [15] (Figure 7.9). In the same figure another numerical solution [14] is also indicated.

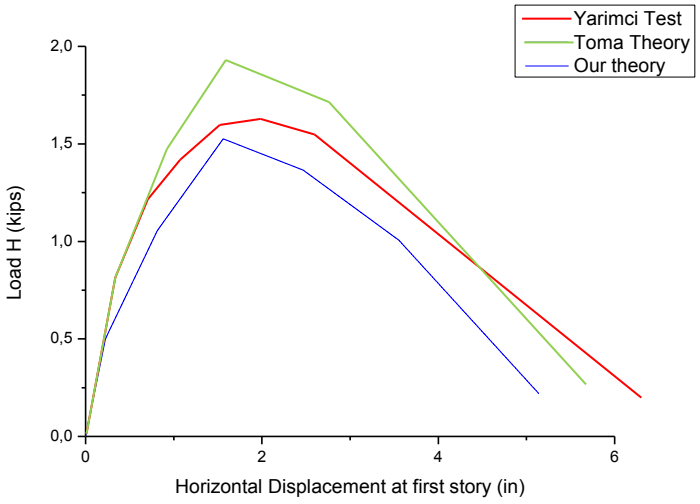


Figure 7.9 Comparison of experimental and numerical solutions

## 7.3. Steel Roof

The following example was presented by [16] . The frame consists of beams with section IPE400 and columns with section HEB450 (Figure 7.10). The material considered was steel Fe360 with yield stress 235N/mm$^2$ and the analysis was considered as holonomic.

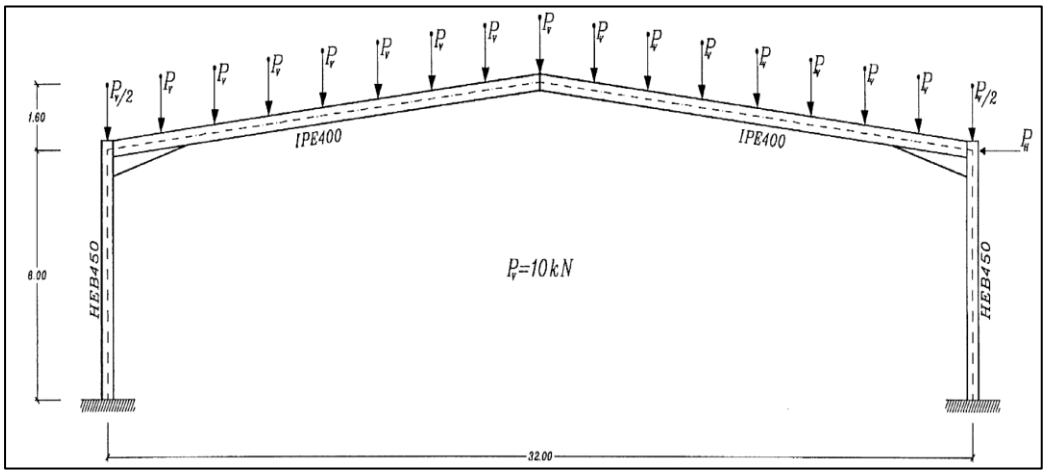


Figure 7.10 The frame with the assigned loads and sections

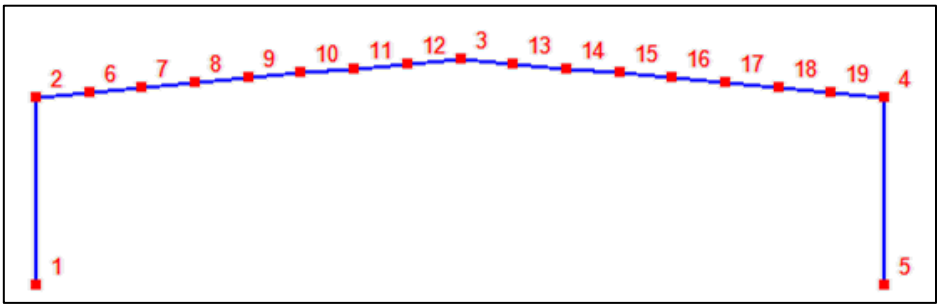


Figure 7.11 The discretized model

The vertical loads were applied first and the horizontal ones followed. The $P_v$ was equal to 10kN. Three types of inelastic analyses with large displacements were carried out, considering different cases of material non linearity

- Case 1: All the elements were considered elastic perfectly plastic
- Case 2: The columns were considered elastic perfectly plastic, while the beams were considered elastic plastic with strain softening with slope equal to -77,39kNm/rad
- Case 3: The columns were considered elastic perfectly plastic, while the beams were considered elastic plastic with strain hardening with slope equal to 77,39kNm/rad

For all the cases, the sequence in the opening of the plastic hinges was the same. Indicative deformed modes of the structure are presented in the next figures

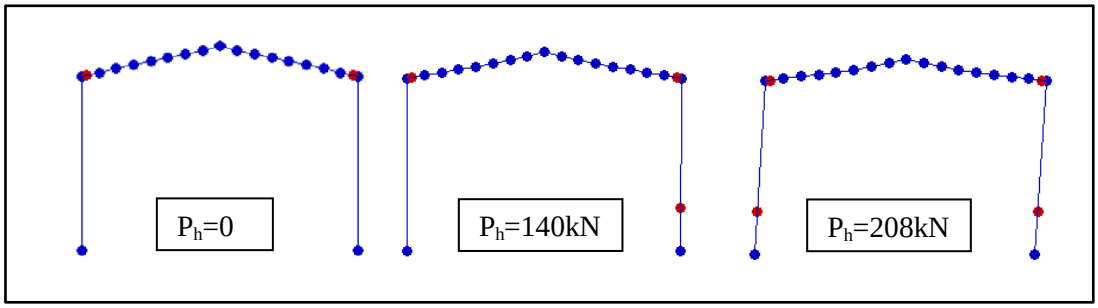


Figure 7.12 Deformed shapes of the structures when plastic hinges open and the corresponding values of the horizontal load

The bending moment diagrams corresponding to the configurations of Figure 7.12 are presented in Figure 7.13. The values of the diagrams are presented in the appendix

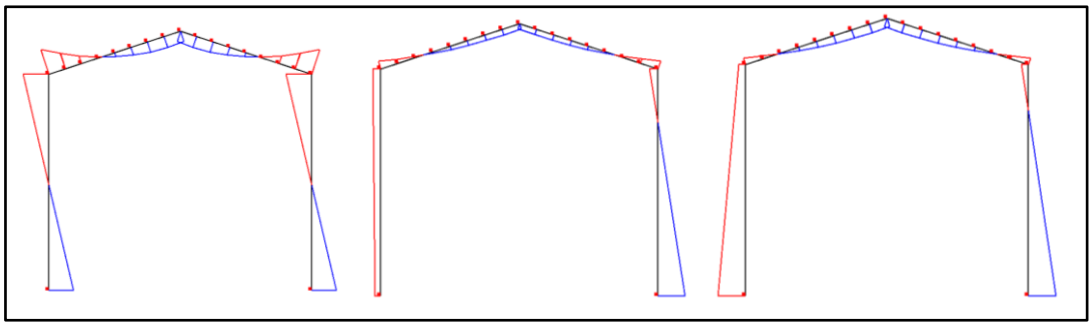

Figure 7.13 Characteristic bending moment diagrams

The force-displacement curve is plotted for the joint where the horizontal force is applied. It is worth-noting that the first two plastic hinges open due to the application of the vertical load. The load displacement curve is the following

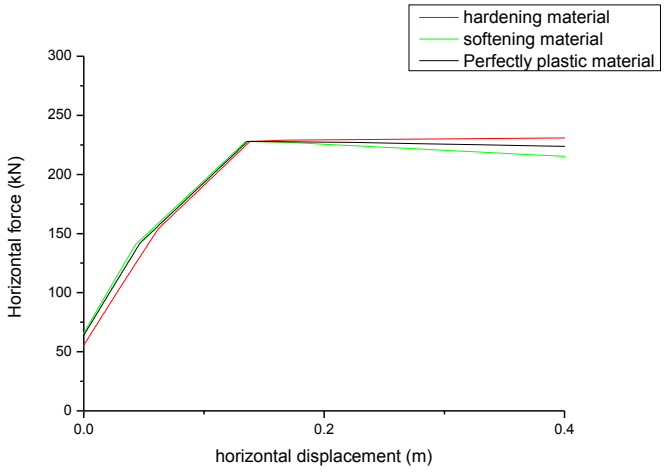


Figure 7.14 Load displacement curve

## 7.4. Frame with three floors

An eccentrically braced frame is introduced (Figure 7.15) consisting of HEB300 columns, IPE200 beams and RHS100/100/4 diagonal support elements. The steel grade is Fe430 with a yield stress of 355N/mm$^2$. The vertical loads Pv are equal to 38kN

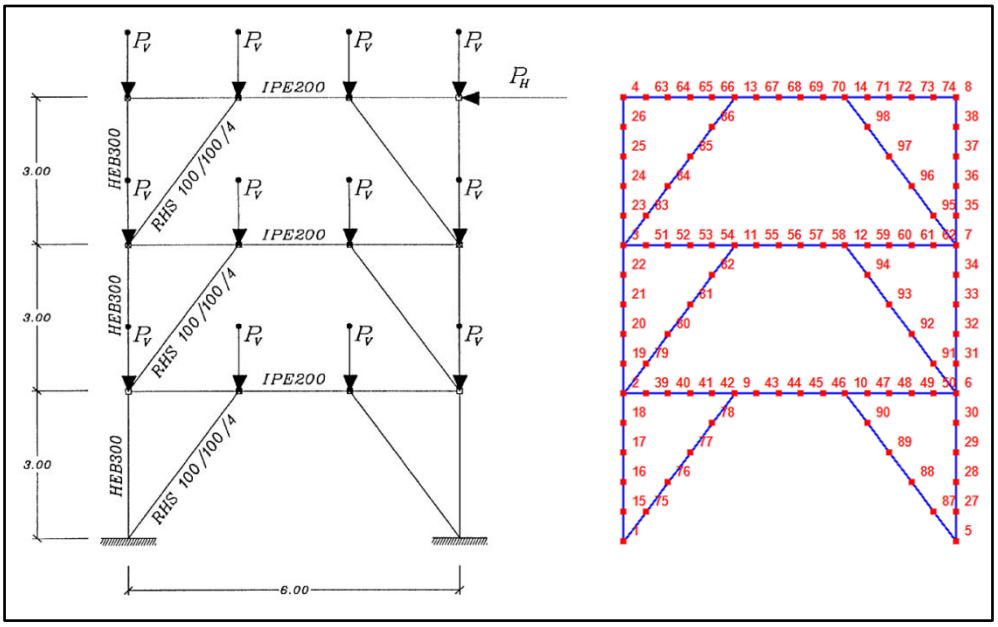


Figure 7.15 The frame's geometry is presented (left), the way it is discretized is presented (right)

Regarding the load sequences, the vertical loads were applied first and the horizontal ones ( $P_H$ ) followed. The number of the elements used were 105, and again three different type of holonomic analyses were performed :

- Case 1: All the elements were considered elastic perfectly plastic
- Case 2: The columns were considered as plastic with strain softening with slope equal to -202.79kNm/rad, while the beams were considered elastic plastic with strain softening with slope equal to -41.04kNm/rad
- Case 3: The columns were considered as plastic with strain softening with slope equal to -202.79kNm/rad, while the beams were considered elastic plastic with strain softening with slope equal to -41.04kNm/rad

For all cases, the sequence in the opening of the plastic hinges was the same. Indicative deformed modes of the structure are presented in the next figures

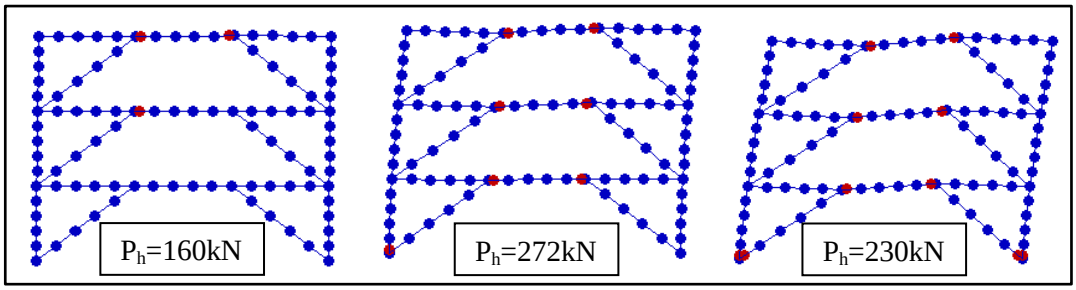


Figure 7.16 Deformed shapes of the structures when plastic hinges open and the corresponding values of the horizontal load

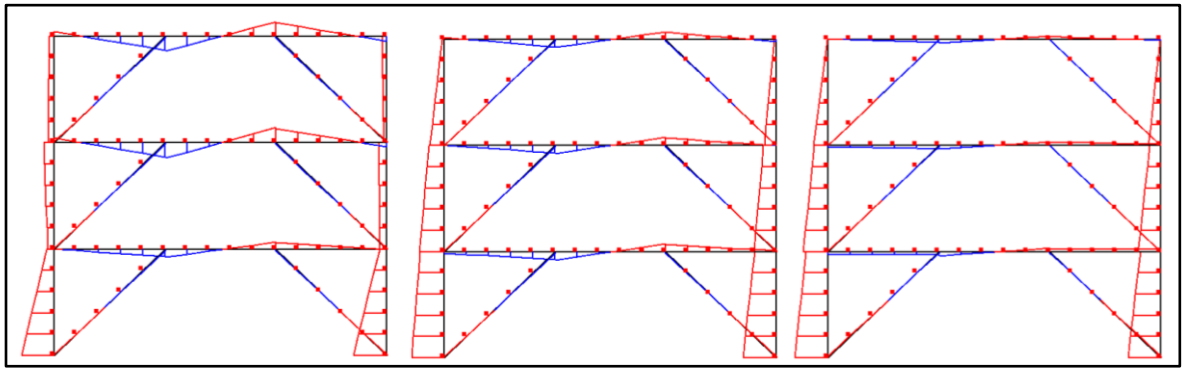

Figure 7.17 Characteristic bending moment diagrams for the above presented deformed configurations, the values of the diagrams are presented in the appendix

The load displacement curve, was created for the last floor and is the following

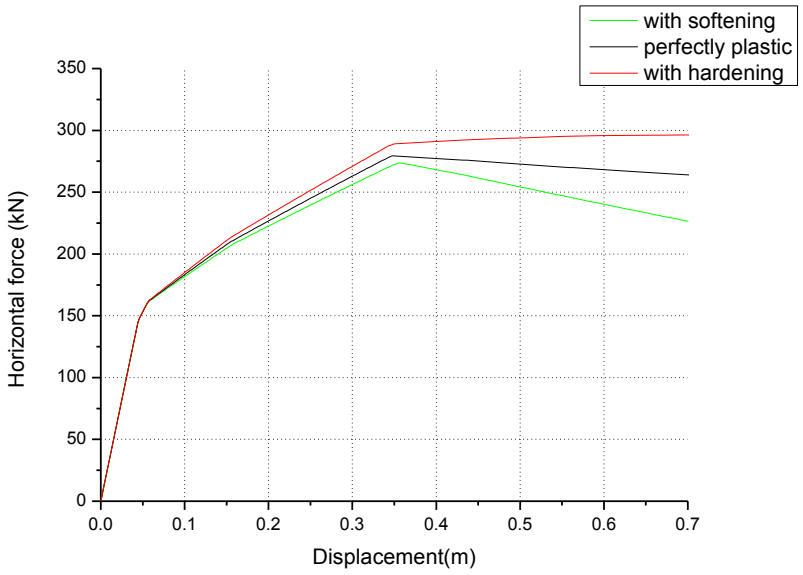


Figure 7.18 Load displacement curve presenting the full load path

Additionally, the current example was solved by SAP2000v15. The discretization and the sections used were exactly the same. Regarding the plastic hinge definition the P-M3 interaction surface was selected, with axial force-displacement relationship proportional to moment-rotation. The initial interaction surface was defined as “user

definded” , in order to be the same with the one presented in present work. The hardening rule, which was implemented in program, is presented in next figures

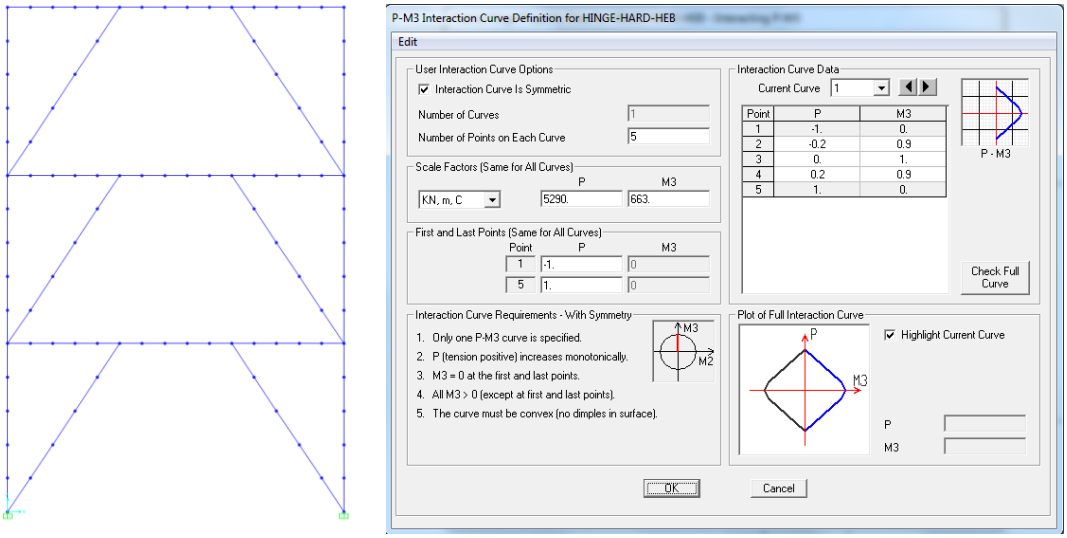


Figure 7.19 The goemetry of the structure in SAP2000 (left), the implementation of the interaction surface (right)

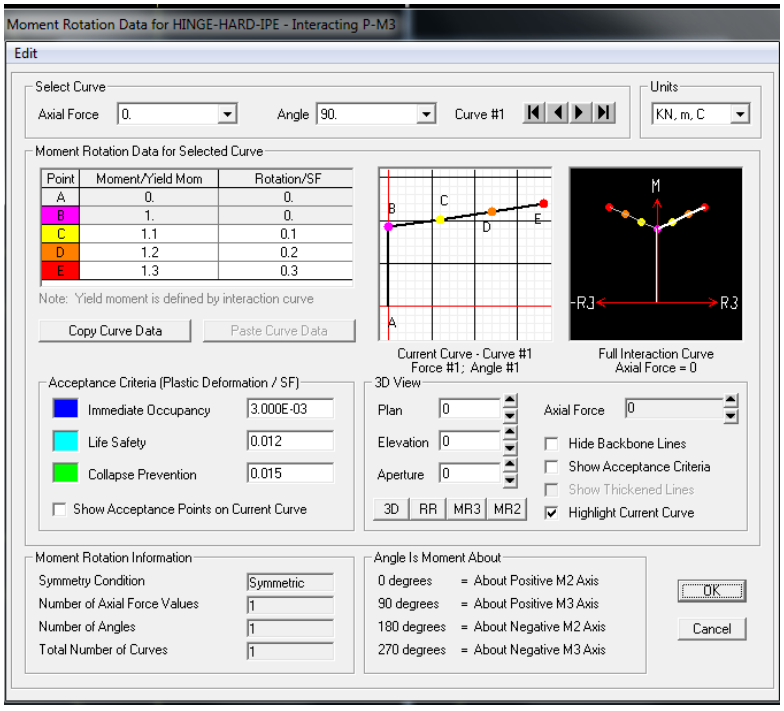


Figure 7.20 The moment plastic rotation law in SAP2000

The comparison between SAP2000 and the present work is presented in Figure 7.21.. The software SAP2000 cannot trace the whole equilibrium. It is worth noting that, SAP2000 confronted serious convergence instabilities at point A.

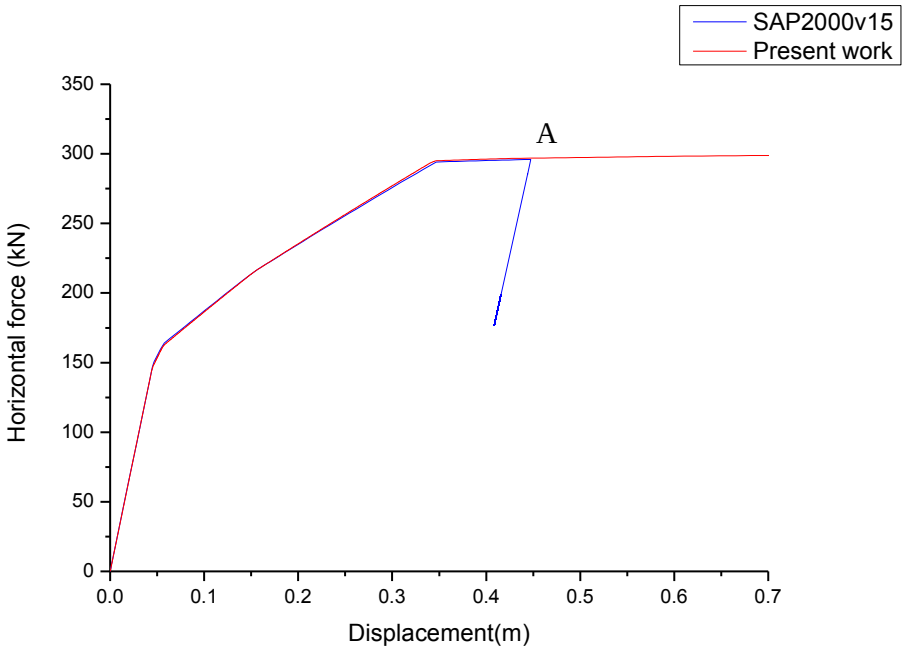


Figure 7.21 Load displacement curve comparing SAP2000 with present work

It is pointed out that this example was proposed and examined by [16]. The load displacement curve produced by those researchers, is the following

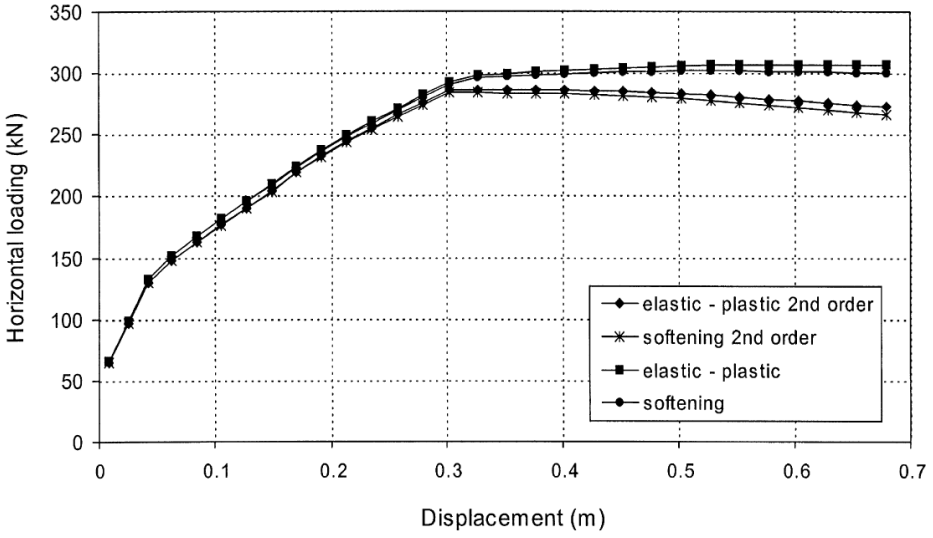


Figure 7.22 Load displacement curves according to **[16]**

## 7.5. Two bay rectangular frame

A two storey frame is introduced (Figure 7.23(a)) [17]. The structure consists of four different steel elements (table 7.2) with Young's modulus of elasticity 200 GPa.

Table 7.2 Properties of beams and columns

| Section Name | Area($m^2$) | Inertia($m^4$) | wpl | fyf(kPa) | Mp(kNm) | Py(kN) | h(kNm/rad) |
|---|---|---|---|---|---|---|---|
| lower columns | 0.00479 | 2.22E-05 | 0.0003274 | 235000 | 76.9484 | 1125.65 | 768.33 |
| lower beam | 0.00494 | 8.51E-05 | 0.0006443 | 235000 | 151.40815 | 1160.9 | 1214.75 |
| upper columns | 0.00379 | 1.72E-05 | 0.0002577 | 235000 | 60.5595 | 890.65 | 981.33 |
| upper beam | 0.00417 | 4.89E-05 | 0.0004478 | 235000 | 105.24005 | 979.95 | 707.43 |

The structure was discretized as presented in Figure 7.23(b) . The yield stress was taken equal to 235MPa and the vertical loads were applied first, while the horizontal ones followed. Three different types of holonomic analyses were performed :

- Case 1: All the elements were considered elastic perfectly plastic
- Case 2: All elements were considered elastic plastic with hardening moment plastic rotation law, with slopes equal to the h value (table 7.2)
- Case 3: All elements were considered elastic plastic with softening moment plastic rotation law, with slopes equal to the h value (table 7.2)

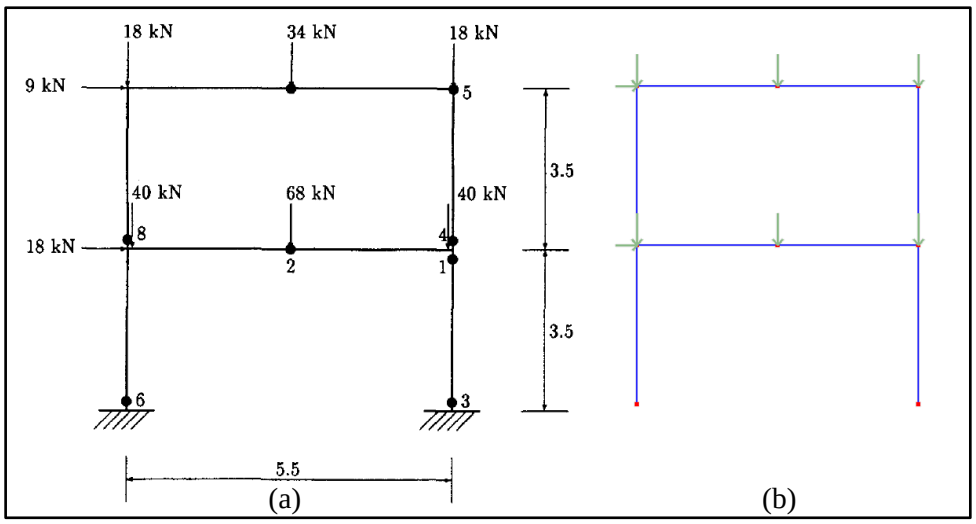


Figure 7.23 (a) The geometry of the frame (b) The discretization of the frame

For all cases, the sequence in the opening of the plastic hinges was the same. Indicative deformed modes of the structure are presented in the next figures

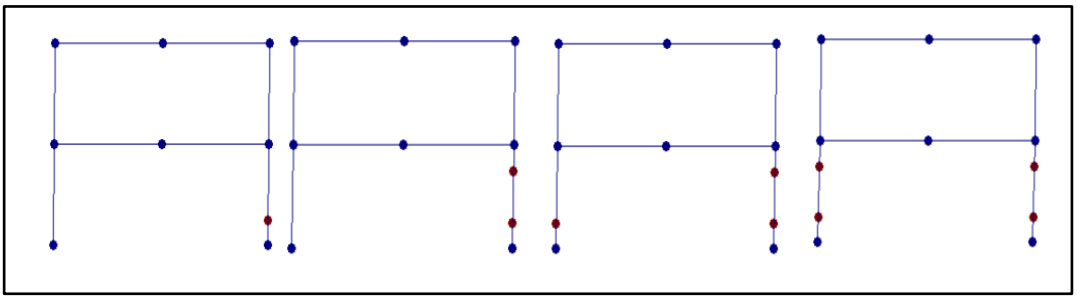

Figure 7.24 Sequence of plastic hinge formation for the softening case

The moment diagrams that correspond to the first and the last plastic hinge are the following

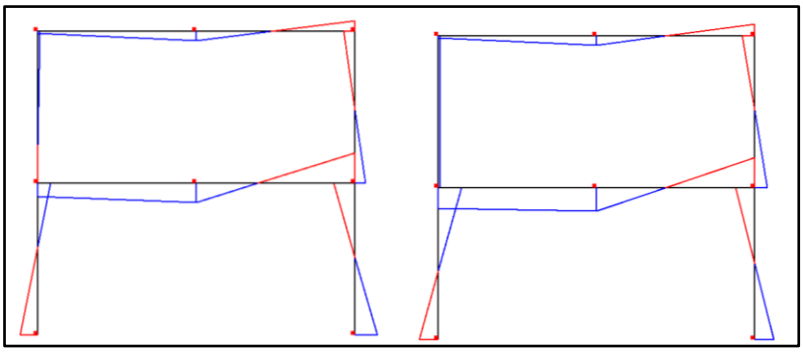

Figure 7.25 Bending moment diagram for the first (left) and the last (right) plastic hinge, in the softening case

The values of the diagrams of Figure 7.25 are presented in the appendix. The last equilibrium is presented in Figure 7.26

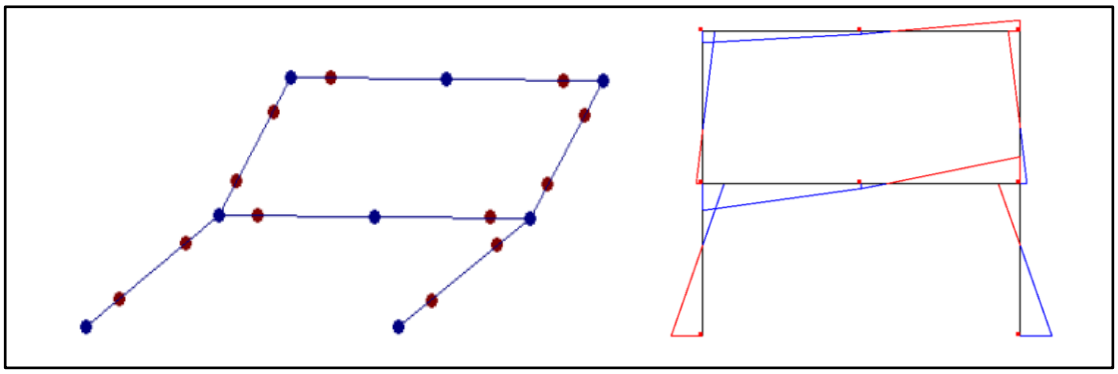

Figure 7.26 Deformed configuration and the corresponding bending moment diagram for the last equilibrium in the hardening case

The load displacement curve, which is shown below corresponds to the left node of the last floor.

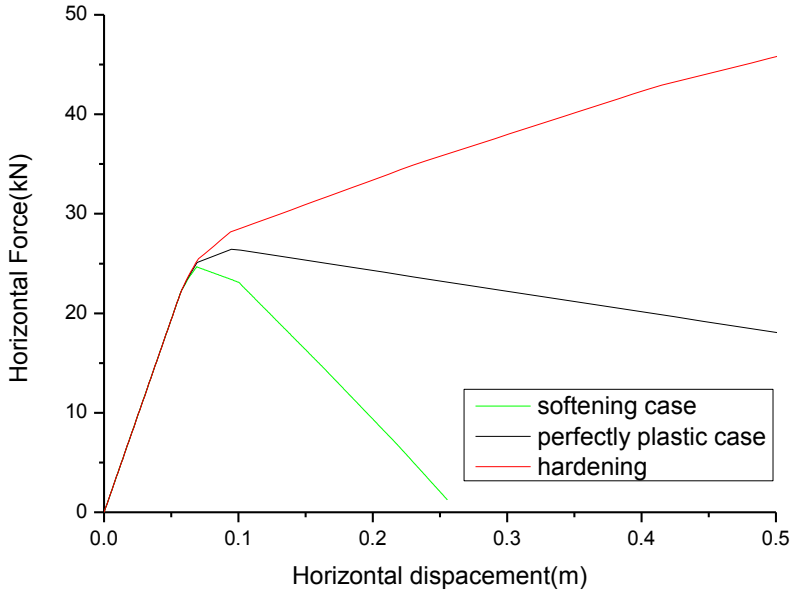

## Bibliography


[1] K. V. Spiliopoulos and I. A. Kapogiannis, "Elastoplastic analysis of frames with large displacements and plastic unstressing," in *International Congress on Mechanics*, Chania, 2013.

[2] W.F. Chen and I. Sohal, Plastic design and Second-Order Analysis of steel frames, New York: Springer-Verlag, 1995.

[3] K.V.Spiliopoulos, Advanced plastic analysis of framed structures (in greek), Athens, 2013.

[4] J. Argyris, "Finite element method the natural approach," *Comp. Meths. Appl. Mech Engrg.*, vol. 17/18, pp. 1-106, 1979.

[5] Hsiao K.M., Hou F.Y. and Spiliopoulos K.V., "Large displacement analysis of elasto-plastic frames," *Computers and Structures*, vol. 28, pp. 627-633.

[6] C. R., Markus, P. M.E. and Witt, Concepts and applications of finite element analysis, J. Willey, 2002.

[7] M. Crisfield, "A fast incremental/iterative solution procedure that handles ‘snap-through," *Computers and Structures*, vol. 13, pp. 55-62, 1981.

[8] AISC, Load and Resistance Factor Design Specification for Structural Steel Buildings, Chicago, 1993.

[9] Mroz, "An Attempt to Describe the Behavior of Metals under Cyclic Loads Using a More General Workhardening Model," *Acta Mechanica*, pp. 199-212, 1969.

[10] Cofie and Krawinkle, "Uniaxial Cyclic Stress-Strain Behavior of Structural Steel," *Engineering Mechanics ASCE*, vol. 11, no. 9, pp. 1105-1120, 1985.

[11] B. Mosaddad and G. H. Powell, "Computational models for cyclic plasticity rate depedence and creep in finite element analysis," *EERC Reports*, 1982.

[12] Krenk S, Vissing-Jorgensen C. and Thesberg L., "Efficient collapse analysis techniques for framed structures," *Computers and Structures*, no. 72, pp. 481-496, 1999.

[13] W. Chen, N. Kishi and M. Komuro, Semi-rigid Connections Handbook, New York: J.Ross, 2011.

[14] S. Toma, W. Chen and D. White, "A selection of calibration frames in North America for second-order inelastic analysis," *Engng Struct*, vol. 17, pp. 104-112, 1993.

[15] Yarimci, "Incremental inelastic analysis of framed structures and some experimental

verifications," Bethlehem, 1966.

[16] S. Karakostas. E. Mistakidis, "Evaluation of the ductility features in steel structures with softening moment-rotation behaviour based on a nonconvex optimization formulation," *Engineering Computations*, vol. 17, no. 5, pp. 573-592, 2000.

[17] C. P. Roth and W. W. Bird, "Internal variable formulations for the plastic analysis of plane frames," *Engineering Structures*, vol. 17, no. 3, pp. 214-220, 1995.

# APPENDIX

## Steel roof results

| Softening Case | | | | | | | | |
|---|---|---|---|---|---|---|---|---|
| 1st Plastic hinge | | | | | | | | |
| | NODE 1 | | | NODE 2 | | | | |
| | FX | FY | MZ | FX | FY | MZ | Θpl1 | Θpl2 |
| 1 | 73.278 | 66.381 | -286.31 | -73.278 | -66.381 | -301.05 | 0 | 0 |
| 2 | 73.278 | 62.232 | 301.05 | -73.278 | -62.232 | -190.33 | 1.60E-02 | 0 |
| 3 | 73.278 | 53.934 | 190.33 | -73.278 | -53.934 | -94.953 | 0 | 0 |
| 4 | 73.278 | 45.637 | 94.953 | -73.278 | -45.637 | -15.573 | 0 | 0 |
| 5 | 73.278 | 37.339 | 15.573 | -73.278 | -37.339 | 47.302 | 0 | 0 |
| 6 | 73.278 | 29.042 | -47.302 | -73.278 | -29.042 | 93.275 | 0 | 0 |
| 7 | 73.278 | 20.744 | -93.275 | -73.278 | -20.744 | 122.07 | 0 | 0 |
| 8 | 73.278 | 12.446 | -122.07 | -73.278 | -12.446 | 133.51 | 0 | 0 |
| 9 | 73.278 | 41.488 | -133.51 | -73.278 | -41.488 | 127.55 | 0 | 0 |
| 10 | 73.278 | -41.488 | -127.55 | -73.278 | 41.488 | 133.51 | 0 | 0 |
| 11 | 73.278 | -12.446 | -133.51 | -73.278 | 12.446 | 122.07 | 0 | 0 |
| 12 | 73.278 | -20.744 | -122.07 | -73.278 | 20.744 | 93.275 | 0 | 0 |
| 13 | 73.278 | -29.042 | -93.275 | -73.278 | 29.042 | 47.302 | 0 | 0 |
| 14 | 73.278 | -37.339 | -47.302 | -73.278 | 37.339 | -15.573 | 0 | 0 |
| 15 | 73.278 | -45.637 | 15.573 | -73.278 | 45.637 | -94.953 | 0 | 0 |
| 16 | 73.278 | -53.934 | 94.953 | -73.278 | 53.934 | -190.33 | 0 | 0 |
| 17 | 73.278 | -62.232 | 190.33 | -73.278 | 62.232 | -301.05 | 0 | -1.60E-02 |
| 18 | 73.278 | -66.381 | 301.05 | -73.278 | 66.381 | 286.31 | 0 | 0 |
| 2nd Plastic hinge | | | | | | | | |
| 1 | 10.028 | 80.185 | 201.12 | -10.028 | -80.185 | -277.86 | 0 | 0 |
| 2 | 151.02 | 75.149 | 277.85 | -151.02 | -75.149 | -150.12 | 0.007791 | 0 |
| 3 | 151.02 | 65.091 | 150.12 | -151.02 | -65.091 | -40.512 | 0 | 0 |
| 4 | 151.02 | 55.029 | 40.512 | -151.02 | -55.029 | 49.485 | 0 | 0 |
| 5 | 151.02 | 44.967 | -49.485 | -151.02 | -44.967 | 118.71 | 0 | 0 |
| 6 | 151.03 | 34.905 | -118.71 | -151.03 | -34.905 | 166.3 | 0 | 0 |
| 7 | 151.03 | 24.842 | -166.3 | -151.03 | -24.842 | 191.65 | 0 | 0 |
| 8 | 151.03 | 14.78 | -191.65 | -151.03 | -14.78 | 194.48 | 0 | 0 |
| 9 | 151.03 | 47.182 | -194.48 | -151.03 | -47.182 | 174.77 | 0 | 0 |
| 10 | 151.03 | -5.344 | -174.77 | -151.03 | 5.344 | 193.07 | 0 | 0 |
| 11 | 151.03 | -15.406 | -193.07 | -151.03 | 15.406 | 188.84 | 0 | 0 |
| 12 | 151.03 | -25.468 | -188.84 | -151.03 | 25.468 | 162.13 | 0 | 0 |
| 13 | 151.03 | -35.53 | -162.13 | -151.03 | 35.53 | 113.23 | 0 | 0 |
| 14 | 151.02 | -45.592 | -113.23 | -151.02 | 45.592 | 42.757 | 0 | 0 |
| 15 | 151.02 | -55.655 | -42.757 | -151.02 | 55.655 | -48.396 | 0 | 0 |
| 16 | 151.02 | -65.717 | 48.396 | -151.02 | 65.717 | -159.06 | 0 | 0 |
| 17 | 151.02 | -75.776 | 159.06 | -151.02 | 75.776 | -287.64 | 0 | -0.0338 |

| | | | | | | | | |
|---|---|---|---|---|---|---|---|---|
| 18 | 151.03 | -80.805 | 287.64 | -151.03 | 80.805 | 928.56 | 0 | 4.53E-01 |
| 3rd Plastic hinge | | | | | | | | |
| 1 | -75.065 | 80.484 | 929.61 | 75.065 | -80.484 | -233.47 | 0.14406 | 0 |
| 2 | 133.23 | 75.449 | 233.46 | -133.23 | -75.449 | -94.613 | -0.12757 | 0 |
| 3 | 133.23 | 65.394 | 94.613 | -133.23 | -65.394 | 24.685 | 0 | 0 |
| 4 | 133.23 | 55.331 | -24.685 | -133.23 | -55.331 | 123.54 | 0 | 0 |
| 5 | 133.23 | 45.269 | -123.54 | -133.23 | -45.269 | 200.83 | 0 | 0 |
| 6 | 133.23 | 35.207 | -200.83 | -133.23 | -35.207 | 255.72 | 0 | 0 |
| 7 | 133.23 | 25.145 | -255.72 | -133.23 | -25.145 | 287.59 | 0 | 0 |
| 8 | 133.23 | 15.083 | -287.59 | -133.23 | -15.083 | 296.13 | 0 | 0 |
| 9 | 133.23 | 50.207 | -296.13 | -133.23 | -50.207 | 281.27 | 0 | 0 |
| 10 | 133.23 | -50.414 | -281.27 | -133.23 | 50.414 | 296.41 | 0 | 0 |
| 11 | 133.23 | -15.104 | -296.41 | -133.23 | 15.104 | 288.15 | 0 | 0 |
| 12 | 133.23 | -25.166 | -288.15 | -133.23 | 25.166 | 256.55 | 0 | 0 |
| 13 | 133.23 | -35.228 | -256.55 | -133.23 | 35.228 | 201.93 | 0 | 0 |
| 14 | 133.23 | -45.29 | -201.93 | -133.23 | 45.29 | 124.88 | 0 | 0 |
| 15 | 133.23 | -55.352 | -124.88 | -133.23 | 55.352 | 26.268 | 0 | 0 |
| 16 | 133.23 | -65.414 | -26.268 | -133.23 | 65.414 | -92.809 | 0 | 0 |
| 17 | 133.23 | -75.478 | 92.809 | -133.23 | 75.478 | -229.86 | 0 | -0.22192 |
| 18 | 133.23 | -80.502 | 229.85 | -133.23 | 80.502 | 930.61 | 0 | 0.15924 |

| perfectly plastic Case | | | | | | | | |
|---|---|---|---|---|---|---|---|---|
| 1st Plastic hinge | | | | | | | | |
| | NODE 1 | | | NODE 2 | | | | |
| | FX | FY | MZ | FX | FY | MZ | Θpl1 | Θpl2 |
| 1 | 73.46 | 66.525 | -287.09 | -73.46 | -66.525 | -301.73 | 0 | 0 |
| 2 | 73.46 | 62.367 | 301.73 | -73.46 | -62.367 | -190.76 | 1.95E-02 | 0 |
| 3 | 73.46 | 54.051 | 190.76 | -73.46 | -54.051 | -95.18 | 0 | 0 |
| 4 | 73.46 | 45.736 | 95.18 | -73.46 | -45.736 | -15.621 | 0 | 0 |
| 5 | 73.46 | 37.42 | 15.621 | -73.46 | -37.42 | 47.396 | 0 | 0 |
| 6 | 73.46 | 29.105 | -47.396 | -73.46 | -29.105 | 93.475 | 0 | 0 |
| 7 | 73.46 | 20.789 | -93.475 | -73.46 | -20.789 | 122.33 | 0 | 0 |
| 8 | 73.46 | 12.473 | -122.33 | -73.46 | -12.473 | 133.8 | 0 | 0 |
| 9 | 73.46 | 41.578 | -133.8 | -73.46 | -41.578 | 127.82 | 0 | 0 |
| 10 | 73.46 | -41.578 | -127.82 | -73.46 | 41.578 | 133.8 | 0 | 0 |
| 11 | 73.46 | -12.473 | -133.8 | -73.46 | 12.473 | 122.33 | 0 | 0 |
| 12 | 73.46 | -20.789 | -122.33 | -73.46 | 20.789 | 93.475 | 0 | 0 |
| 13 | 73.46 | -29.105 | -93.475 | -73.46 | 29.105 | 47.396 | 0 | 0 |
| 14 | 73.46 | -37.42 | -47.396 | -73.46 | 37.42 | -15.621 | 0 | 0 |
| 15 | 73.46 | -45.736 | 15.621 | -73.46 | 45.736 | -95.18 | 0 | 0 |
| 16 | 73.46 | -54.051 | 95.18 | -73.46 | 54.051 | -190.76 | 0 | 0 |
| 17 | 73.46 | -62.367 | 190.76 | -73.46 | 62.367 | -301.73 | 0 | -1.95E-02 |
| 18 | 73.46 | -66.525 | 301.73 | -73.46 | 66.525 | 287.09 | 0 | 0 |
| 2nd Plastic hinge | | | | | | | | |

| | | | | | | | | |
|---|---|---|---|---|---|---|---|---|
| 1 | 89.722 | 80.664 | 227.72 | -89.722 | -80.664 | -295.63 | 0 | 0 |
| 2 | 151.97 | 75.622 | 295.63 | -151.97 | -75.622 | -168.93 | 0.00042 | 0 |
| 3 | 151.97 | 65.54 | 168.93 | -151.97 | -65.54 | -60.189 | 0 | 0 |
| 4 | 151.97 | 55.456 | 60.189 | -151.97 | -55.456 | 29.166 | 0 | 0 |
| 5 | 151.97 | 45.373 | -29.166 | -151.97 | -45.373 | 97.973 | 0 | 0 |
| 6 | 151.97 | 35.289 | -97.973 | -151.97 | -35.289 | 145.35 | 0 | 0 |
| 7 | 151.97 | 25.206 | -145.35 | -151.97 | -25.206 | 170.72 | 0 | 0 |
| 8 | 151.97 | 15.123 | -170.72 | -151.97 | -15.123 | 173.76 | 0 | 0 |
| 9 | 151.97 | 50.393 | -173.76 | -151.97 | -50.393 | 154.47 | 0 | 0 |
| 10 | 151.97 | -5.044 | -154.47 | -151.97 | 5.044 | 173.76 | 0 | 0 |
| 11 | 151.97 | -15.127 | -173.76 | -151.97 | 15.127 | 170.72 | 0 | 0 |
| 12 | 151.97 | -25.211 | -170.72 | -151.97 | 25.211 | 145.35 | 0 | 0 |
| 13 | 151.97 | -35.294 | -145.35 | -151.97 | 35.294 | 97.973 | 0 | 0 |
| 14 | 151.97 | -45.377 | -97.973 | -151.97 | 45.377 | 29.165 | 0 | 0 |
| 15 | 151.97 | -55.461 | -29.165 | -151.97 | 55.461 | -60.189 | 0 | 0 |
| 16 | 151.97 | -65.544 | 60.189 | -151.97 | 65.544 | -168.93 | 0 | 0 |
| 17 | 151.97 | -75.627 | 168.93 | -151.97 | 75.627 | -295.63 | 0 | -0.02813 |
| 18 | 151.97 | -80.67 | 295.63 | -151.97 | 80.67 | 928.11 | 0 | 0.000105 |
| 3rd Plastic hinge | | | | | | | | |
| 1 | -76.786 | 80.672 | 928.14 | 76.786 | -80.672 | -295.77 | 0.01122 | 0 |
| 2 | 150.28 | 75.618 | 295.77 | -150.28 | -75.618 | -168.64 | -0.02705 | 0 |
| 3 | 150.28 | 65.534 | 168.64 | -150.28 | -65.534 | -59.508 | 0 | 0 |
| 4 | 150.28 | 55.45 | 59.508 | -150.28 | -55.45 | 30.22 | 0 | 0 |
| 5 | 150.28 | 45.367 | -30.22 | -150.28 | -45.367 | 99.391 | 0 | 0 |
| 6 | 150.28 | 35.284 | -99.391 | -150.28 | -35.284 | 147.13 | 0 | 0 |
| 7 | 150.28 | 25.2 | -147.13 | -150.28 | -25.2 | 172.85 | 0 | 0 |
| 8 | 150.28 | 15.117 | -172.85 | -150.28 | -15.117 | 176.24 | 0 | 0 |
| 9 | 150.28 | 50.336 | -176.24 | -150.28 | -50.336 | 157.29 | 0 | 0 |
| 10 | 150.28 | -50.497 | -157.29 | -150.28 | 50.497 | 176.24 | 0 | 0 |
| 11 | 150.28 | -15.133 | -176.24 | -150.28 | 15.133 | 172.85 | 0 | 0 |
| 12 | 150.28 | -25.216 | -172.85 | -150.28 | 25.216 | 147.13 | 0 | 0 |
| 13 | 150.28 | -35.3 | -147.13 | -150.28 | 35.3 | 99.39 | 0 | 0 |
| 14 | 150.28 | -45.383 | -99.39 | -150.28 | 45.383 | 30.219 | 0 | 0 |
| 15 | 150.28 | -55.466 | -30.219 | -150.28 | 55.466 | -59.508 | 0 | 0 |
| 16 | 150.28 | -65.55 | 59.508 | -150.28 | 65.55 | -168.64 | 0 | 0 |
| 17 | 150.28 | -75.634 | 168.64 | -150.28 | 75.634 | -295.77 | 0 | -0.05104 |
| 18 | 150.28 | -80.701 | 295.76 | -150.28 | 80.701 | 928.42 | 0 | 0.022589 |

| Hardening Case | | | | | | | | |
|---|---|---|---|---|---|---|---|---|
| 1st Plastic hinge | | | | | | | | |
| | NODE 1 | | | NODE 2 | | | | |
| | FX | FY | MZ | FX | FY | MZ | Θpl1 | Θpl2 |
| 1 | 73.46 | 66.525 | -287.09 | -73.46 | -66.525 | -301.73 | 0 | 0 |
| 2 | 73.46 | 62.367 | 301.73 | -73.46 | -62.367 | -190.76 | 1.95E-02 | 0 |

| | | | | | | | | |
|---|---|---|---|---|---|---|---|---|
| 3 | 73.46 | 54.051 | 190.76 | -73.46 | -54.051 | -95.18 | 0 | 0 |
| 4 | 73.46 | 45.736 | 95.18 | -73.46 | -45.736 | -15.621 | 0 | 0 |
| 5 | 73.46 | 37.42 | 15.621 | -73.46 | -37.42 | 47.396 | 0 | 0 |
| 6 | 73.46 | 29.105 | -47.396 | -73.46 | -29.105 | 93.475 | 0 | 0 |
| 7 | 73.46 | 20.789 | -93.475 | -73.46 | -20.789 | 122.33 | 0 | 0 |
| 8 | 73.46 | 12.473 | -122.33 | -73.46 | -12.473 | 133.8 | 0 | 0 |
| 9 | 73.46 | 41.578 | -133.8 | -73.46 | -41.578 | 127.82 | 0 | 0 |
| 10 | 73.46 | -41.578 | -127.82 | -73.46 | 41.578 | 133.8 | 0 | 0 |
| 11 | 73.46 | -12.473 | -133.8 | -73.46 | 12.473 | 122.33 | 0 | 0 |
| 12 | 73.46 | -20.789 | -122.33 | -73.46 | 20.789 | 93.475 | 0 | 0 |
| 13 | 73.46 | -29.105 | -93.475 | -73.46 | 29.105 | 47.396 | 0 | 0 |
| 14 | 73.46 | -37.42 | -47.396 | -73.46 | 37.42 | -15.621 | 0 | 0 |
| 15 | 73.46 | -45.736 | 15.621 | -73.46 | 45.736 | -95.18 | 0 | 0 |
| 16 | 73.46 | -54.051 | 95.18 | -73.46 | 54.051 | -190.76 | 0 | 0 |
| 17 | 73.46 | -62.367 | 190.76 | -73.46 | 62.367 | -301.73 | 0 | -1.95E-02 |
| 18 | 73.46 | -66.525 | 301.73 | -73.46 | 66.525 | 287.09 | 0 | 0 |
| 2nd Plastic hinge | | | | | | | | |
| 1 | 0.0568 | 80.825 | 325.53 | -0.0568 | -80.825 | -320.98 | 0 | 0 |
| 2 | 154.06 | 75.795 | 320.98 | -154.06 | -75.795 | -197.61 | -0.01295 | 0 |
| 3 | 154.06 | 65.724 | 197.61 | -154.06 | -65.724 | -91.866 | 0 | 0 |
| 4 | 154.06 | 55.656 | 91.866 | -154.06 | -55.656 | -5.036 | 0 | 0 |
| 5 | 154.06 | 45.589 | 5.036 | -154.06 | -45.589 | 61.733 | 0 | 0 |
| 6 | 154.06 | 35.521 | -61.733 | -154.06 | -35.521 | 107.57 | 0 | 0 |
| 7 | 154.06 | 25.454 | -107.57 | -154.06 | -25.454 | 131.9 | 0 | 0 |
| 8 | 154.06 | 15.386 | -131.9 | -154.06 | -15.386 | 134.42 | 0 | 0 |
| 9 | 154.06 | 5.319 | -134.42 | -154.06 | -5.319 | 115.12 | 0 | 0 |
| 10 | 154.06 | -47.484 | -115.12 | -154.06 | 47.484 | 135.74 | 0 | 0 |
| 11 | 154.06 | -14.816 | -135.74 | -154.06 | 14.816 | 134.52 | 0 | 0 |
| 12 | 154.06 | -24.883 | -134.52 | -154.06 | 24.883 | 111.46 | 0 | 0 |
| 13 | 154.06 | -34.951 | -111.46 | -154.06 | 34.951 | 66.843 | 0 | 0 |
| 14 | 154.06 | -45.018 | -66.843 | -154.06 | 45.018 | 12.273 | 0 | 0 |
| 15 | 154.06 | -55.086 | -12.273 | -154.06 | 55.086 | -84.531 | 0 | 0 |
| 16 | 154.06 | -65.153 | 84.531 | -154.06 | 65.153 | -189.3 | 0 | 0 |
| 17 | 154.06 | -75.224 | 189.3 | -154.06 | 75.224 | -311.62 | 0 | -0.01789 |
| 18 | 154.06 | -80.254 | 311.61 | -154.06 | 80.254 | 928.62 | 0 | 1.02E-01 |
| 3rd Plastic hinge | | | | | | | | |
| 1 | -73.877 | 80.878 | 931.79 | 73.877 | -80.878 | -327.36 | 0.003536 | 0 |
| 2 | 155.11 | 75.861 | 327.38 | -155.11 | -75.861 | -204.85 | -0.03378 | 0 |
| 3 | 155.11 | 65.78 | 204.85 | -155.11 | -65.78 | -99.974 | 0 | 0 |
| 4 | 155.11 | 55.712 | 99.974 | -155.11 | -55.712 | -13.892 | 0 | 0 |
| 5 | 155.11 | 45.645 | 13.892 | -155.11 | -45.645 | 52.251 | 0 | 0 |
| 6 | 155.11 | 35.577 | -52.251 | -155.11 | -35.577 | 97.587 | 0 | 0 |
| 7 | 155.11 | 25.51 | -97.587 | -155.11 | -25.51 | 121.53 | 0 | 0 |
| 8 | 155.11 | 15.443 | -121.53 | -155.11 | -15.443 | 123.79 | 0 | 0 |

| | | | | | | | | |
|---|---|---|---|---|---|---|---|---|
| 9 | 155.11 | 53.752 | -123.79 | -155.11 | -53.752 | 104.36 | 0 | 0 |
| 10 | 155.11 | -46.922 | -104.36 | -155.11 | 46.922 | 125.4 | 0 | 0 |
| 11 | 155.11 | -14.76 | -125.4 | -155.11 | 14.76 | 124.73 | 0 | 0 |
| 12 | 155.11 | -24.827 | -124.73 | -155.11 | 24.827 | 102.33 | 0 | 0 |
| 13 | 155.11 | -34.894 | -102.33 | -155.11 | 34.894 | 58.477 | 0 | 0 |
| 14 | 155.11 | -44.962 | -58.477 | -155.11 | 44.962 | -62.603 | 0 | 0 |
| 15 | 155.11 | -55.029 | 62.603 | -155.11 | 55.029 | -91.038 | 0 | 0 |
| 16 | 155.11 | -65.097 | 91.038 | -155.11 | 65.097 | -194.73 | 0 | 0 |
| 17 | 155.11 | -75.163 | 194.73 | -155.11 | 75.163 | -315.82 | 0 | -0.02799 |
| 18 | 155.11 | -80.193 | 315.82 | -155.11 | 80.193 | 940.61 | 0 | 0.012632 |

## Frame with three floors

| 1st Configuration-softening case | | | | | | | | |
|---|---|---|---|---|---|---|---|---|
| | NODE 1 | | | NODE 2 | | | | |
| | FX | FY | MZ | FX | FY | MZ | Θpl1 | Θpl2 |
| 1 | -40337 | 59003 | 158000 | 40337 | -59003 | -133760 | 0 | 0 |
| 2 | -40337 | 59003 | 133760 | 40337 | -59003 | -109480 | 0 | 0 |
| 3 | -40337 | 59003 | 109480 | 40337 | -59003 | -85150 | 0 | 0 |
| 4 | -40337 | 59003 | 85150 | 40337 | -59003 | -60786 | 0 | 0 |
| 5 | -40337 | 59003 | 60786 | 40337 | -59003 | -36398 | 0 | 0 |
| 6 | 7636.5 | 88470 | 30380 | -7636.5 | -88470 | -34659 | 0 | 0 |
| 7 | 7636.5 | 88470 | 34659 | -7636.5 | -88470 | -38917 | 0 | 0 |
| 8 | 7636.5 | 88470 | 38917 | -7636.5 | -88470 | -43152 | 0 | 0 |
| 9 | 7636.5 | 88470 | 43152 | -7636.5 | -88470 | -47360 | 0 | 0 |
| 10 | 7636.5 | 88470 | 47360 | -7636.5 | -88470 | -51541 | 0 | 0 |
| 11 | 553.09 | 83649 | 25437 | -553.09 | -83649 | -25367 | 0 | 0 |
| 12 | 553.09 | 83649 | 25367 | -553.09 | -83649 | -25284 | 0 | 0 |
| 13 | 553.09 | 83649 | 25284 | -553.09 | -83649 | -25185 | 0 | 0 |
| 14 | 553.09 | 83649 | 25185 | -553.09 | -83649 | -25073 | 0 | 0 |
| 15 | 553.09 | 83649 | 25073 | -553.09 | -83649 | -24946 | 0 | 0 |
| 16 | -40950 | 323970 | 160490 | 40950 | -323970 | -135760 | 0 | 0 |
| 17 | -40950 | 323970 | 135760 | 40950 | -323970 | -110720 | 0 | 0 |
| 18 | -40950 | 323970 | 110720 | 40950 | -323970 | -85445 | 0 | 0 |
| 19 | -40950 | 323970 | 85445 | 40950 | -323970 | -59978 | 0 | 0 |
| 20 | -40950 | 323970 | 59978 | 40950 | -323970 | -34378 | 0 | 0 |
| 21 | 2943.2 | 140860 | 31902 | -2943.2 | -140860 | -33182 | 0 | 0 |
| 22 | 2943.2 | 140860 | 33182 | -2943.2 | -140860 | -34431 | 0 | 0 |
| 23 | 2943.2 | 140860 | 34431 | -2943.2 | -140860 | -35647 | 0 | 0 |
| 24 | 2943.2 | 140860 | 35647 | -2943.2 | -140860 | -36829 | 0 | 0 |
| 25 | 2943.2 | 140860 | 36829 | -2943.2 | -140860 | -37975 | 0 | 0 |
| 26 | 2938.8 | -8537.6 | 14322 | -2938.8 | 8537.6 | -16124 | 0 | 0 |
| 27 | 2938.8 | -8537.6 | 16124 | -2938.8 | 8537.6 | -17927 | 0 | 0 |
| 28 | 2938.8 | -8537.6 | 17927 | -2938.8 | 8537.6 | -19731 | 0 | 0 |
| 29 | 2938.8 | -8537.6 | 19731 | -2938.8 | 8537.6 | -21537 | 0 | 0 |

| | | | | | | | | |
|---|---|---|---|---|---|---|---|---|
| 30 | 2938.8 | -8537.6 | 21537 | -2938.8 | 8537.6 | -23343 | 0 | 0 |
| 31 | 13591 | 18910 | 2888.2 | -13591 | -18910 | 4705.7 | 0 | 0 |
| 32 | 13591 | 18910 | -4705.7 | -13591 | -18910 | 12297 | 0 | 0 |
| 33 | 13591 | 18910 | -12297 | -13591 | -18910 | 19882 | 0 | 0 |
| 34 | 13591 | 18910 | -19882 | -13591 | -18910 | 27456 | 0 | 0 |
| 35 | 13591 | 18910 | -27456 | -13591 | -18910 | 35016 | 0 | 0 |
| 36 | -1549.5 | -38070 | -38987 | 1549.5 | 38070 | 23762 | 0 | 0 |
| 37 | -1549.5 | -38070 | -23762 | 1549.5 | 38070 | 8537.8 | 0 | 0 |
| 38 | -1549.5 | -38070 | -8537.8 | 1549.5 | 38070 | -6685.5 | 0 | 0 |
| 39 | -1549.5 | -38070 | 6685.5 | 1549.5 | 38070 | -21909 | 0 | 0 |
| 40 | -1549.5 | -38070 | 21909 | 1549.5 | 38070 | -37134 | 0 | 0 |
| 41 | -65122 | 16406 | 33398 | 65122 | -16406 | -26802 | 0 | 0 |
| 42 | -65122 | 16406 | 26802 | 65122 | -16406 | -20274 | 0 | 0 |
| 43 | -65122 | 16406 | 20274 | 65122 | -16406 | -13797 | 0 | 0 |
| 44 | -65122 | 16406 | 13797 | 65122 | -16406 | -7356.3 | 0 | 0 |
| 45 | -65122 | 16406 | 7356.3 | 65122 | -16406 | -934 | 0 | 0 |
| 46 | 64607 | 47355 | 23393 | -64607 | -47355 | -4229.9 | 0 | 0 |
| 47 | 64607 | 47355 | 4229.9 | -64607 | -47355 | 14944 | 0 | 0 |
| 48 | 64607 | 47355 | -14944 | -64607 | -47355 | 34081 | 0 | 0 |
| 49 | 64607 | 47355 | -34081 | -64607 | -47355 | 53131 | 0 | 0 |
| 50 | 64607 | 47355 | -53131 | -64607 | -47355 | 72047 | 0 | 0 |
| 51 | 3041.9 | -77118 | -78359 | -3041.9 | 77118 | 47504 | -6.27E-06 | 0 |
| 52 | 3042.1 | -77117 | -47504 | -3042.1 | 77117 | 16645 | 0 | 0 |
| 53 | 3042.2 | -77117 | -16645 | -3042.2 | 77117 | -14216 | 0 | 0 |
| 54 | 3042.2 | -77117 | 14216 | -3042.2 | 77117 | -45075 | 0 | 0 |
| 55 | 3042.2 | -77117 | 45075 | -3042.2 | 77117 | -75931 | 0 | 0 |
| 56 | -105970 | 46311 | 71042 | 105970 | -46311 | -52448 | 0 | 0 |
| 57 | -105970 | 46311 | 52448 | 105970 | -46311 | -34072 | 0 | 0 |
| 58 | -105970 | 46311 | 34072 | 105970 | -46311 | -15839 | 0 | 0 |
| 59 | -105970 | 46311 | 15839 | 105970 | -46311 | 2328.8 | 0 | 0 |
| 60 | -105970 | 46311 | -2328.8 | 105970 | -46311 | 20506 | 0 | 0 |
| 61 | 160550 | 45602 | 24946 | -160550 | -45602 | -6056.6 | 0 | 0 |
| 62 | 160550 | 45602 | 6056.6 | -160550 | -45602 | 12871 | 0 | 0 |
| 63 | 160550 | 45602 | -12871 | -160550 | -45602 | 31718 | 0 | 0 |
| 64 | 160550 | 45602 | -31718 | -160550 | -45602 | 50365 | 0 | 0 |
| 65 | 160550 | 45602 | -50365 | -160550 | -45602 | 68697 | 0 | 0 |
| 66 | 103030 | -73026 | -74477 | -103030 | 73026 | 44823 | -0.0066477 | 0 |
| 67 | 103030 | -73026 | -44823 | -103030 | 73026 | 14972 | 0 | 0 |
| 68 | 103030 | -73026 | -14972 | -103030 | 73026 | -14940 | 0 | 0 |
| 69 | 103030 | -73026 | 14940 | -103030 | 73026 | -44792 | 0 | 0 |
| 70 | 103030 | -73026 | 44792 | -103030 | 73026 | -74449 | 0 | -0.0054647 |
| 71 | -2938.5 | 46585 | 69785 | 2938.5 | -46585 | -51151 | 0 | 0 |
| 72 | -2938.6 | 46585 | 51151 | 2938.6 | -46585 | -32524 | 0 | 0 |
| 73 | -2938.6 | 46585 | 32524 | 2938.6 | -46585 | -13900 | 0 | 0 |

| | | | | | | | | |
|---|---|---|---|---|---|---|---|---|
| 74 | -2938.6 | 46585 | 13900 | 2938.6 | -46585 | 4721.3 | 0 | 0 |
| 75 | -2938.6 | 46585 | -4721.3 | 2938.6 | -46585 | 23343 | 0 | 0 |
| 76 | -15141 | -18933 | 3301 | 15141 | 18933 | -1825.9 | 0 | 0 |
| 77 | -15141 | -18933 | 1825.9 | 15141 | 18933 | -398.09 | 0 | 0 |
| 78 | -15141 | -18933 | 398.09 | 15141 | 18933 | 1019.4 | 0 | 0 |
| 79 | -15141 | -18933 | -1019.4 | 15141 | 18933 | 2463.3 | 0 | 0 |
| 80 | -15141 | -18933 | -2463.3 | 15141 | 18933 | 3971.1 | 0 | 0 |
| 81 | -61565 | -86424 | 3130.2 | 61565 | 86424 | -1325.8 | 0 | 0 |
| 82 | -61565 | -86424 | 1325.8 | 61565 | 86424 | 326.17 | 0 | 0 |
| 83 | -61565 | -86424 | -326.17 | 61565 | 86424 | 2015.7 | 0 | 0 |
| 84 | -61565 | -86424 | -2015.7 | 61565 | 86424 | 3937.2 | 0 | 0 |
| 85 | -61565 | -86424 | -3937.2 | 61565 | 86424 | 6311.8 | 0 | 0 |
| 86 | -57523 | -80581 | 2710.6 | 57523 | 80581 | -1103.2 | 0 | 0 |
| 87 | -57523 | -80581 | 1103.2 | 57523 | 80581 | 385.82 | 0 | 0 |
| 88 | -57523 | -80581 | -385.82 | 57523 | 80581 | 1916.3 | 0 | 0 |
| 89 | -57523 | -80581 | -1916.3 | 57523 | 80581 | 3652.5 | 0 | 0 |
| 90 | -57523 | -80581 | -3652.5 | 57523 | 80581 | 5780.5 | 0 | 0 |
| 91 | -63572 | 92524 | 3172.7 | 63572 | -92524 | -1874.1 | 0 | 0 |
| 92 | -63572 | 92524 | 1874.1 | 63572 | -92524 | -353.91 | 0 | 0 |
| 93 | -63572 | 92524 | 353.91 | 63572 | -92524 | 1208.1 | 0 | 0 |
| 94 | -63572 | 92524 | -1208.1 | 63572 | -92524 | 2627.3 | 0 | 0 |
| 95 | -63572 | 92524 | -2627.3 | 63572 | -92524 | 3736 | 0 | 0 |
| 96 | -109020 | 161480 | 3410.8 | 109020 | -161480 | -1520.6 | 0 | 0 |
| 97 | -109020 | 161480 | 1520.6 | 109020 | -161480 | 678.44 | 0 | 0 |
| 98 | -109020 | 161480 | -678.44 | 109020 | -161480 | 2739.8 | 0 | 0 |
| 99 | -109020 | 161480 | -2739.8 | 109020 | -161480 | 4245.2 | 0 | 0 |
| 100 | -109020 | 161480 | -4245.2 | 109020 | -161480 | 4889 | 0 | 0 |
| 101 | -105970 | 157660 | 3147.5 | 105970 | -157660 | -1337.2 | 0 | 0 |
| 102 | -105970 | 157660 | 1337.2 | 105970 | -157660 | 738.1 | 0 | 0 |
| 103 | -105970 | 157660 | -738.1 | 105970 | -157660 | 2667.4 | 0 | 0 |
| 104 | -105970 | 157660 | -2667.4 | 105970 | -157660 | 4068.6 | 0 | 0 |
| 105 | -105970 | 157660 | -4068.6 | 105970 | -157660 | 4664.2 | 0 | 0 |
| 2st Configuration-softening case | | | | | | | | |
| | NODE 1 | | | NODE 2 | | | | |
| | FX | FY | MZ | FX | FY | MZ | Θpl1 | Θpl2 |
| 1 | -23762 | 76015 | 283410 | 23762 | -76015 | -269080 | 0 | 0 |
| 2 | -23762 | 76015 | 269080 | 23762 | -76015 | -254610 | 0 | 0 |
| 3 | -23762 | 76015 | 254610 | 23762 | -76015 | -240010 | 0 | 0 |
| 4 | -23762 | 76015 | 240010 | 23762 | -76015 | -225290 | 0 | 0 |
| 5 | -23762 | 76015 | 225290 | 23762 | -76015 | -210450 | 0 | 0 |
| 6 | -25755 | 82324 | 214740 | 25755 | -82324 | -198540 | 0 | 0 |
| 7 | -25755 | 82324 | 198540 | 25755 | -82324 | -182220 | 0 | 0 |
| 8 | -25755 | 82324 | 182220 | 25755 | -82324 | -165810 | 0 | 0 |
| 9 | -25755 | 82324 | 165810 | 25755 | -82324 | -149300 | 0 | 0 |

| | | | | | | | | |
|---|---|---|---|---|---|---|---|---|
| 10 | -25755 | 82324 | 149300 | 25755 | -82324 | -132710 | 0 | 0 |
| 11 | -33825 | 76115 | 126540 | 33825 | -76115 | -105130 | 0 | 0 |
| 12 | -33825 | 76115 | 105130 | 33825 | -76115 | -83670 | 0 | 0 |
| 13 | -33825 | 76115 | 83670 | 33825 | -76115 | -62162 | 0 | 0 |
| 14 | -33825 | 76115 | 62162 | 33825 | -76115 | -40623 | 0 | 0 |
| 15 | -33825 | 76115 | 40623 | 33825 | -76115 | -19063 | 0 | 0 |
| 16 | -31323 | 303340 | 289120 | 31323 | -303340 | -270040 | 0 | 0 |
| 17 | -31323 | 303340 | 270040 | 31323 | -303340 | -250400 | 0 | 0 |
| 18 | -31323 | 303340 | 250400 | 31323 | -303340 | -230240 | 0 | 0 |
| 19 | -31323 | 303340 | 230240 | 31323 | -303340 | -209610 | 0 | 0 |
| 20 | -31323 | 303340 | 209610 | 31323 | -303340 | -188540 | 0 | 0 |
| 21 | -24954 | 142340 | 194250 | 24954 | -142340 | -178020 | 0 | 0 |
| 22 | -24954 | 142340 | 178020 | 24954 | -142340 | -161620 | 0 | 0 |
| 23 | -24954 | 142340 | 161620 | 24954 | -142340 | -145070 | 0 | 0 |
| 24 | -24954 | 142340 | 145070 | 24954 | -142340 | -128380 | 0 | 0 |
| 25 | -24954 | 142340 | 128380 | 24954 | -142340 | -111560 | 0 | 0 |
| 26 | -29049 | -3921.6 | 105080 | 29049 | 3921.6 | -87713 | 0 | 0 |
| 27 | -29049 | -3921.6 | 87713 | 29049 | 3921.6 | -70345 | 0 | 0 |
| 28 | -29049 | -3921.6 | 70345 | 29049 | 3921.6 | -52979 | 0 | 0 |
| 29 | -29049 | -3921.6 | 52979 | 29049 | 3921.6 | -35614 | 0 | 0 |
| 30 | -29049 | -3921.6 | 35614 | 29049 | 3921.6 | -18251 | 0 | 0 |
| 31 | 57709 | 29060 | -10239 | -57709 | -29060 | 22169 | 0 | 0 |
| 32 | 57709 | 29060 | -22169 | -57709 | -29060 | 34049 | 0 | 0 |
| 33 | 57709 | 29060 | -34049 | -57709 | -29060 | 45852 | 0 | 0 |
| 34 | 57709 | 29060 | -45852 | -57709 | -29060 | 57552 | 0 | 0 |
| 35 | 57709 | 29060 | -57552 | -57709 | -29060 | 69122 | 0 | 0 |
| 36 | 5315.6 | -78202 | -78257 | -5315.6 | 78202 | 46960 | -0.0007734 | 0 |
| 37 | 5315.4 | -78209 | -46960 | -5315.4 | 78209 | 15650 | 0 | 0 |
| 38 | 5314.9 | -78209 | -15650 | -5314.9 | 78209 | -15663 | 0 | 0 |
| 39 | 5314.1 | -78209 | 15663 | -5314.1 | 78209 | -46973 | 0 | 0 |
| 40 | 5313 | -78202 | 46973 | -5313 | 78202 | -78273 | 0 | -6.25E-05 |
| 41 | -95807 | 30181 | 70367 | 95807 | -30181 | -58179 | 0 | 0 |
| 42 | -95806 | 30181 | 58179 | 95806 | -30181 | -46210 | 0 | 0 |
| 43 | -95806 | 30181 | 46210 | 95806 | -30181 | -34414 | 0 | 0 |
| 44 | -95806 | 30181 | 34414 | 95806 | -30181 | -22749 | 0 | 0 |
| 45 | -95806 | 30181 | 22749 | 95806 | -30181 | -11169 | 0 | 0 |
| 46 | 58258 | 34532 | 2358.7 | -58258 | -34532 | 12003 | 0 | 0 |
| 47 | 58258 | 34532 | -12003 | -58258 | -34532 | 26338 | 0 | 0 |
| 48 | 58258 | 34532 | -26338 | -58258 | -34532 | 40613 | 0 | 0 |
| 49 | 58258 | 34532 | -40613 | -58258 | -34532 | 54797 | 0 | 0 |
| 50 | 58258 | 34532 | -54797 | -58258 | -34532 | 68856 | 0 | 0 |
| 51 | 2541.6 | -76928 | -76890 | -2541.6 | 76928 | 46160 | -0.034843 | 0 |
| 52 | 2541.7 | -76932 | -46160 | -2541.7 | 76932 | 15371 | 0 | 0 |
| 53 | 2541.7 | -76932 | -15371 | -2541.7 | 76932 | -15418 | 0 | 0 |

| | | | | | | | | |
|---|---|---|---|---|---|---|---|---|
| 54 | 2541.7 | -76932 | 15418 | -2541.7 | 76932 | -46207 | 0 | 0 |
| 55 | 2541.6 | -76928 | 46207 | -2541.6 | 76928 | -76944 | 0 | -0.033171 |
| 56 | -99633 | 38154 | 70304 | 99633 | -38154 | -55401 | 0 | 0 |
| 57 | -99633 | 38154 | 55401 | 99633 | -38154 | -40716 | 0 | 0 |
| 58 | -99633 | 38154 | 40716 | 99633 | -38154 | -26191 | 0 | 0 |
| 59 | -99633 | 38154 | 26191 | 99633 | -38154 | -11770 | 0 | 0 |
| 60 | -99633 | 38154 | 11770 | 99633 | -38154 | 2605.8 | 0 | 0 |
| 61 | 174780 | 38068 | 19063 | -174780 | -38068 | -1841.5 | 0 | 0 |
| 62 | 174780 | 38068 | 1841.5 | -174780 | -38068 | 15392 | 0 | 0 |
| 63 | 174780 | 38068 | -15392 | -174780 | -38068 | 32522 | 0 | 0 |
| 64 | 174780 | 38068 | -32522 | -174780 | -38068 | 49430 | 0 | 0 |
| 65 | 174780 | 38068 | -49430 | -174780 | -38068 | 66001 | 0 | 0 |
| 66 | 124590 | -66351 | -72194 | -124590 | 66351 | 43549 | -0.059648 | 0 |
| 67 | 124590 | -66351 | -43549 | -124590 | 66351 | 14531 | 0 | 0 |
| 68 | 124590 | -66351 | -14531 | -124590 | 66351 | -14556 | 0 | 0 |
| 69 | 124590 | -66351 | 14556 | -124590 | 66351 | -43573 | 0 | 0 |
| 70 | 124590 | -66351 | 43573 | -124590 | 66351 | -72226 | 0 | -0.057097 |
| 71 | 29049 | 41969 | 67013 | -29049 | -41969 | -50033 | 0 | 0 |
| 72 | 29049 | 41969 | 50033 | -29049 | -41969 | -32998 | 0 | 0 |
| 73 | 29049 | 41969 | 32998 | -29049 | -41969 | -15926 | 0 | 0 |
| 74 | 29049 | 41969 | 15926 | -29049 | -41969 | 1162.8 | 0 | 0 |
| 75 | 29049 | 41969 | -1162.8 | -29049 | -41969 | 18251 | 0 | 0 |
| 76 | -52394 | -69222 | 7381.2 | 52394 | 69222 | -3920.2 | 0 | 0 |
| 77 | -52394 | -69222 | 3920.2 | 52394 | 69222 | -826.78 | 0 | 0 |
| 78 | -52394 | -69222 | 826.78 | 52394 | 69222 | 2189.1 | 0 | 0 |
| 79 | -52394 | -69222 | -2189.1 | 52394 | 69222 | 5410.2 | 0 | 0 |
| 80 | -52394 | -69222 | -5410.2 | 52394 | 69222 | 9138.7 | 0 | 0 |
| 81 | -55716 | -73416 | 5947 | 55716 | 73416 | -3057.8 | 0 | 0 |
| 82 | -55716 | -73416 | 3057.8 | 55716 | 73416 | -472.27 | 0 | 0 |
| 83 | -55716 | -73416 | 472.27 | 55716 | 73416 | 2066.7 | 0 | 0 |
| 84 | -55716 | -73416 | -2066.7 | 55716 | 73416 | 4811.6 | 0 | 0 |
| 85 | -55716 | -73416 | -4811.6 | 55716 | 73416 | 8035.5 | 0 | 0 |
| 86 | -50189 | -66371 | 3808.5 | 50189 | 66371 | -1814.7 | 0 | 0 |
| 87 | -50189 | -66371 | 1814.7 | 50189 | 66371 | 16.418 | 0 | 0 |
| 88 | -50189 | -66371 | -16.418 | 50189 | 66371 | 1849.2 | 0 | 0 |
| 89 | -50189 | -66371 | -1849.2 | 50189 | 66371 | 3848.4 | 0 | 0 |
| 90 | -50189 | -66371 | -3848.4 | 50189 | 66371 | 6193.3 | 0 | 0 |
| 91 | -101120 | 146440 | 6941.8 | 101120 | -146440 | -4265.1 | 0 | 0 |
| 92 | -101120 | 146440 | 4265.1 | 101120 | -146440 | -795.96 | 0 | 0 |
| 93 | -101120 | 146440 | 795.96 | 101120 | -146440 | 2821.1 | 0 | 0 |
| 94 | -101120 | 146440 | -2821.1 | 101120 | -146440 | 5914 | 0 | 0 |
| 95 | -101120 | 146440 | -5914 | 101120 | -146440 | 7908.1 | 0 | 0 |
| 96 | -102170 | 153130 | 5464 | 102170 | -153130 | -3139.7 | 0 | 0 |
| 97 | -102170 | 153130 | 3139.7 | 102170 | -153130 | -210.23 | 0 | 0 |

| | | | | | | | | |
|---|---|---|---|---|---|---|---|---|
| 98 | -102170 | 153130 | 210.23 | 102170 | -153130 | 2760.7 | 0 | 0 |
| 99 | -102170 | 153130 | -2760.7 | 102170 | -153130 | 5201.3 | 0 | 0 |
| 100 | -102170 | 153130 | -5201.3 | 102170 | -153130 | 6641.6 | 0 | 0 |
| 101 | -95537 | 146370 | 3872.8 | 95537 | -146370 | -1980.4 | 0 | 0 |
| 102 | -95537 | 146370 | 1980.4 | 95537 | -146370 | 274.73 | 0 | 0 |
| 103 | -95537 | 146370 | -274.73 | 95537 | -146370 | 2480.2 | 0 | 0 |
| 104 | -95537 | 146370 | -2480.2 | 95537 | -146370 | 4232.8 | 0 | 0 |
| 105 | -95537 | 146370 | -4232.8 | 95537 | -146370 | 5212 | 0 | 0 |
| 3st Configuration-softening case | | | | | | | | |
| | NODE 1 | | | NODE 2 | | | | |
| | FX | FY | MZ | FX | FY | MZ | Θpl1 | Θpl2 |
| 1 | -67849 | 67655 | 626490 | 67849 | -67655 | -585190 | 0.012358 | 0 |
| 2 | -67907 | 67656 | 585190 | 67907 | -67656 | -543550 | 0 | 0 |
| 3 | -67907 | 67656 | 543550 | 67907 | -67656 | -501660 | 0 | 0 |
| 4 | -67907 | 67656 | 501660 | 67907 | -67656 | -459550 | 0 | 0 |
| 5 | -67907 | 67656 | 459550 | 67907 | -67656 | -417240 | 0 | 0 |
| 6 | -65948 | 79412 | 466640 | 65948 | -79412 | -424990 | 0 | 0 |
| 7 | -65948 | 79412 | 424990 | 65948 | -79412 | -383120 | 0 | 0 |
| 8 | -65948 | 79412 | 383120 | 65948 | -79412 | -341050 | 0 | 0 |
| 9 | -65948 | 79412 | 341050 | 65948 | -79412 | -298810 | 0 | 0 |
| 10 | -65948 | 79412 | 298810 | 65948 | -79412 | -256410 | 0 | 0 |
| 11 | -85895 | 61449 | 279610 | 85895 | -61449 | -225830 | 0 | 0 |
| 12 | -85895 | 61450 | 225830 | 85895 | -61450 | -171950 | 0 | 0 |
| 13 | -85895 | 61450 | 171950 | 85895 | -61450 | -118010 | 0 | 0 |
| 14 | -85895 | 61450 | 118010 | 85895 | -61450 | -64029 | 0 | 0 |
| 15 | -85895 | 61450 | 64029 | 85895 | -61450 | -10021 | 0 | 0 |
| 16 | -70271 | 306290 | 616610 | 70271 | -306290 | -571980 | 0.010325 | 0 |
| 17 | -70329 | 306290 | 571980 | 70329 | -306290 | -526080 | 0 | 0 |
| 18 | -70329 | 306290 | 526080 | 70329 | -306290 | -479090 | 0 | 0 |
| 19 | -70329 | 306290 | 479090 | 70329 | -306290 | -431120 | 0 | 0 |
| 20 | -70329 | 306290 | 431120 | 70329 | -306290 | -382240 | 0 | 0 |
| 21 | -65893 | 139430 | 427840 | 65893 | -139430 | -384910 | 0 | 0 |
| 22 | -65893 | 139430 | 384910 | 65893 | -139430 | -341610 | 0 | 0 |
| 23 | -65893 | 139430 | 341610 | 65893 | -139430 | -298000 | 0 | 0 |
| 24 | -65893 | 139430 | 298000 | 65893 | -139430 | -254110 | 0 | 0 |
| 25 | -65893 | 139430 | 254110 | 65893 | -139430 | -209980 | 0 | 0 |
| 26 | -72548 | 6209.8 | 229370 | 72548 | -6209.8 | -185690 | 0 | 0 |
| 27 | -72548 | 6209.8 | 185690 | 72548 | -6209.8 | -142020 | 0 | 0 |
| 28 | -72548 | 6209.8 | 142020 | 72548 | -6209.8 | -98344 | 0 | 0 |
| 29 | -72548 | 6209.8 | 98344 | 72548 | -6209.8 | -54667 | 0 | 0 |
| 30 | -72548 | 6209.8 | 54667 | 72548 | -6209.8 | -10989 | 0 | 0 |
| 31 | 41748 | -522.25 | -59142 | -41748 | 522.25 | 59586 | 0 | 0 |
| 32 | 41748 | -522.25 | -59586 | -41748 | 522.25 | 59931 | 0 | 0 |
| 33 | 41748 | -522.25 | -59931 | -41748 | 522.25 | 60179 | 0 | 0 |

| | | | | | | | | |
|---|---|---|---|---|---|---|---|---|
| 34 | 41748 | -522.25 | -60179 | -41748 | 522.25 | 60328 | 0 | 0 |
| 35 | 41748 | -522.25 | -60328 | -41748 | 522.25 | 60379 | 0 | 0 |
| 36 | 3729.5 | -75926 | -75858 | -3729.5 | 75926 | 45582 | -0.058213 | 0 |
| 37 | 3729.8 | -75931 | -45582 | -3729.8 | 75931 | 15174 | 0 | 0 |
| 38 | 3729.8 | -75931 | -15174 | -3729.8 | 75931 | -15235 | 0 | 0 |
| 39 | 3729.8 | -75931 | 15235 | -3729.8 | 75931 | -45643 | 0 | 0 |
| 40 | 3729.5 | -75925 | 45643 | -3729.5 | 75925 | -75926 | 0 | -0.05623 |
| 41 | -81837 | 6009.4 | 61793 | 81837 | -6009.4 | -59834 | 0 | 0 |
| 42 | -81837 | 6009.4 | 59834 | 81837 | -6009.4 | -58068 | 0 | 0 |
| 43 | -81837 | 6009.4 | 58068 | 81837 | -6009.4 | -56488 | 0 | 0 |
| 44 | -81837 | 6009.4 | 56488 | 81837 | -6009.4 | -55090 | 0 | 0 |
| 45 | -81837 | 6009.4 | 55090 | 81837 | -6009.4 | -53870 | 0 | 0 |
| 46 | 50661 | 14406 | -28555 | -50661 | -14406 | 35541 | 0 | 0 |
| 47 | 50661 | 14406 | -35541 | -50661 | -14406 | 42458 | 0 | 0 |
| 48 | 50661 | 14406 | -42458 | -50661 | -14406 | 49293 | 0 | 0 |
| 49 | 50661 | 14406 | -49293 | -50661 | -14406 | 56031 | 0 | 0 |
| 50 | 50661 | 14406 | -56031 | -50661 | -14406 | 62659 | 0 | 0 |
| 51 | 6954.6 | -72918 | -72967 | -6954.6 | 72918 | 43869 | -0.12846 | 0 |
| 52 | 6955 | -72922 | -43869 | -6955 | 72922 | 14569 | 0 | 0 |
| 53 | 6955 | -72922 | -14569 | -6955 | 72922 | -14731 | 0 | 0 |
| 54 | 6955 | -72922 | 14731 | -6955 | 72922 | -44031 | 0 | 0 |
| 55 | 6954.6 | -72919 | 44031 | -6954.6 | 72919 | -73142 | 0 | -0.12387 |
| 56 | -79319 | 23853 | 64292 | 79319 | -23853 | -55973 | 0 | 0 |
| 57 | -79319 | 23853 | 55973 | 79319 | -23853 | -47831 | 0 | 0 |
| 58 | -79319 | 23853 | 47831 | 79319 | -23853 | -39840 | 0 | 0 |
| 59 | -79319 | 23853 | 39840 | 79319 | -23853 | -31974 | 0 | 0 |
| 60 | -79319 | 23853 | 31974 | 79319 | -23853 | -24209 | 0 | 0 |
| 61 | 175930 | 23402 | 10021 | -175930 | -23402 | 4303.5 | 0 | 0 |
| 62 | 175930 | 23402 | -4303.5 | -175930 | -23402 | 18599 | 0 | 0 |
| 63 | 175930 | 23402 | -18599 | -175930 | -23402 | 32767 | 0 | 0 |
| 64 | 175930 | 23402 | -32767 | -175930 | -23402 | 46712 | 0 | 0 |
| 65 | 175930 | 23402 | -46712 | -175930 | -23402 | 60338 | 0 | 0 |
| 66 | 145210 | -49135 | -66955 | -145210 | 49135 | 40561 | -0.18291 | 0 |
| 67 | 145210 | -49136 | -40561 | -145210 | 49136 | 13476 | 0 | 0 |
| 68 | 145210 | -49136 | -13476 | -145210 | 49136 | -13683 | 0 | 0 |
| 69 | 145210 | -49136 | 13683 | -145210 | 49136 | -40767 | 0 | 0 |
| 70 | 145210 | -49135 | 40767 | -145210 | 49135 | -67177 | 0 | -0.17594 |
| 71 | 72549 | 31838 | 61331 | -72549 | -31838 | -47047 | 0 | 0 |
| 72 | 72549 | 31838 | 47047 | -72549 | -31838 | -32633 | 0 | 0 |
| 73 | 72549 | 31838 | 32633 | -72549 | -31838 | -18129 | 0 | 0 |
| 74 | 72549 | 31838 | 18129 | -72549 | -31838 | -3575.3 | 0 | 0 |
| 75 | 72549 | 31838 | 3575.3 | -72549 | -31838 | 10989 | 0 | 0 |
| 76 | -38019 | -37361 | 18578 | 38019 | 37361 | -11245 | 0.0022989 | 0 |
| 77 | -38018 | -37361 | 11245 | 38018 | 37361 | -4544.3 | 0 | 0 |

| | | | | | | | | |
|---|---|---|---|---|---|---|---|---|
| 78 | -38019 | -37361 | 4544.3 | 38019 | 37361 | 1900.4 | 0 | 0 |
| 79 | -38019 | -37361 | -1900.4 | 38019 | 37361 | 8452.5 | 0 | 0 |
| 80 | -38019 | -37361 | -8452.5 | 38019 | 37361 | 15481 | 0 | 0 |
| 81 | -43706 | -49281 | 9734.5 | 43706 | 49281 | -5491.5 | 0 | 0 |
| 82 | -43706 | -49281 | 5491.5 | 43706 | 49281 | -1635.1 | 0 | 0 |
| 83 | -43706 | -49281 | 1635.1 | 43706 | 49281 | 2106.3 | 0 | 0 |
| 84 | -43706 | -49281 | -2106.3 | 43706 | 49281 | 5996.7 | 0 | 0 |
| 85 | -43706 | -49281 | -5996.7 | 43706 | 49281 | 10310 | 0 | 0 |
| 86 | -30714 | -34491 | 5352.3 | 30714 | 34491 | -2900.1 | 0 | 0 |
| 87 | -30714 | -34491 | 2900.1 | 30714 | 34491 | -590.96 | 0 | 0 |
| 88 | -30714 | -34491 | 590.96 | 30714 | 34491 | 1689.2 | 0 | 0 |
| 89 | -30714 | -34491 | -1689.2 | 30714 | 34491 | 4053.1 | 0 | 0 |
| 90 | -30714 | -34491 | -4053.1 | 30714 | 34491 | 6617.2 | 0 | 0 |
| 91 | -85568 | 119990 | 15972 | 85568 | -119990 | -11466 | 8.33E-05 | 0 |
| 92 | -85567 | 119990 | 11467 | 85567 | -119990 | -5186.5 | 0 | 0 |
| 93 | -85567 | 119990 | 5186.5 | 85567 | -119990 | 1897.2 | 0 | 0 |
| 94 | -85567 | 119990 | -1897.2 | 85567 | -119990 | 8688.3 | 0 | 0 |
| 95 | -85567 | 119990 | -8688.3 | 85567 | -119990 | 14136 | 0 | 0 |
| 96 | -86273 | 134820 | 8269.3 | 86273 | -134820 | -5330.7 | 0 | 0 |
| 97 | -86273 | 134820 | 5330.7 | 86273 | -134820 | -1494.6 | 0 | 0 |
| 98 | -86273 | 134820 | 1494.6 | 86273 | -134820 | 2594 | 0 | 0 |
| 99 | -86273 | 134820 | -2594 | 86273 | -134820 | 6247.7 | 0 | 0 |
| 100 | -86273 | 134820 | -6247.7 | 86273 | -134820 | 8851.9 | 0 | 0 |
| 101 | -72664 | 119020 | 4826.7 | 72664 | -119020 | -2804.9 | 0 | 0 |
| 102 | -72664 | 119020 | 2804.9 | 72664 | -119020 | -370.62 | 0 | 0 |
| 103 | -72664 | 119020 | 370.62 | 72664 | -119020 | 2118.8 | 0 | 0 |
| 104 | -72664 | 119020 | -2118.8 | 72664 | -119020 | 4297.9 | 0 | 0 |
| 105 | -72664 | 119020 | -4297.9 | 72664 | -119020 | 5846.5 | 0 | 0 |

## Two bay rectangular frame

| Figure 6.22 (a) | | | | | | | | |
|---|---|---|---|---|---|---|---|---|
| | NODE 1 | | | NODE 2 | | | | |
| | FX | FY | MZ | FX | FY | MZ | Θpl1 | Θpl2 |
| 1 | -27.731 | 74.535 | 58.276 | 27.731 | -74.535 | 41.369 | 0 | 0 |
| 2 | -24.301 | 27.139 | 23.303 | 24.301 | -27.139 | 67.842 | 0 | 0 |
| 3 | 19.796 | 91.254 | -67.842 | -19.796 | -91.254 | 32.007 | 0 | 0 |
| 4 | 19.796 | -24.901 | -32.007 | -19.796 | 24.901 | -36.592 | 0 | 0 |
| 5 | 19.796 | -42.91 | 36.592 | -19.796 | 42.91 | 33.652 | 0 | 0 |
| 6 | 38.943 | -143.61 | 69.213 | -38.943 | 143.61 | 72.053 | 0 | 2.67E-02 |
| 7 | 19.153 | 73.762 | -43.699 | -19.153 | -73.762 | 64.125 | 0 | 0 |
| 8 | 19.153 | -60.678 | -64.125 | -19.153 | 60.678 | -102.87 | 0 | 0 |
| Figure 6.22 (b) | | | | | | | | |
| | NODE 1 | | | NODE 2 | | | | |
| | FX | FY | MZ | FX | FY | MZ | Θpl1 | Θpl2 |
| 1 | -37.59 | 69.478 | 62.203 | 37.59 | -69.478 | 74.586 | 0.016044 | 0.00016 |
| 2 | -0.18573 | 26.655 | -47.886 | 0.18573 | -26.655 | 60.957 | 0 | 0 |
| 3 | 22.891 | 86.407 | -60.957 | -22.891 | -86.407 | 29.993 | 0 | 0 |
| 4 | 22.891 | -25.386 | -29.993 | -22.891 | 25.386 | -39.935 | 0 | 0 |
| 5 | 22.891 | -43.401 | 39.935 | -22.891 | 43.401 | 41.243 | 0 | 0 |
| 6 | 31.593 | -148.69 | 60.665 | -31.593 | 148.69 | 61.134 | 0.014348 | 0.013932 |
| 7 | 87.366 | 27.912 | -69.791 | -87.366 | -27.912 | 77.559 | 0 | 0 |
| 8 | 87.374 | -65.263 | -77.559 | -87.374 | 65.263 | -102 | 0 | 0 |
| Figure 6.23 | | | | | | | | |
| | NODE 1 | | | NODE 2 | | | | |
| | FX | FY | MZ | FX | FY | MZ | Θpl1 | Θpl2 |
| 1 | -468.45 | -140.47 | 543.16 | 468.45 | 140.47 | 365.32 | 0.60995 | 0.37814 |
| 2 | -110.68 | -38.869 | 112.62 | 110.68 | 38.869 | 198.87 | 0.053871 | 0.14136 |
| 3 | 55.864 | -57.001 | -198.87 | -55.864 | 57.001 | 45.072 | -0.13522 | 0 |
| 4 | 55.864 | -91.306 | -45.072 | -55.864 | 91.306 | -204.04 | 0 | -0.14239 |
| 5 | 55.862 | -109.45 | 204.04 | -55.862 | 109.45 | 118.18 | 0.14801 | 0.061188 |
| 6 | 31.224 | -360.32 | 370.34 | -31.224 | 360.32 | 541.82 | 0.38857 | 0.61156 |
| 7 | -24.669 | -141.91 | -477.95 | 24.669 | 141.91 | 88.369 | -0.2704 | 0 |
| 8 | -24.669 | -210.52 | -88.369 | 24.669 | 210.52 | -488.51 | 0 | -0.27871 |